Hiroshima University Doctoral Thesis

2‐(4‐Nitrophenyl)‐1*H* indole: A Versatile Chromophore in Photoreaction

(2‐（4‐ニトロフェニル）‐1*H*‐インドール：光反応で多様性を持つ発色団)

2021

Department of Chemistry,

Graduate School of Science,

Hiroshima University

Lin Qianghua

Contents

Chapter 1.

General Introduction

1-1. Caged compounds

The human brain is the central organ of the human nervous system, which controls activities of the body, processing, integrating, and coordinating the information it receives from the sense organs, and making decisions as to the instructions sent to the rest of the body by neurons and their release of neurotransmitters. To understand the role of neurotransmitters and their associated mechanisms is a meaningful but challenge work because it is hard to monitor also control the release of neurotransmitters precisely, especially in vivo condition.

The fluorophore is a fluorescent chemical compound that can re-emit light upon light excitation[1]. Based on this feature, fluorophores can work as probes to monitor how neurotransmitters works: use biological fluorescent stains, immunofluorescence, and fluorescent proteins to generate real-time images of life phenomena, from which the active sites and functionalization of bioactive compounds can be clarified.[1,2]

Recently, a "caging & uncaging" strategy has attracted attention,[3] in which the bioactive substances can be masked temporally (caging) by photoremovable protecting groups (PPGs)[4–10] and unmasked (uncaging) by photolysis (Figure 1). By employ such caged compounds, the concentration jumps[11] of neurotransmitters or other bioactive compounds can be controlled by light:

$$Y = \frac{\emptyset \times I}{M}$$

Which, Y is yield of the released bioactive compounds (mol); $\emptyset$ is the quantum yield of bioactive compounds formation (%); I is the intensity of light source; M is the Avogadro constant.

Therefore, spatiotemporal control of the release of bioactive molecules, which achieved by caged compounds can be a weapon for biological research.

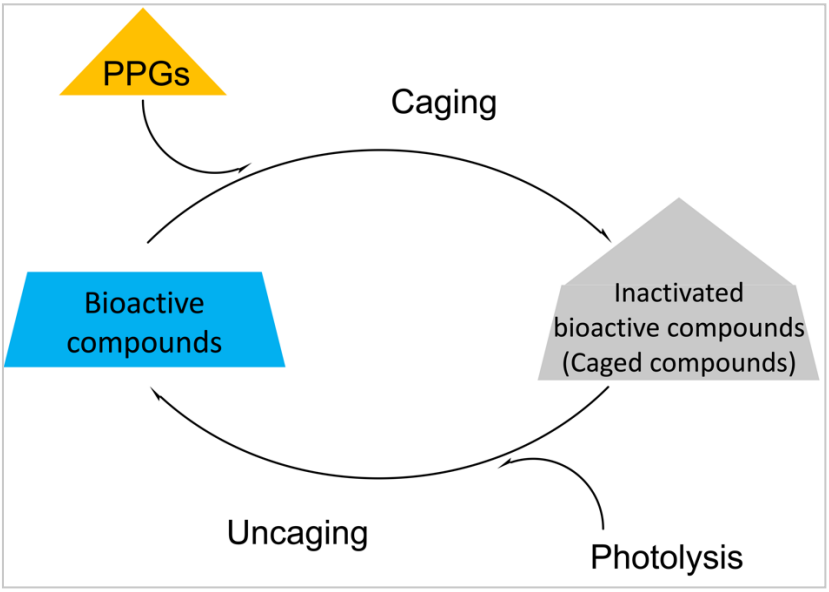

Figure 1. Caging and uncaging of bioactive compounds.

The application of PPGs for biology can be chased from 1977 by Engels and Schlaeger, who first achieved the photorelease of cyclic adenosine monophosphate (cAMP).[3] Until nowadays, several types of PPGs have been used in physiological studies to understand the bioactivity of substrates. Based on the photorelease uncaging mechanism, those PPGs can be categorized into two groups: First one is the ortho-nitrophenyl-type PPGs,[12–21] which can release leaving groups by intramolecular rearrangement. Another is photo S_N1-type,[22–25] by which PPGs are directly cleaved (Figure 2).

The ortho-nitrophenyl-type PPG was the first PPG that applied in physiological studies. However, this PPG has the potential to thermally hydrolyze at the benzylic position to produce bioactive substances during such studies. Coumarin chromophore worked as a photo S_N1-type PPG was

reported in 1984 by Givens and coworkers[22]. Recently, BODIPY[26–28] chromophore become an attractive PPG, which can release leaving group efficiently (Ø >90%) by visible light.

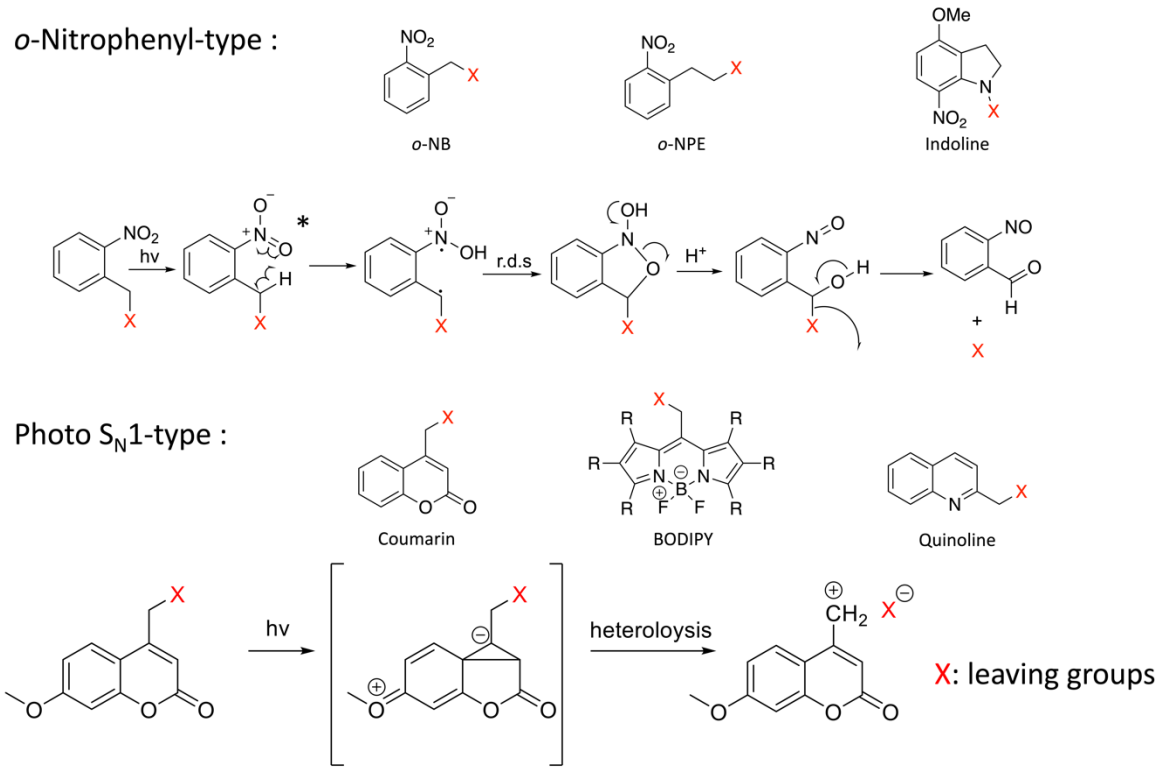

Figure 2. Typical photoremovable protecting groups (PPGs) and their photorelease uncaging mechanism.

1.2 Two-photon excitation for uncaging

The excitation energy of those typical PPGs is high, which requires ultraviolet (UV) light to activate, i.e., ortho-nitrophenyl PPGs has λ_{max} at 270 nm; 7-methoxycoumarin has λ_{max} at 320 nm.[10] However, UV light leads damage to living tissues.[29] To avoid cell damage, several visible-light-responsive PPGs, such as organometallic complexes[30,31] and organic chromophores[32–35] have been reported recently. Another strategy to reduce cell damage caused by light irradiation utilizes PPGs that

respond to two-photon (2P) excitation, with bioactive compounds released using less-toxic near-infrared (NIR) light.

2P excitation is a nonlinear process that two photons are absorbed simultaneously by the same molecule to generate excited state, this concept was proposed by Maria Göppert-Mayer in 1931.[36] Benefit from this, if there is a chromophore can be activated by 400 nm photon to generate electronically excited state, which means it may also absorb two 800 nm photons to generate the same excited state (Figure 3a). Therefore, 2P excitation can use lower energy photons to bring ground state molecules to their excited state. When 2P excitation applies for uncaging reaction, it becomes possible to activate PPGs by NIR light. Another feature of 2P excitation is that only the molecules on focal point can be excited (Figure 3b), thus more precise spatial control can be achieved.[37] Compared to one-photon (1P) visible light uncaging, 2P uncaging promise more advantages: (1) Less toxic to living tissues; (2) High spatial resolution and temporal control; (3) Deeper penetration in living tissues; (4) Low scattering.

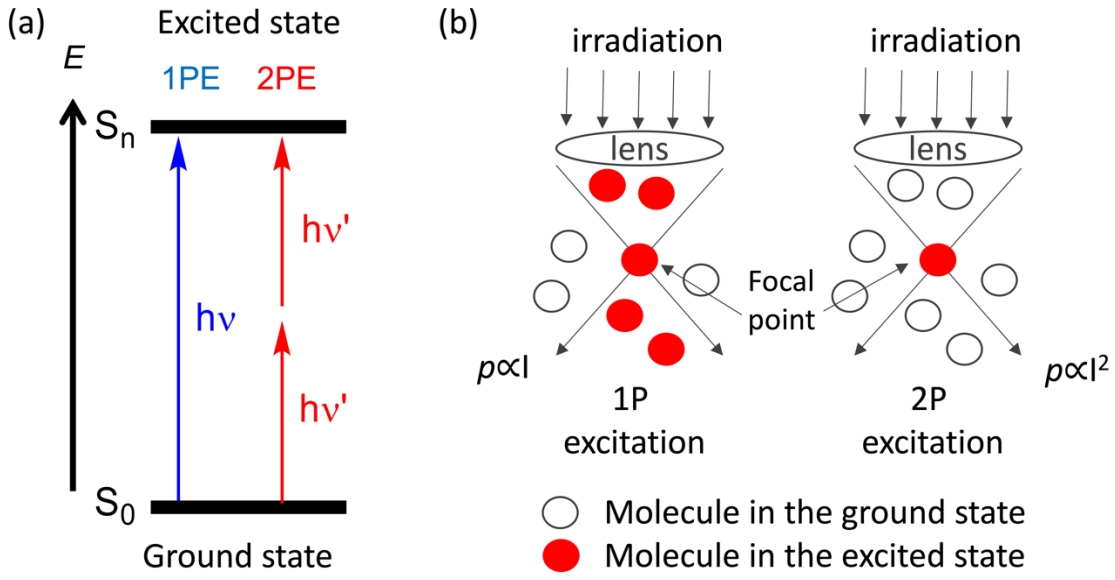

Figure 3. (a) 2P excitation and (b) difference between 1P and 2P excitation.

To apply 2P excitation for uncaging reaction, the 2P uncaging efficiency (δ_u) should be considered, it can be determined by:

$$\delta_u = \sigma_2 \times \phi_u$$

Where σ_2 is the 2P absorption cross-section (GM), ϕ is the uncaging quantum yield (%). The most important features of a strong 2P responsive molecule were found to be: (1) a long conjugation system; (2) substitution by strong donor and acceptor groups. And the 2P uncaging quantum yield should be same with 1P excitation because they provide the same excited state for uncaging reaction.

1.3 Molecular design of 2P responsive chromophores

To design suitable 2P responsive chromophores for caged compounds, several factors should be considered. The 2P absorption band should be around NIR region, 650 nm to 1050 nm. Also, a high 2P absorption cross section will be required to promise the efficiency of 2P uncaging reaction. To increase the 2P absorption cross section, there are two strategies.

1. Extension of π conjugation: Benzene has no 2P responsive character, while naphthalene gives 0.9 GM at 530 nm.[38] When a double bond introduced between two benzene rings to form a bridge connected compound stilbene, the 2P absorption cross section is improved significantly, with 12 GM at 514 nm (Figure 4).[39] The tendency clearly indicates the π-conjugation is directly correlated with TP absorption character. Long π-conjugation brings high 2P absorption cross section but also results poor water solubility. The water solubility is needed for biological studies; thus, it is important to design a suitable size of π conjugation chromophores.

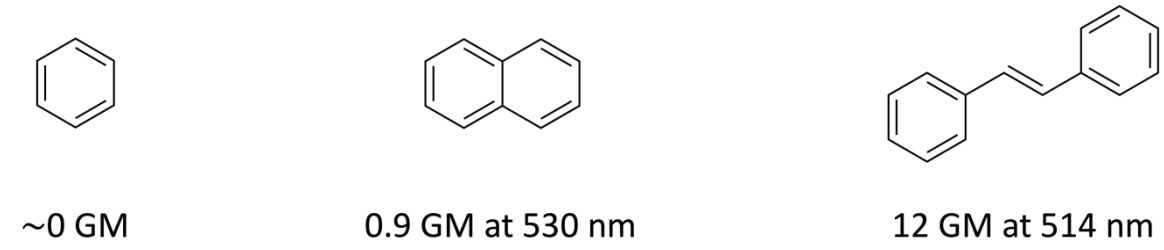

Figure 4. Conjugation effect on 2P absorption cross section

2. Donor and acceptor groups: The donor and acceptor groups can be thought of as inducing nonlinearity in the system and increasing the potential for charge-transfer, which can increase 2P cross section efficiently. When a donor and acceptor group introduced to a stilbene structure to form the (D-π-A) dipolar system, the 2P cross section can be improve from 12 GM to ~100 GM (Figure 5).[40] Similar D-π-D quadrupolar system can also bring over 100 GM to a stilbene skeleton. The branched chromophores i.e., the triangular structure (Figure 5) exploit the same principle and gather the sizable 2P cross section than dipolar system.[41]

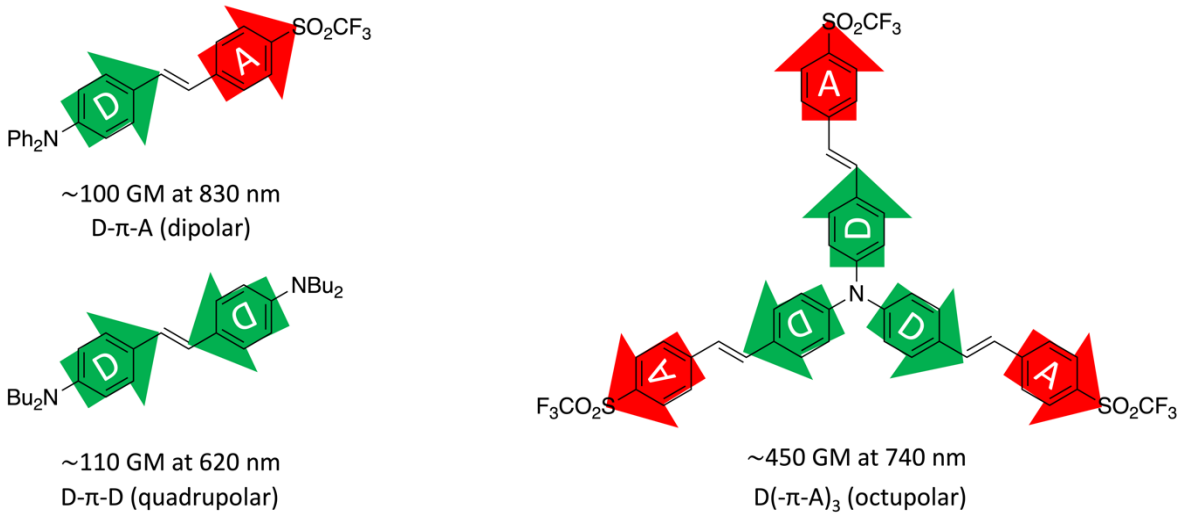

Figure 5. Strategy to improve 2P absorption cross section.

1.4 Target of this work

To design and synthesize 2P responsive chromophores for efficient uncaging is our purpose. Our lab has developed a series of NIR-2P-responsive PPGs based on stilbene scaffolds, e.g., NPNA,[42] NPBF,[43,44] DEACP[45] and APHI[46] (Figure 6). The NPNA Chromophore has good performance in 2P absorption with 120 GM at 680 nm, however, it has low quantum yield of uncaging (~0.01). More efficient 2P uncaging was required, because physiologists suggested that the 2P uncaging efficiency (δ_u) should be over 3 GM.[47] Later, the NPBF was designed, which possessed the 2P uncaging efficiency (δ_u) of ~5.0 GM at 740 nm. This feature makes the NPBF a promising TP photoremovable protecting group for physiological studies. Recently, the DEACP and APHI were developed, nominated by their high uncaging efficiency, but suffered from poor 2P absorption cross section. In the present study, 2-(4-nitrophenyl)-1*H*-indole (NPI) chromophore is designed as a new 2P responsive chromophores for caged compounds.

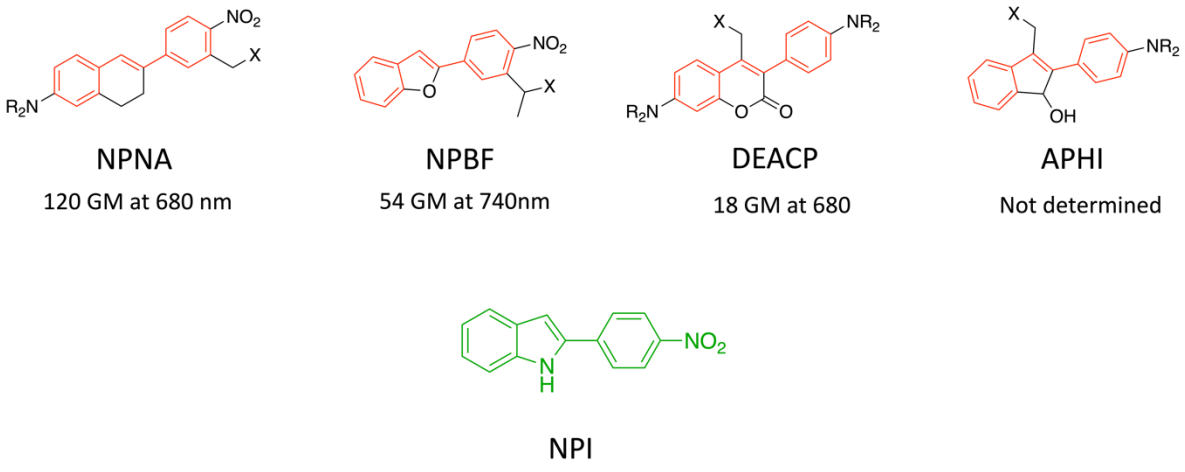

Figure 6. Several 2P responsive PPGs based on stilbene structure.

Reference:

1 (a) In Fluorescence Microscopy, Cornea, A.; Conn, P. M. Eds.Elsevier, 2014. (b)R. Yuste, Fluorescence microscopy today, *Nat. Methods*, 2005, **2**, 902–904.

2 H. M. Kim and B. R. Cho, Small-Molecule Two-Photon Probes for Bioimaging Applications, *Chem. Rev.*, 2015, **115**, 5014–5055.

3 J. Engels and E. J. Schlaeger, Synthesis, structure, and reactivity of adenosine cyclic 3',5'-phosphate-benzyltriesters, *J. Med. Chem.*, 1977, **20**, 907–911.

4 J. A. Barltrop and P. Schofield, Photosensitive Protecting Groups, *Tetrahedron Lett.*, 1962, **3**, 697–699.

5 J. A. Barltrop, P. J. Plant and P. Schofield, Photosensitive protective groups, *Chem. Commun.*, 1966, 822.

6 R. S. Givens, P. G. I. Conrad, A. L. Yousef and J.-I. Lee, *In CRC Handbook of Organic Photochemistry and Photobiology, 2nd ed*, 2003.

7 C. G. Bochet, Photolabile protecting groups and linkers, *J. Chem. Soc. Perkin Trans. 1*, 2002, **2**, 125–142.

8 N. Hoffmann, Photochemical Reactions as Key Steps in Organic Synthesis, *Chem. Rev.*, 2008, **108**, 1052–1103.

9 P. Wang, Photolabile Protecting Groups: Structure and Reactivity, *Asian J. Org. Chem.*, 2013, **2**, 452–464.

10 P. Klán, T. Šolomek, C. G. Bochet, A. Blanc, R. Givens, M. Rubina, V. Popik, A. Kostikov and J. Wirz, Photoremovable Protecting Groups in Chemistry and Biology: Reaction Mechanisms and Efficacy, *Chem. Rev.*, 2013, **113**, 119–191.

11 M. Goeldner and R. Givens, Eds., *Dynamic Studies in Biology: Phototriggers, Photoswitches and Caged Biomolecules*, Wiley-VCH: Weinheim, 2005.

12 A. Patchornik, B. Amit and R. B. Woodward, Photosensitive protecting groups, *J. Am. Chem. Soc.*, 1970, **92**, 6333–6335.

13 J. H. Kaplan, B. Forbush and J. F. Hoffman, Rapid Photolytic Release of Adenosine 5′-Triphosphate from a Protected Analogue: Utilization by the Na:K Pump of Human Red Blood Cell Ghosts, *Biochemistry*, 1978, **17**, 1929–1935.

14 A. Hasan, K.-P. Stengele, H. Giegrich, P. Cornwell, K. R. Isham, R. A. Sachleben, W. Pfleiderer and R. S. Foote, Photolabile protecting groups for nucleosides: Synthesis and photodeprotection rates, *Tetrahedron*, 1997, **53**, 4247–4264.

15 A. Specht, F. Bolze, L. Donato, C. Herbivo, S. Charon, D. Warther, S. Gug, J.-F.

Nicoud and M. Goeldner, The donor–acceptor biphenyl platform: A versatile chromophore for the engineering of highly efficient two-photon sensitive photoremovable protecting groups, *Photochem. Photobiol. Sci.*, 2012, **11**, 578.

16 L. Donato, A. Mourot, C. M. Davenport, C. Herbivo, D. Warther, J. Léonard, F. Bolze, J.-F. Nicoud, R. H. Kramer, M. Goeldner and A. Specht, Water-Soluble, Donor-Acceptor Biphenyl Derivatives in the 2-(o-Nitrophenyl)propyl Series: Highly Efficient Two-Photon Uncaging of the Neurotransmitter γ-Aminobutyric Acid at λ=800 nm, *Angew. Chemie Int. Ed.*, 2012, **51**, 1840–1843.

17 B. Amit and A. Patchornik, The photorearrangement of N-substituted -nitroanilides and nitroveratramides. A potential photosensitive protecting group, *Tetrahedron Lett.*, 1973, **14**, 2205–2208.

18 B. Amit, D. A. Ben-Efraim and A. Patchornik, Light-sensitive amides. The photosolvolysis of substituted 1-acyl-7-nitroindolines, *J. Am. Chem. Soc.*, 1976, **98**, 843–844.

19 J. Morrison, P. Wan, J. E. T. Corrie and G. Papageorgiou, Mechanisms of photorelease of carboxylic acids from 1-acyl-7-nitroindolines in solutions of varying water content, *Photochem. Photobiol. Sci.*, 2002, **1**, 960.

20 G. Papageorgiou, D. C. Ogden, A. Barth and J. E. T. Corrie, Photorelease of Carboxylic Acids from 1-Acyl-7-nitroindolines in Aqueous Solution: Rapid and Efficient Photorelease of <scp>l</scp> -Glutamate [1], *J. Am. Chem. Soc.*, 1999, **121**, 6503–6504.

21 M. Matsuzaki, T. Hayama, H. Kasai and G. C. R. Ellis-Davies, Two-photon uncaging of γ-aminobutyric acid in intact brain tissue, *Nat. Chem. Biol.*, 2010, **6**, 255–257.

22 R. S. Givens and B. Matuszewski, Photochemistry of phosphate esters: an efficient method for the generation of electrophiles, *J. Am. Chem. Soc.*, 1984, **106**, 6860–6861.

23 N. Kamatham, D. C. Mendes, J. P. Da Silva, R. S. Givens and V. Ramamurthy, Photorelease of Incarcerated Caged Acids from Hydrophobic Coumaryl Esters into Aqueous Solution, *Org. Lett.*, 2016, **18**, 5480–5483.

24 O. D. Fedoryak and T. M. Dore, Brominated Hydroxyquinoline as a Photolabile Protecting Group with Sensitivity to Multiphoton Excitation, *Org. Lett.*, 2002, **4**, 3419–3422.

25 Y. Zhu, C. M. Pavlos, J. P. Toscano and T. M. Dore, 8-Bromo-7-hydroxyquinoline as a Photoremovable Protecting Group for Physiological Use: Mechanism and Scope, *J. Am. Chem. Soc.*, 2006, **128**, 4267–4276.

26 P. P. Goswami, A. Syed, C. L. Beck, T. R. Albright, K. M. Mahoney, R. Unash, E. A. Smith and A. H. Winter, BODIPY-Derived Photoremovable Protecting Groups Unmasked with Green Light, *J. Am. Chem. Soc.*, 2015, **137**, 3783–3786.

27 E. Palao, T. Slanina, L. Muchová, T. Šolomek, L. Vítek and P. Klán, Transition-Metal-Free CO-Releasing BODIPY Derivatives Activatable by Visible to NIR Light as Promising Bioactive Molecules, *J. Am. Chem. Soc.*, 2016, **138**, 126–133.

28 T. Slanina, P. Shrestha, E. Palao, D. Kand, J. A. Peterson, A. S. Dutton, N. Rubinstein, R. Weinstain, A. H. Winter and P. Klán, In Search of the Perfect Photocage: Structure-Reactivity Relationships in meso-Methyl BODIPY Photoremovable Protecting Groups, *J. Am. Chem. Soc.*, 2017, **139**, 15168–15175.

29 J. R. Pehrson, Thymine dimer formation as a probe of the path of DNA in and between nucleosomes in intact chromatin, *Proc. Natl. Acad. Sci.*, 1989, **86**, 9149 LP – 9153.

30 L. Zayat, M. G. Noval, J. Campi, C. I. Calero, D. J. Calvo and R. Etchenique, A new inorganic photolabile protecting group for highly efficient visible light GABA uncaging, *ChemBioChem*, 2007, **8**, 2035–2038.

31 O. Filevich and R. Etchenique, RuBiGABA-2: a hydrophilic caged GABA with long wavelength sensitivity, *Photochem. Photobiol. Sci.*, 2013, **12**, 1565.

32 P. Šebej, J. Wintner, P. Müller, T. Slanina, J. Al Anshori, L. A. P. Antony, P. Klán and J. Wirz, Fluorescein analogues as photoremovable protecting groups absorbing at ∼520 nm, *J. Org. Chem.*, 2013, **78**, 1833–1843.

33 J. P. Olson, M. R. Banghart, B. L. Sabatini and G. C. R. Ellis-Davies, Spectral evolution of a photochemical protecting group for orthogonal two-color uncaging with visible light, *J. Am. Chem. Soc.*, 2013, **135**, 15948–15954.

34 N. Umeda, H. Takahashi, M. Kamiya, T. Ueno, T. Komatsu, T. Terai, K. Hanaoka, T. Nagano and Y. Urano, Boron dipyrromethene as a fluorescent caging group for single-photon uncaging with long-wavelength visible light, *ACS Chem. Biol.*, 2014, **9**, 2242–2246.

35 R. R. Nani, A. P. Gorka, T. Nagaya, H. Kobayashi and M. J. Schnermann, Near-IR Light-Mediated Cleavage of Antibody-Drug Conjugates Using Cyanine Photocages, *Angew. Chemie*, 2015, **127**, 13839–13842.

36 M. Saigo, K. Miyata, S. Tanaka, H. Nakanotani, C. Adachi and K. Onda, Suppression of Structural Change upon S1-T1 Conversion Assists the Thermally Activated

Delayed Fluorescence Process in Carbazole-Benzonitrile Derivatives, *J. Phys. Chem. Lett.*, 2019, **10**, 2475–2480.

37 T. Hosokai, H. Matsuzaki, H. Nakanotani, K. Tokumaru, T. Tsutsui, A. Furube, K. Nasu, H. Nomura, M. Yahiro and C. Adachi, Evidence and mechanism of efficient thermally activated delayed fluorescence promoted by delocalized excited states, *Sci. Adv.*, 2017, **3**, e1603282.

38 S. Z. Weisz, A. B. Zahlan, J. Gileeath, R. C. Jarnagin and M. Silver, Two-photon absorption in crystalline anthracene and naphthalene excited with a xenon flash, *J. Chem. Phys.*, 1964, **41**, 3491–3495.

39 R. J. M. Anderson, G. R. Holtom and W. M. McClain, Two-photon absorptivities of the all t r a n s α, ω-diphenylpolyenes from stilbene to diphenyloctatetraene via three wave mixing, *J. Chem. Phys.*, 1979, **70**, 4310–4315.

40 F. Terenziani, C. Sissa and A. Painelli, Symmetry breaking in octupolar chromophores: Solvatochromism and electroabsorption, *J. Phys. Chem. B*, 2008, **112**, 5079–5087.

41 F. Terenziani, C. Katan, E. Badaeva, S. Tretiak and M. Blanchara-Desce, *Enhanced two-photon absorption of organic chromophores: Theoretical and experimental assessments*, 2008, vol. 20.

42 S. Boinapally, B. Huang, M. Abe, C. Katan, J. Noguchi, S. Watanabe, H. Kasai, B. Xue and T. Kobayashi, Caged Glutamates with π-Extended 1,2-Dihydronaphthalene Chromophore: Design, Synthesis, Two-Photon Absorption Property, and Photochemical Reactivity, *J. Org. Chem.*, 2014, **79**, 7822–7830.

43 N. Komori, S. Jakkampudi, R. Motoishi, M. Abe, K. Kamada, K. Furukawa, C. Katan, W. Sawada, N. Takahashi, H. Kasai, B. Xue and T. Kobayashi, Design and synthesis of a new chromophore, 2-(4-nitrophenyl)benzofuran, for two-photon uncaging using near-IR light, *Chem. Commun.*, 2016, **52**, 331–334.

44 S. Jakkampudi, M. Abe, N. Komori, R. Takagi, K. Furukawa, C. Katan, W. Sawada, N. Takahashi and H. Kasai, Design and Synthesis of a 4-Nitrobromobenzene Derivative Bearing an Ethylene Glycol Tetraacetic Acid Unit for a New Generation of Caged Calcium Compounds with Two-Photon Absorption Properties in the Near-IR Region and Their Application in Vivo, *ACS Omega*, 2016, **1**, 193–201.

45 Y. Chitose, M. Abe, K. Furukawa, J. Y. Lin, T. C. Lin and C. Katan, Design and Synthesis of a Caged Carboxylic Acid with a Donor-π-Donor Coumarin Structure: One-photon and Two-photon Uncaging Reactions Using Visible and Near-Infrared

Lights, *Org. Lett.*, 2017, **19**, 2622–2625.

46 M. Sasaki, L. Tran Bao Nguyen, S. Yabumoto, T. Nakagawa and M. Abe, Structural Transformation of the 2-(p -Aminophenyl)-1-hydroxyinden-3-ylmethyl Chromophore as a Photoremovable Protecting Group, *ChemPhotoChem*, 2020, **4**, 5392–5398.

47 N. I. Kiskin, Rod Chillingworth, James, The efficiency of two-photon photolysis of a 'caged' fluorophore, o -1-(2-nitrophenyl)ethylpyranine, in relation to photodamage of synaptic terminals, *Eur. Biophys. J.*, 2002, **30**, 588–604.

Chapter 2

Light-triggered elimination of CO_2 and absorption of O_2 (artificial breathing reaction) in photolysis of 2-(4-nitrophenyl)-1*H*-indole derivatives

2-1. Introduction

In the origin, I chose 2-(4-nitrophenyl)-1*H*-indole (NPI) chromophore as basic skeleton for designing PPG. The electron-donating character of the indole nitrogen atom and electron-withdrawing nitrophenyl group can form a push-pull system to promise a sizable 2P sensitivity. A polar group (CH_2CO_2H), which may increase the water solubility, has been introduced on the nitrogen atom.[1]

Compounds **1** and **2**, which are the caged benzoic acid equivalents, were synthesized and their photochemical reactions were investigated in detail. Interestingly, upon photolysis of **2** under air, in addition to the expected release of benzoic acid, it was observed an efficient transformation of the "R = CH_2CO_2H" group to the "R = CHO" moiety. To understand the generality and mechanism of this interesting reaction, **3** and **4** were synthesized and their photolysis was conducted under similar conditions. Further, I employed transient absorption spectroscopy and computational studies to understand the novel chemical transformation.

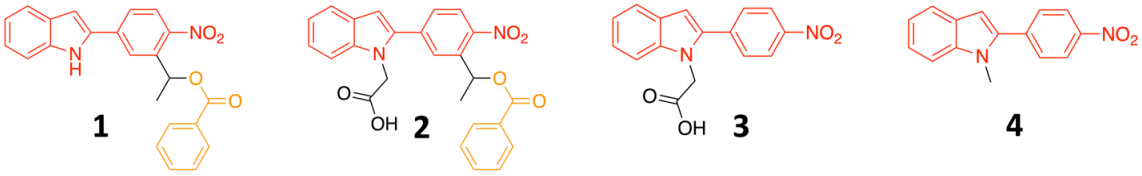

Figure 7. 2-(4-nitrophenyl)-1*H*-indole (NPI) derivatives.

2-2. Results and discussion

Synthesis of compounds 1-4. The synthesis of compounds **1**–**4** is shown in Scheme 1. The selective nitration of bromide **5** afforded compound **6** in 60%, followed by the reduction of the ketone moiety produced alcohol **7** in 95% (Scheme 1a). The

Suzuki-Miyaura coupling with indole derivative **9** gave 2-(4-nitrophenyl)indole **10** in 90%. The condensation with benzoic acid (**11**) gave compound **1** in 95%. A polar substituent, CH_2CO_2H, was introduced at the nitrogen atom using *t*-butyl bromoacetate to afford compound **2** via compound **12** in 86% in two steps from **1**. The synthesis of compound **3** was achieved by Suzuki-Miyaura coupling of compound **13** with compound **9**, and followed by the introduction of CH_2CO_2H group (Scheme 1b). Compound **4** was synthesized by the N-methylation of compound **14** in 81%. The molecular structures were confirmed by ^{1}H NMR, ^{13}C NMR, and ESI-MS (experimental section).

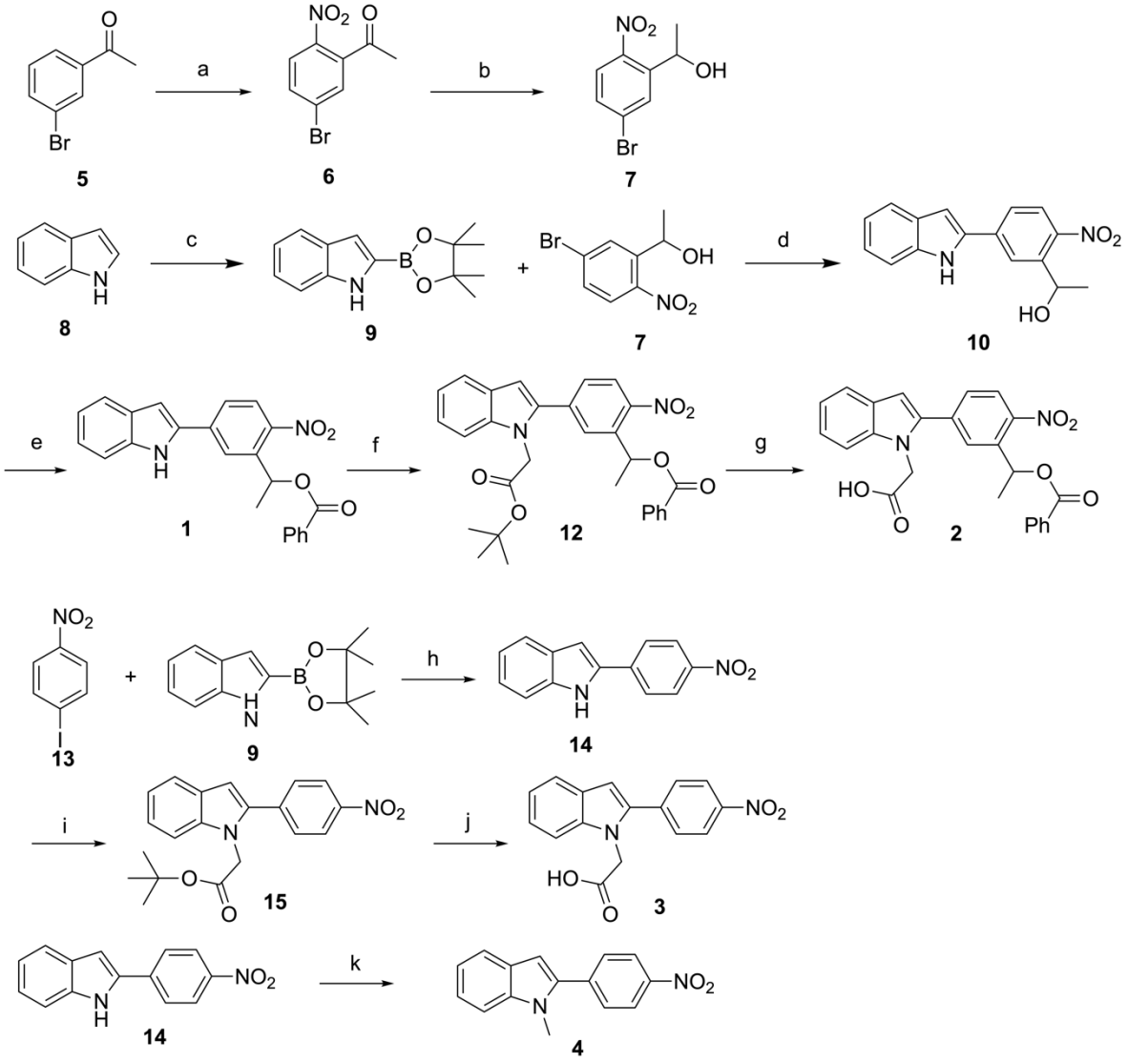

Scheme 1. Reagents and conditions: (a) KNO_3, H_2SO_4, 0°C to RT, 2 h, 60%. (b) $NaBH_4$, MeOH, 0°C to RT, 1 h, 95%. (c) (1,5-Cyclooctadiene)(methoxy)iridium dimer, 4,4'-di-tert-buyl-2,2'-bipyridine, bis (pinacolato) diboron, RT, 18 h, 90%. (d) $Pd(PPh_3)_4$, K_2CO_3, THF/H_2O, reflux, 15 h, 88%. (e) Benzoic acid (**11**), DMAP, DCC, CH_2Cl_2, RT, 16 h, 95%. (f) t-butyl bromoacetate, KI, K_2CO_3, MeCN, RT, 12 h, 95%. (g) TFA, CH_2Cl_2, RT, 12 h, 91%. (h) $Pd(PPh_3)_4$, K_2CO_3, THF/H_2O, reflux, 15 h, 81%. (i) *t*-butyl bromoacetate, KI, K_2CO_3, MeCN, RT, 12 h, 68%. (j) TFA, CH_2Cl_2, RT, 12 h, 9%. (k) Iodomethane, KOH, MeCN, RT, 3 h, 72%.

Photophysical property of compounds 1-4. Table 1 summarizes the photophysical properties, i.e., absorption maximum (λ_{max}), molar absorption coefficient (ε), fluorescence 0-0 band ($\lambda_{f0\text{-}0}$), phosphorescence 0-0 bands ($\lambda_{p0\text{-}0}$), quantum yield of fluorescence (Φ_f), fluorescence lifetime (τ), fluorescence rate constant (k_f), and the maximum of intersystem crossing (ISC) rate constant (k_{ISC}) of **1**–**4** in 2-methyltetrahydrofuran (2-MTHF). The absorption and emission spectra in polar solvents are shown in the Figure 8. The relatively large Stokes shift (~200 nm) and solvent effect on the emission maxima of **1**–**4** suggest that the emission is originated from their charge-transfer state.[2,3] Indeed, the fluorescence maxima of **1**-**4** in DMSO were bathochromically shifted by ~90 nm compared to those in 2-MeTHF (Figure S27-31). Accordingly, the charge transfer character renders small energy gaps ($\Delta E_{ST} = E_{S1} - E_{T1}$) of the excited singlet (λ_{f00}) and triplet states (λ_{p00}) of **1**-**4**,[4,5] which would lead to a smooth ISC and causes weak fluorescence (Table 1). The nitro group would also accelerate the ISC process.[6] Because ΔE_{ST} is small (Table 1), thermally activated delayed fluorescence of **3** was observed in the laser flash photolysis (LFP) experiments (Figure S32).[7-10]

Table 1. Photophysical data for **1**–**4**.

Entry		λ_{abs} (/nm)[a]	ε (M^{-1} cm^{-1})[a]	λ_{f0-0} (/nm)[a] (E_{S1} /kJ mol^{-1})	λ_{p0-0} (/nm)[a] (E_{T1} /kJ mol^{-1})	Φ_f %[b]	τ (ns)[a]	k_f (10^9 s^{-1})	k_{isc} (10^9 s^{-1})[c]
1	**1**	381	15,783	453 (264)	540 (222)	7.3	0.9	1.1	14
2	**2**	363	13,334	472 (253)	517 (231)	2.1	0.6	1.7	78
3	**3**	369	16,146	440 (271)	463 (258)	3.1	1.1	0.9	28
4	**4**	374	21,322	452 (265)	493 (242)	2.2	0.7	0.15	66

[a] Absorbance, molar extinction coefficient, fluorescence, and fluorescence lifetime (τ) determined in 2-MeTHF at ~25 °C. Phosphorescence was measured at 77 K in 2-MeTHF. The 0-0 bands were determined from the onset of the emission spectra. E_{S1} is the energy of the singlet excited state. E_{T1} is the energy of the triplet state. [b] Fluorescence quantum yield (Φ_f) determined using 9,10-diphenylanthracene as a reference standard.[11] [c] The maximum of k_{isc} is calculated using $k_{isc} = k_f / \Phi_f - k_f$.

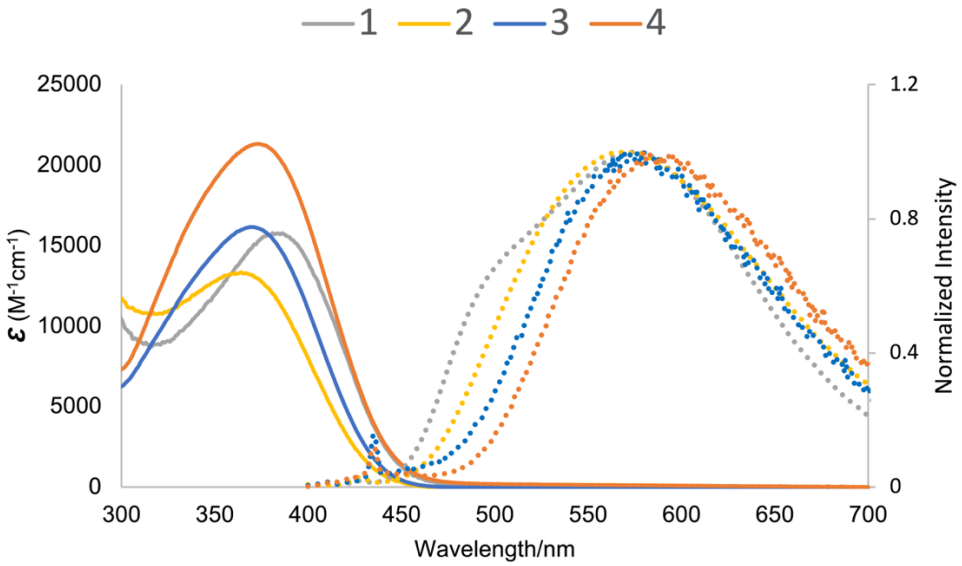

Figure 8. Absorption (solid) and fluorescence emission (dashed) spectra of the NPI derivatives **1**-**4** in 2-MTHF.

Photochemical reaction of compounds 1-4. First, the photochemical reactions of **1** and **2** were carried out in DMSO and MeOH, respectively, at 370 ± 10 nm with a Xe-lamp under air at ~25°C (Table 2), as the solubility of **1** is poor in MeOH. The reaction progress during the irradiation of compound **1** was monitored in DMSO-d_6 by ^{1}H NMR spectroscopy (Figure 9). The formation of benzoic acid (**11**) was confirmed by comparison with the authentic NMR signals of **11**, and the chemical yield of the released benzoic acid was found to be 50% (entry 1 in Table 2, Figure 9). The thermally and photochemically labile nitroso compound derived from the nitrophenyl unit was not isolated.

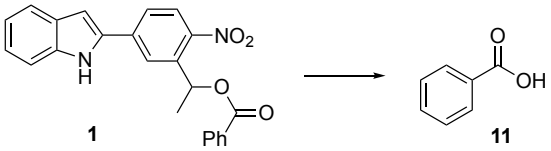

1 11

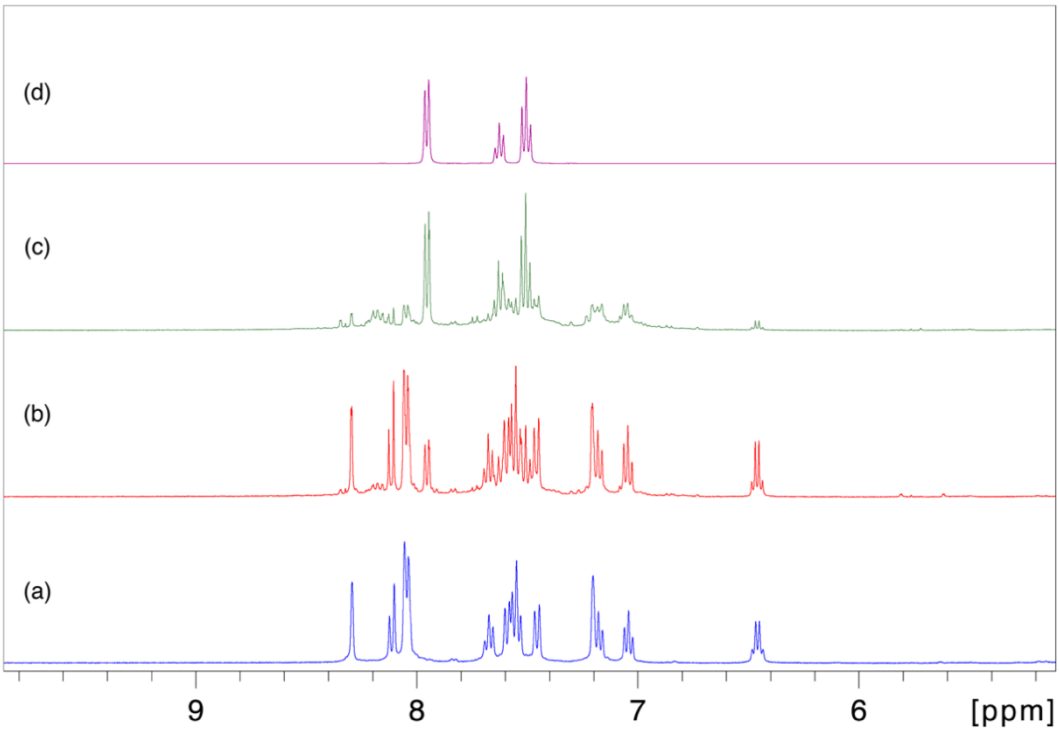

Figure 9. ^{1}H NMR spectroscopy analysis during the photolysis of compound **1** (34.6 mM) at 370 nm in DMSO-d_6 under Air (a) before irradiation; (b) after 6h irradiation; (c) after 12h irradiation; (d) ^{1}H NMR spectrum of benzoic acid in DMSO-d_6, δ 6-9 ppm.

In the photolysis of **2**, benzoic acid (**11**) was isolated in 40% yield (entry 2 in Table 2). Interestingly, during purification of the products, an aldehyde, 1-(5-(1-formyl-1H-indol-2-yl)-2-nitrophenyl)ethyl benzoate (**16**), was isolated in 20% yield (Figure 10, entry 2 in Table 2). Surprisingly, this indicated that the methyl carboxylic acid group (CH_2CO_2H) was transformed to the aldehyde moiety (CHO) during photolysis. The quantum yield of the photochemical decomposition of **2** was determined to be 17% by the ferrioxalate actinometer method (see, SI) and was considerably higher than the yield (2%) of the photochemical decomposition of **1**.

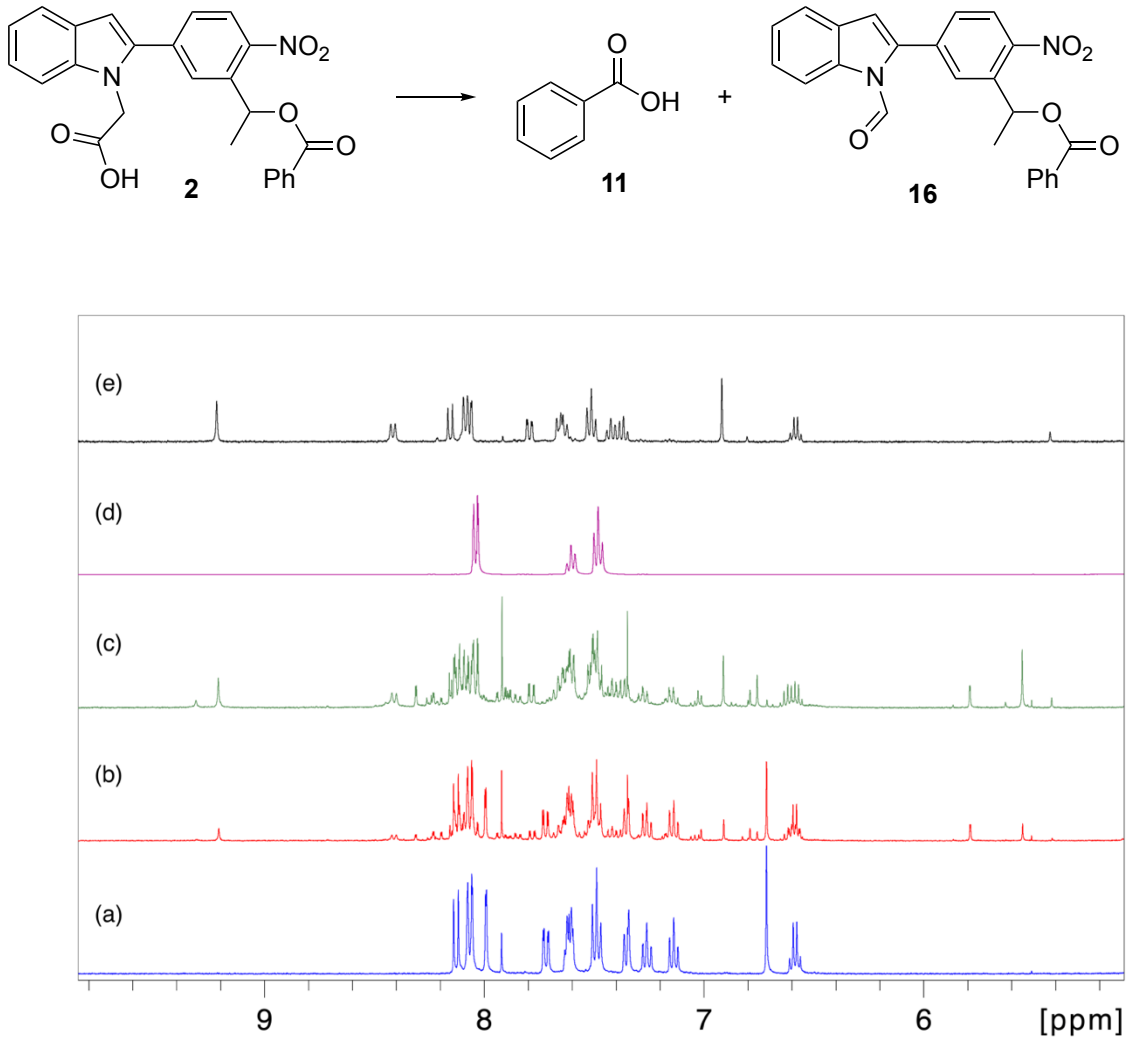

Figure 10. ^{1}H NMR spectroscopy analysis during the photolysis of compound **2** (11.7 mM) at 370 nm in CD_3OD; (a) before irradiation; (b) after 3.5h irradiation; (c) after 9h irradiation; (d) ^{1}H NMR spectrum of benzoic acid in CD_3OD; (e) the ^{1}H NMR spectrum of 1-(5-(1-formyl-1H-indol-2-yl)-2-nitrophenyl)ethyl benzoate **16** in CD_3OD, δ 6-9 ppm.

Table 2. Reaction of **1** and **2** under various conditions

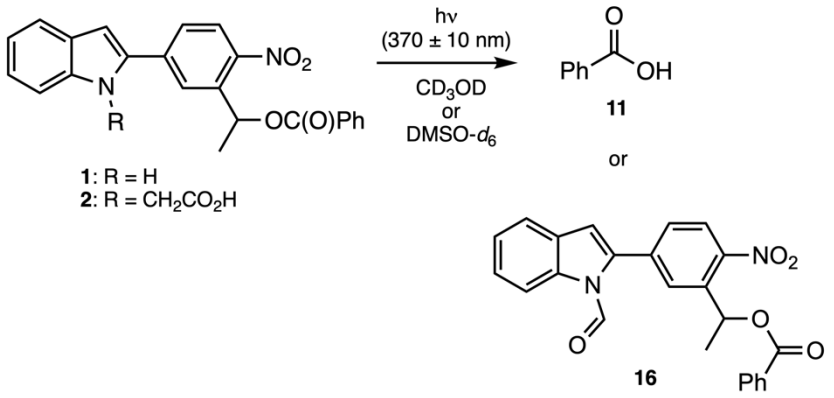

Entry	compound	Solvent	Reaction conditions	benzoic acid (**11**)	aldehyde **16**
1	**1**	DMSO-d_6	hν (370 ± 10 nm) under air, r.t	50%	–
2	**2**	CD_3OD	hν (370 ± 10 nm) under air, r.t	40%	20%
3	**2**	CD_3OD	hν (370 ± 10 nm) under N2	61%	not detected
4	**2**	CD_3OD	under dark for one week, under air, r.t	not detected	not detected
5	**2**	DMSO-d_6	heat at 100 °C for 10 h	not detected	not detected

To understand the mechanism of this novel chemical transformation, I carried out control experiments with **2** under photochemical and thermal conditions (entries 3–5). Under a nitrogen atmosphere, the aldehyde was not detected in the reaction, and benzoic acid alone was isolated in 61% yield (entry 3), indicating that molecular oxygen is required for

the aldehyde formation. In contrast to the photochemical behavior, **2** was stable under dark conditions in MeOH and DMSO at 100°C (entries 4,5). Thus, the formation of the aldehyde required both the irradiation and the presence of molecular oxygen.

Because the benzoate moiety in **2** was intact under the photolysis conditions during the formation of **16**, compound **3** without the benzoate group was synthesized to probe the photochemical behavior. The photochemical reaction of **3** (Figure 11) was carried out under conditions (air and 370 nm irradiation) similar with those used for the photolysis of **2**. Aldehyde **18** was formed in 11% together with **17** and **19** in 43 and 32% yield, respectively. As shown in Figure 11b, hydroperoxide **17** (Figure 11d) was the primary photolysis product from **3**, because a clear NMR signal at 5.9 ppm was observed after 30 min of irradiation. The other two products, aldehyde **18** (Figure 11e) and alcohol **19** (Figure 11f), were detected after 1 h of photolysis (Figure 11c). The total chemical yield of the products isolated from the photolysis of **3** was over 85%. In addition to **17**–**19**, 2-(4-nitrophenyl)-1*H*-indole (**14**), which was not detected in the photolysate, was obtained in a small amount through silica gel column chromatography of the crude products. The formation of **14** is attributed to the decomposition of alcohol **19** owing to the instability of the methanol amine under acidic conditions.[12] Results similar to such a photoreaction were also observed in different solvents such as acetonitrile (Figure S33) and DMSO (34). Because of the poor solubility of **3**, nonpolar solvents could not be used for the photoreaction. Analysis of the products of the photochemical reaction of **3** revealed that molecular oxygen (O_2) was absorbed, and carbon dioxide (CO_2) was eliminated during the photolysis, in a phenomenon reminiscent of “breathing”. In contrast to the high

photoreactivity of **3**, compound **4** was intact after 1 h irradiation at 365 nm in DMSO at rt.

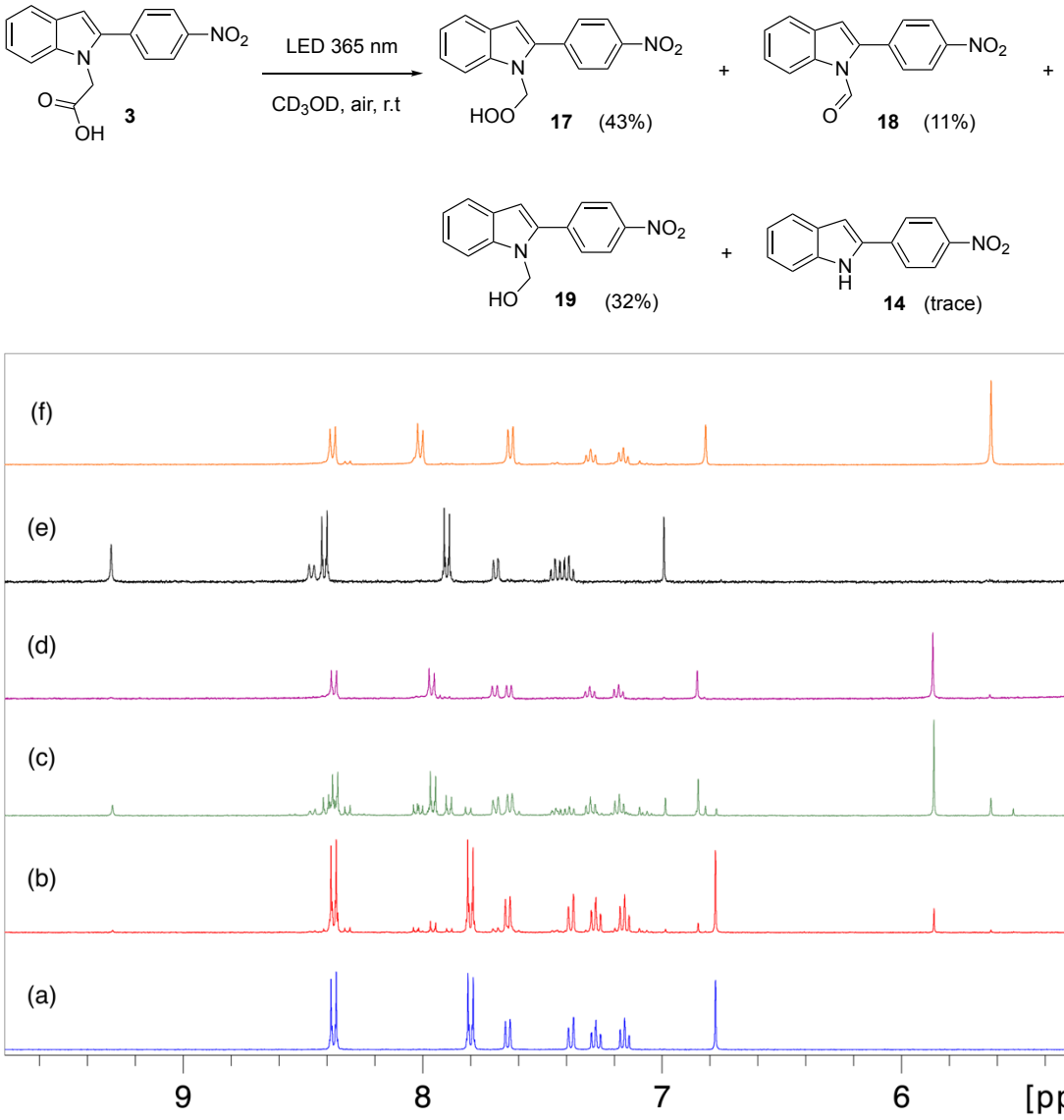

Figure 11. ^{1}H NMR spectroscopy analysis of **3** photolysis (18 mM) at 365 nm in CD_3OD; (a) before irradiation; (b) after 30 min irradiation; (c) after 1 h irradiation; (d) ^{1}H NMR spectrum of 1-(hydroperoxymethyl)-2-(4-nitrophenyl)-1*H*-indole (**17**); (e) 2-(4-nitrophenyl)-1*H*-indole-1-carbaldehyde (**18**); (f) (2-(4-nitrophenyl)-1*H*- indol-1-yl)methanol (**19**) in CD_3OD, δ 6–9 ppm.

Transient absorption spectroscopy of compounds 3 and 4. To gain more insights into the reaction mechanism of the breathing-type phenomenon, I employed transient absorption (TA) spectroscopy at sub-nanosecond and sub-microsecond time scales by using the randomly interleaved pulse train (RIPT) method[13] for the photolysis of **3** and **4**. The TA spectrum observed in the photolysis of **3** looks similar to that obtained in the photolysis of **4** (Figures 12a,c). However, the significant difference was found by the careful analysis of the wavelength-dependence of their time profiles (Figures 12b,d).

Figure 12a shows the TA spectra of **3** in the Ar-saturated acetonitrile solution using a 355 nm laser (25 ps pulse, 80 μJ). The absorption maxima were observed at around 600 and 800 nm immediately after the flash photolysis. However, the maximum shifted to ~820 nm after 700 ns (Figure 12a), indicating at least two transient species are generated in the photolysis of **3**. The decay rate constants at 620 and 820 nm were determined to be 2.0×10^6 s^{-1} (blue, 500 ns at 620 nm) and 1.3×10^6 s^{-1} (orange, 770 ns at 820 nm), respectively (Figure 12b). Thus, a transient at 820 nm decayed more slowly than that at 620 nm. These signals were assigned to paramagnetic species, because significant quenching of the decay rate constants was observed under air ($[O_2] = 1.9 \times 10^{-3}$ M), $k_d = 4.6 \times 10^6$ s^{-1} (grey, 217 ns at 620 nm) and 4.4×10^6 s^{-1} (yellow, 227 ns at 820 nm), respectively (Figure 12b). The decay constants under air were twice larger than those under the degassed conditions, from which the oxygen quenching rate constants at 620 and 820 nm were determined to be 1.37×10^9 and 1.63×10^9 M^{-1} s^{-1}, respectively.

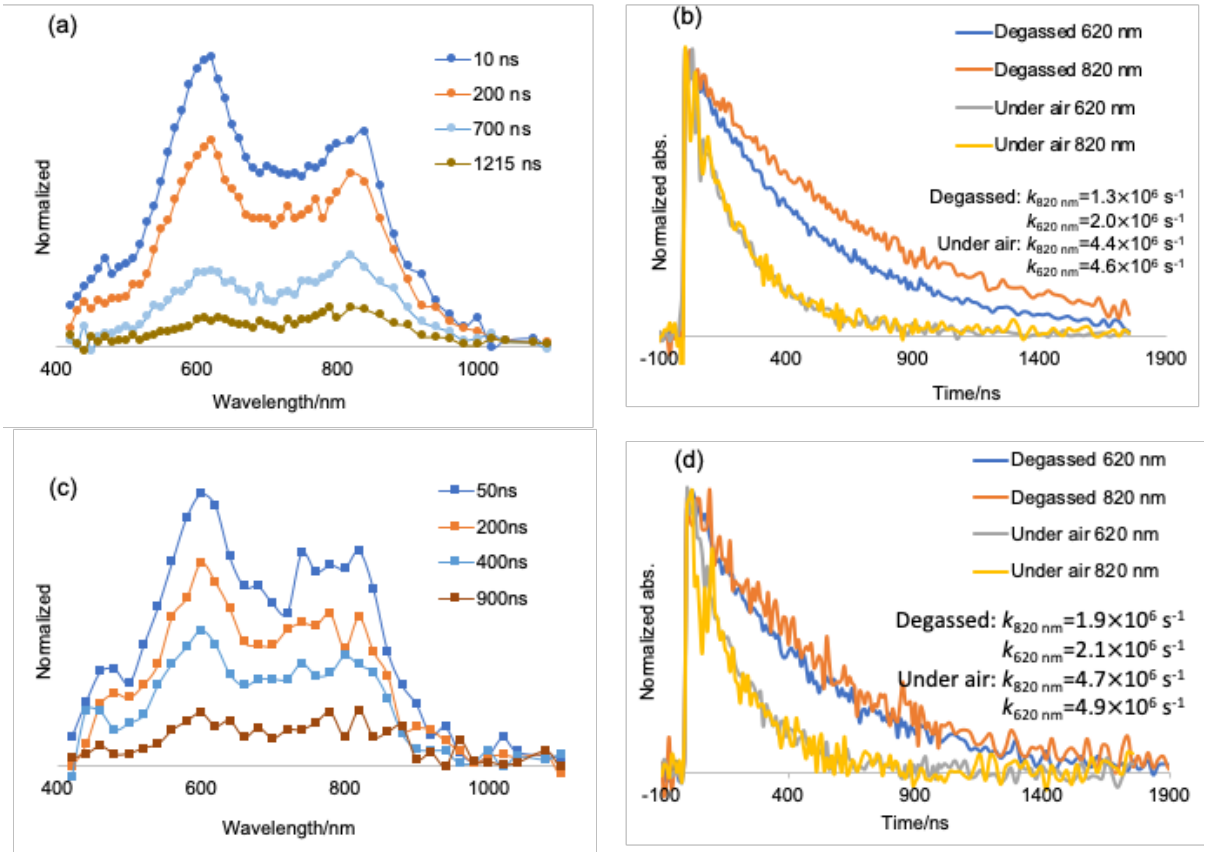

Figure 12. TA spectra observed after the 355 nm laser irradiation (25 ps pulse, 80 μJ). (a) photolysis of **3** (8.5×10^{-5} M) and (c) photolysis of **4** (1.0×10^{-4} M) in acetonitrile under argon (Ar) atmosphere at 298 K. The kinetic traces for (b) **3** and (d) **4** in the nanosecond time region.

A similar TA spectrum with ~600 and ~800 nm bands was observed after the flash photolysis of compound **4** under the similar conditions for **3** (Figure 12c). The corresponding kinetic decay-traces at 620 and 820 nm are summarized in Figure 12d. In contrast to the rate constants observed for the photolysis of **3**, in which dual decay was observed, the fall rate constants at 620 (blue in Figure 12d) and 820 nm (orange in Figure 12d) were both single exponentials and were determined to be ~2.0×10^6 s^{-1} (~500 ns).

Under air conditions ($[O_2]$ = 1.9 x 10^{-3} M), the quenching of the signals was observed to obtain the decay rate constants of 4.9 x 10^6 s^{-1} (204 ns) at 620 nm and 4.7 x 10^6 s^{-1} (213 ns) at 820 nm (Figure 12d), from which the oxygen quenching rate constant was determined to be 1.47 x 10^9 M^{-1} s^{-1}. Thus, the TA spectrum in the photolysis of **4** is also assigned to a paramagnetic species. Since compound **4** was quantitatively recovered after the photolysis, the TA spectrum observed in Figure 12c can be assigned to the T-T absorption of the triplet excited state of **4**.

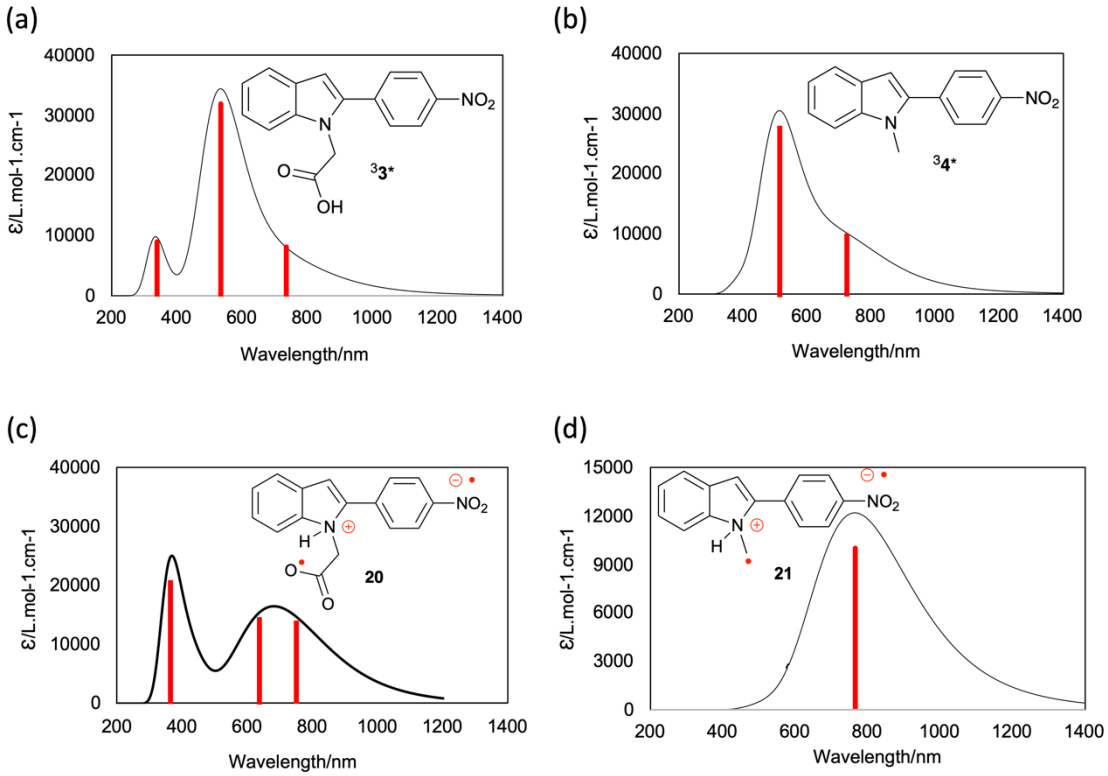

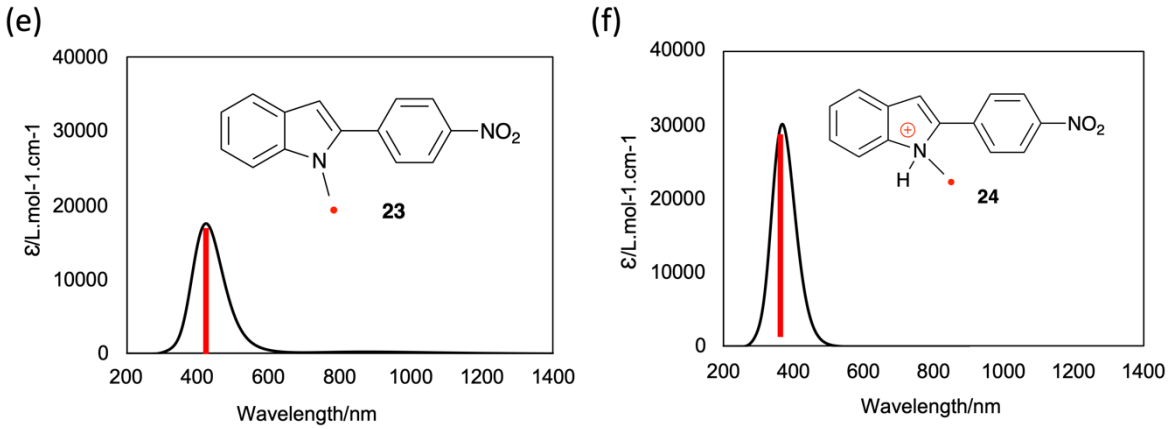

Figure 13. Computationally predicted UV-vis spectrum at TD-B3LYP/6-31G(d) level of theory in acetonitrile: (a) triplet state of **3**, (b) triplet state of **4**, (c) triplet state of **20**, (d) triplet state of **21**, (e) doublet state of **23**, (f) doublet state of **24**. The red-bars are computed values of the electronic transitions at the TD-UB3LYP/6-31G(d) level of theory in acetonitrile using SMD model for the solvation.

Mechanism of photo-induced breathing reaction. A plausible mechanism for the photo-induced breathing-type reaction of **3** is shown in Scheme 2. Compound **3** undergoes excitation to its electronically excited state upon exposure to light and undergoes intramolecular electron transfer (ET) to generate the ammonium intermediate **20**. The electron transfer process would be accelerated by the zwitterionic form **ZI** of the amino acid moiety in **3** because compound **15**, in which the *t*-Bu group protects the carboxylic acid, was intact under the photolysis conditions. The elimination of CO_2 produces the intermediate **21**. The radical intermediate **21** is then trapped by O_2 to afford hydroperoxide **17**. As the photoreactivity of hydroperoxides is well known,[14-16] **17** undergoes O–O bond scission to produce aldehyde **18** and alcohol **19** via **22**. The similar decarboxylation and

generation of alkyl radicals have been reported in intermolecular photo-induced electron transfer reactions of carboxylic acids.[17-26]

As mentioned in the TA spectroscopy analysis of compound **3**, two paramagnetic species were identified at ~600 nm and ~800 nm (Figures 12a,b). One transient species was detected for compound **4** (Figures 12c,d). The transient species is also proposed to be paramagnetic because the very fast oxygen quenching reactions was observed. To understand the results from the time-resolved spectroscopy, first, the UV-vis spectra in acetonitrile were computed for the triplet states of **3** and **4** at the TD-UB3LYP/6-31G(d) level of theory using SMD model for the solvation (Figures 13a,b). The triplet **3** was predicted to possess the electronic transitions mainly at 343 nm (f = 0.15), 526 nm (f = 0.59), and 735 nm (f = 0.18) (Figure 13a), which are fit to the TA spectrum in Figure 13a under Ar just after the laser flash of compound **3**. The transitions at 521 nm (f = 0.53) and 721 nm (f = 0.21) were found for the triplet state of compound **4** (Figure 13b), which reproduces well the TA spectrum observed in the laser flash photolysis of compound **4** (Figure 13c).

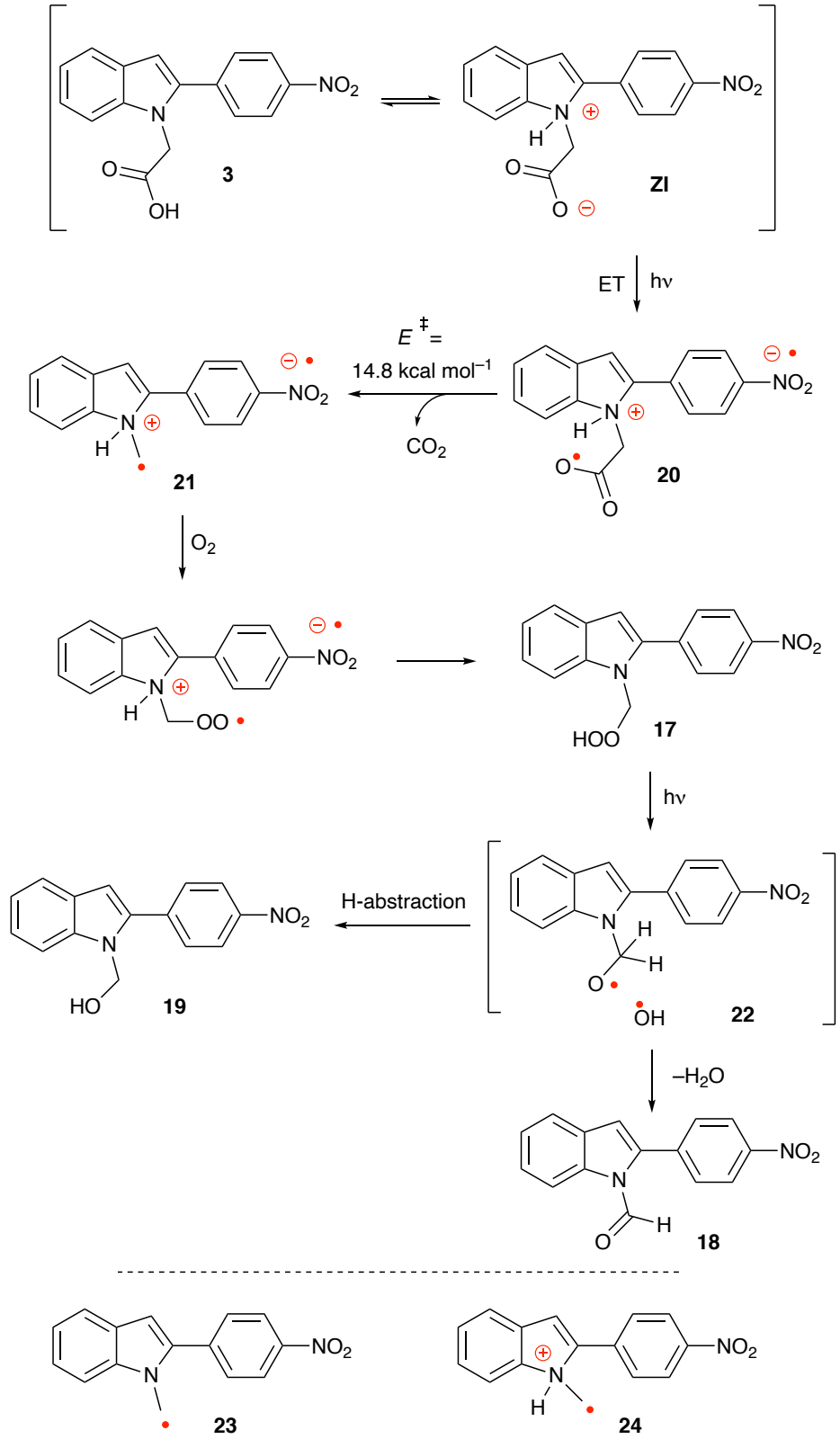

Scheme 2. Proposed mechanism for the breathing reaction in the photolysis of 3.

Next, I conducted quantum chemical computations for the possible paramagnetic intermediates **20**, **21**, **23**, and **24** in the photo-induced breathing reaction of **3**. Those intermediates were found as equilibrium structures in the triplet states for **20**,**21** and doublet states for **23**,**24** at the UB3LYP/6-31G(d) level of theory. The UV-vis spectra in acetonitrile were computed at the TD-B3LYP/6-31G(d) level of theory (Figures 13c-f). Three main excitations, 359 nm (f = 0.32), 621 nm (f = 0.19), 752 nm (f = 0.23), were found in the triplet state of **20** (Figure 13c). One excitation band at 765 nm with f = 0.30 was computed in the visible region for the triplet state of **21** at the same level of theory (Figure 13d). No strong absorption bands were computed in the visible region for compounds **23** (422 nm, f = 0.39, Figure 13e) and **24** (384 nm, f = 0.168, Figure 13f). As judged by the computed absorption spectra, a transient species at ~820 nm in the TA analysis of compound **3** is proposed to be assigned to compound **21**. Because the computed ε value for the triplet state of **3** was 34000 (Figure 13a), which was much larger than that of **21** (ε = 12000, Figure 13d), the T-T absorption spectrum of **3** dominates the TA spectrum in the photolysis compound **3** (Figure 13a). The weak absorption spectrum of **21** is overlapped with that of triplet **3**. Furthermore, the CO_2 elimination process from **20** to **21** was computed at the UB3LYP/6-31G(d) level of theory (Scheme 2). The relatively small energy barrier, 14.8 kcal mol^{-1}, was found to the CO_2 elimination process. Thus, the smooth elimination of CO_2 is expected from intermediate **20**.

2-3. Conclusions

In summary, a new photolabile protecting group, 2-(4-nitrophenyl)-1*H*-indole (NPI), was synthesized in this study. Caged benzoic acids were prepared, and their photochemical reactions were examined. Benzoic acid was released in a moderate chemical yield of 40–60%. In addition to the formation of benzoic acid, an unexpected aldehyde was isolated during product analysis. The identification of the aldehyde product prompted us to investigate the mechanism of the transformation and the excited-state dynamics. Based on the TA spectroscopy and TD-DFT computational results, the intramolecular electron transfer to the excited state was proposed for the initial step of the chemical transformation to generate the zwitterion intermediate. The successive CO_2 elimination and absorption of O_2 (breathing reaction) produced the hydroperoxide together with its photoinduced decomposition products, the alcohol and aldehyde. The photoinduced breathing-type reaction may apply to transition metal free oxidation of amino acids.

2-4. Supporting information

Experimental section

Dry acetonitrile (ACN, Spectro grade), tetrahydrofuran (THF, super dehydrated, stabilizer free), acetone (Spectro grade) and dimethylformamide (DMF, super dehydrated) were purchased from commercial suppliers and stored at least 24 h under nitrogen gas over activated 3 Å molecular sieves (3 Å MS), which were predried at 300 °C for 24 h before use. ^{1}H NMR spectra were obtained at 400 MHz, chemical shifts are reported in ppm, and referenced to the $CHCl_3$ singlet at 7.26 ppm. ^{13}C NMR spectra were obtained at 100 MHz

and referenced to the center peak of the $CDCl_3$ triplet at 77.02 ppm. The abbreviations s, d, t, and m stand for the resonance multiplicities singlet, doublet, triplet, and multiplet, respectively. UV-vis spectra were recorded on a SIMADZU UV-3600 Plus spectrophotometer. Mass-spectrometric data were measured with a mass spectrometric Thermo Fisher Scientific LTQ Orbitrap XL.

1-(5-Bromo-2-nitrophenyl)ethan-1-one (6):[27] A flask was charged with KNO_3 (0.28 g, 2.76 mmol) and was cooled to 0 °C, to which H_2SO_4 (5 mL) was added slowly and mixture allowed to stir for 10 min. 3-bromoacetophenone **5** (0.50 g, 2.51 mmol) was added at 0°C. Temperature was raised to room temperature and stirred for 2 h. Subsequently the reaction mixture was poured into crushed ice. Aqueous layer was extracted with CH_2Cl_2. Organic layer was washed with brine, dried over Na_2SO_4, and purified through silica gel column chromatography to give required product (365.4 mg, 60%). ^{1}H NMR (400 MHz, $CDCl_3$): δ = 8.00 (d, J = 8.7 Hz, 1 H), 7.73 (dd, J = 8.7 and 2.1 Hz, 1H), 7.54 (d, J = 2.1 Hz, 1 H), 2.55 (s, 3H).

1-(5-Bromo-2-nitrophenyl)ethan-1-ol (7):[27] To a stirred solution of 1-(5-bromo-2-nitrophenyl)ethane-1-one **6** (2.7 g, 0.011 mol) in methanol (30 mL) was added $NaBH_4$ (0.45 g, 0.010 mol) in portion at 0 °C. Temperature was slowly raised to room temperature. Stirring was continued for additional 1 h. After completion of the reaction, methanol was removed under reduced pressure. Reaction mixture was partitioned between the ethyl acetate and water, organic layer was combined, washed with brine, dried over Na_2SO_4, filtered and evaporated under reduced pressure to give the required compound which

requires no further purification (2.6 g, 95%). ^{1}H NMR (400 MHz, $CDCl_3$): δ = 8.03 (d, J = 2.1 Hz, 1 H), 7.82 (d, J = 8.7 Hz, 1 H), 7.55 (dd, J = 8.7 and 2.1 Hz, 1 H), 5.47 (m, 1 H), 2.24 (d, J = 3.9Hz, 1 H), 1.57 (d, J = 1.3, 3 H).

2-(4,4,5,5-Tetramethyl-1,3,2-dioxaborolan-2-yl)-1H-indole (9):[28] Inside a glove box, $[Ir(cod)OMe]_2$ (6.4 mg, 0.0096 mmol), dtbpy (5.2 mg, 0.019 mmol), bis(pinacolato)diboron (162.2 mg, 0.64 mmol), the indole (150.1 mg, 1.28 mmol), and THF (2 mL) were added consecutively to a dry vial with a magnetic stir bar. The vial was sealed and heated at 80 °C for 18 h. The reaction mixture was cooled to room temperature, concentrated and purified by column chromatography to give the product. **9** (278.5 mg, 89.5%), EtOAc : hexane=1 : 9 (Rf = 0.3). ^{1}H NMR (400 MHz, $CDCl_3$): δ = 8.69 (br, 1 H), 7.73 (dd, J = 8.1 and 0.8 Hz, 1 H), 7.43 (dd, J = 8.4 and 1.2 Hz, 1 H), 7.29-7.25 (m, 1 H), 7.17-7.14 (m, 2 H), 1.42 (s, 12 H).

1-(5-(1H-Indol-2-yl)-2-nitrophenyl)ethan-1-ol (10): To a solution of compound **9** (50.1 mg, 0.21 mmol) and **7** (50.0 mg, 0.20 mmol), K_2CO_3 (37.1 mg, 0.22 mmol) in THF/H_2O (1:1) (2 mL) was added $Pd(PPh_3)_4$ (11.5 mg, 0.01 mmol) under N_2. The mixture was heated and reflux for 15 h. The reaction mixture was quenched with saturated NH_4Cl solution (6 mL) and extracted with ethyl acetate. The combined extracts were washed with water, dried (Na_2SO_4), and evaporated under reduced pressure. Flash chromatography on silica gel using hexane/ethyl acetate afforded compound **10**. (52.4 mg, 88.4%) (EtOAc:Hexane = 1 : 5, R_f = 0.24, then change ratio to 1 : 2) ^{1}H NMR (400 MHz, $CDCl_3$): δ = 8.57 (broad, 1 H), 8.15 (d, J = 1.9 Hz, 1 H), 8.08 (d, J = 8.6 Hz,1 H), 7.71 (dd, J = 9 and 1.9 Hz, 1 H), 7.68 (d, J = 8.4 Hz,1 H), 7.46 (d, J = 8.1 Hz, 1 H), 7.28 (t, J = 3.9 Hz,1

H), 7.18 (t, *J* = 8.1 Hz,1 H), 7.06 (d, *J* = 1.4 Hz,1 H), 5.63 (q, *J* = 6.3 Hz, 1 H), 2.36 (broad, 1 H), 1.66 (d, *J* = 6.2 Hz, 3 H). ^{13}C NMR (100 MHz, DMSO-d_6): δ 145.99, 143.94, 138.32, 137.48, 135.99, 128.88, 125.42, 124.38, 124.02, 123.24, 121.14, 120.29, 112.16, 102.16, 64.45, 25.47. mp 175-176°C; HRMS-APCI: calcd for $C_{16}H_{16}O_3N_2$: 283.10772, found 283.10767 [M + H]+.

1-(5-(1H-Indol-2-yl)-2-nitrophenyl)ethyl benzoate (1): Benzoic acid (13.2 mg, 0.11 mmol), DMAP (1.3 mg, 0.01 mmol) and compound **10** (28.3 mg, 0.1 mmol) in anhydrous dichloromethane (5 mL) was stirred for 10 min. To the reaction mixture DCC (20.6 mg, 0.1 mmol) was added and stirred for 16 h at room temperature. Subsequently water was added into reaction mixture and compound was extracted with dichloromethane. The organic layer was washed with sodium bicarbonate solution and water. Dried with anhydrous sodium sulfate and evaporated under reduced pressure. Flash chromatography on silica gel afforded compound **1** (38.4 mg, 95%). Hexane : EtOAc = 5 : 1, R_f = 0.5. ^{1}H NMR (400 MHz, $CDCl_3$): δ = 8.44 (broad, 1 H), 8.12 (q, *J* = 5.44 Hz, 3 H), 7.97 (d, *J* = 1.92 Hz, 1 H), 7.61-7.69 (m, 3 H), 7.51 (t, *J* = 7.8 Hz, 2 H), 7.42 (d, *J* = 7.8 Hz, 1 H), 7.25 (dd, *J* = 8.16 and 0.96Hz, 1 H), 7.16 (t, *J* = 7.16 Hz, 1 H), 6.96 (d, *J* = 1.2 Hz, 1 H), 6.7 (q, *J* = 6.52 Hz, 1 H), 1.87 (d, *J* = 6.48 Hz, 3 H). ^{13}C NMR (100 MHz, DMSO-d_6): δ 165.59, 146.32, 138.42, 138.29, 138, 135.46, 134.11, 129.79, 129.29, 128.8, 125.87, 125.47, 123.71, 123.5, 121.26, 120.4, 112.16, 102.72, 68.79, 21.72. mp 238-239°C; HRMS-ESI: calcd for $C_{23}H_{18}O_4N_2Na$: 409.11588, found 409.11624 $[M + Na]^+$.

1-(5-(1-(2-(tert-Butoxy)-2-oxoethyl)-1H-indol-2-yl)-2-nitrophenyl)ethyl benzoate (12): Compound **1** (39 mg, 0.1 mmol), K_2CO_3 (27.6 mg, 0.2 mmol) in 3 mL MeCN was stirred

for 30min at 60 ℃ oil bath. To the mixture *tert*-butyl 2-bromoacetate (39 mg, 0.2 mmol) and KI (0.87 mg, 0.005 mmol) was added and stirred 12 h. Reaction stopped and poured mixture into water extracted with EtOAc three times, washed with brine, dried with $NaSO_4$, solvent removed to get crude product. Flash chromatography on silica gel afforded pure product (54.5 mg, 95%), EtOAc : Hexane= 1 : 4. R_f = 0.47. ^{1}HNMR (400 MHz, $CDCl_3$): δ = 8.10 (d, *J* = 8.4 Hz, 1H), 8.07 (d, *J* = 7.1 Hz, 2H), 7.91(d, *J* = 1.8 Hz, 1H), 7.66 (d, *J* = 7.9 Hz, 1H), 7.57(t, *J* = 9.5 Hz, 2H), 7.44 (t, *J* = 7.8 Hz, 2H), 7.26 (t, *J* = 9.9 Hz, 1H), 7.18 (t, *J* = 7.8 Hz, 1H), 6.7 (s, 1H), 6.67 (q, *J* = 6.4 Hz, 1H), 4.67 (s, 2H), 1.86 (d, *J* = 6.7 Hz, 3H). 13C NMR (100 MHz, DMSO-d_6): δ 167.88, 165.53, 146.88, 139.06, 139.05, 138.82, 138.11, 133.3, 129.73, 129.69, 128.69, 128.51, 128.01, 127.74, 125.08, 123.32, 121.24, 120.98, 109.67, 104.83, 82.85, 68.65, 68.18, 47.11, 27.92, 22.23. mp 57-59°C; HRMS-ESI: calcd for $C_{29}H_{29}O_6N_2$: 501.20201, found 501.20187 $[M + H]^+$.

2-(2-(3-(1-(Benzoyloxy)ethyl)-4-nitrophenyl)-1H-indol-1-yl)acetic acid (2): Dissolved **12** (54.5 mg, 0.1mmol) in 6 mL DCM with stirring, 2 mL TFA was added dropwise and stirred 12 h. Solvent removed to get crude product, flash chromatography on silica gel afforded pure product (40.8 mg, 91%), first EtOAc : Hexane= 1 : 3 (R_f = 0); then change to EtOAc : MeOH: 5 : 1 (Rf = 0.43). ^{1}H NMR (400 MHz, $CDCl_3$): δ = 8.09 (d, *J* = 8.5 Hz, 1H), 8.05 (dd, *J* = 7.1 and 1.2 Hz, 2H), 7.8 (d, *J* = 1.5 Hz, 1H), 7.6 (d, *J* = 7.8 Hz, 1H), 7.5 (t, *J* = 7.5 Hz, 2H), 7.4 (t, *J* = 7.9 Hz, 2H), 7.2-7.3 (m, 3H), 6.7 (s, 1H), 6.6 (q, *J* = 6.6 Hz, 1H), 4.7 (s, 2H), 1.8 (d, *J* = 6.6 Hz, 3H). ^{13}C NMR (100 MHz, $CDCl_3$): δ 173.0363, 165.58, 146.92, 138.91, 138.85, 138.79, 137.68, 133.38, 129.65, 128.69, 128.53, 127.99, 127.59, 125.31, 123.53, 121.35, 121.27, 109.48, 105.12, 77.21, 68.83, 45.77, 22.11. mp

97-100°C; HRMS-ESI: calcd for $C_{25}H_{20}O_6N_2Na$: 467.12136, found 467.12140 $[M + Na]^+$.

2-(4-Nitrophenyl)-1H-indole (14):[29] To a solution of compound **13** (1.0 g, 4.14 mmol) and **9** (1.0 g, 4.12 mmol), K_2CO_3 (74.1 mg, 0.44 mmol) in THF/H_2O (1:1) (10 mL) was added $Pd(PPh_3)_4$ (230.2 mg, 0.2 mmol) under N_2. The mixture was heated and reflux for 15 h. The reaction mixture was quenched with saturated NH_4Cl solution and extracted with ethyl acetate. The combined extracts were washed with water, dried (Na_2SO_4), and evaporated under reduced pressure. Flash chromatography on silica gel using hexane/ethyl acetate afforded compound **14**. (0.80 g, 81%). ^1H NMR (400 MHz, $CDCl_3$): δ = 8.48 (s, 1H), 8.23 (d, J = 9.1 Hz, 2H), 7.83 (d, J = 9.1 Hz, 2H), 7.69 (t, J = 7.4 Hz, 1H), 7.45 (t, J = 7.4 Hz, 1H), 7.35 (mult, 1H), 7.3 (mult, 1H), 6.96 (1H, s).

***tert*-Butyl 2-(2-(4-nitrophenyl)-1H-indol-1-yl)acetate (15)**: Compound **14** (0.80 g, 3.34 mmol), K_2CO_3 (0.92 g, 6.68 mmol) in 30 mL ACN was stirred for 30min at 60 ℃ oil bath. To the mixture *tert*-butyl 2-bromoacetate (1.3 g, 6.68 mmol) and KI (29 mg, 0.167 mmol) was added and stirred 12h. Reaction stopped and poured mixture into water extracted with EtOAc three times, washed with brine, dried with NaSO4, solvent removed to get crude product. Flash chromatography on silica gel afforded pure product (799.5 mg, 68%). ^1H NMR (400 MHz, $CDCl_3$): δ = 8.35 (d, J = 9.1 Hz, 2H), 7.72 (mult, 2H), 7.31 (mult, 2H), 7.21 (mult, 1H), 6.75 (s, 1H), 4.73 (s, 2H), 1.45 (s, 9H). ^{13}C NMR (100 MHz, $CDCl_3$): δ 167.84, 147.27, 139.20, 139.09, 139.01, 129.62, 128.06, 123.99, 123.40, 121.29, 121.00, 109.72, 105.04, 82.93, 47.18, 27.97. mp 118-120°C; HRMS-ESI: calcd for $C_{20}H_{20}O_4N_2Na$: 375.13208, found 375.13156 $[M + Na]^+$.

2-(2-(4-Nitrophenyl)-1H-indol-1-yl)acetic acid (3): Dissolved tert-butyl

2-(2-(4-nitrophenyl)-1H-indol-1-yl)acetate (536.4 mg, 1.8 mmol) in 20 mL DCM with stirring, 1 mL TFA was added dropwise and stirred 12 h. Solvent removed to get crude product, purified with GPC to get pure product (46.2 mg, 8.7%). ^{1}H NMR (400 MHz, CD_3OD): δ = 8.36 (d, J = 8.3 Hz, 2H), 7.8 (d, J = 8.4 Hz, 2H), 7.64 (d, J = 7.9 Hz, 1H), 7.38 (d, J = 8.2 Hz, 1H), 7.27 (t, J = 7.4 Hz, 1H), 7.15 (t, J = 7.3 Hz, 1H), 6.77 (s, 1H), 4.94 (s, 2H); ^{13}C NMR (100 MHz, CD_3OD): δ 171.10, 147.27, 139.30, 139.04, 138.95, 133.01, 129.45, 128.13, 123.49, 122.69, 122.35, 120.60, 120.30, 109.52, 104.30, 31.50. mp 172-174°C; HRMS-ESI: calcd for $C_{16}H_{11}O_4N_2$: 295.07188, found 295.07196 [M - H]$^-$.

1-Methyl-2-(4-nitrophenyl)-1H-indole (4): Dissolved 1-methyl-2(4-nitrophenyl) -1H-indole (374.4 mg, 1.57 mmol), KOH (95.2 mg, 1.7 mmol) in 20 mL ACN and stirred for 30min at 60 ℃ oil bath. Methyl iodide (392.1 mg, 2.78 mmol) was added into ACN solution and stirred 3 h. Stopped reaction and poured mixture into water, extracted with EtOAc three times, washed with brine, dried with $NaSO_4$, solvent removed to get crude product. Flash chromatography on silica gel afforded pure product (283.2 mg, 72%).[73] ^{1}H NMR (400 MHz, $CDCl_3$): δ = 8.36 (d, J = 8.8 Hz, 2H), 7.71 (t, J = 9.2 Hz, 3H), 7.43 (d, J = 4.0 Hz, 1H), 7.34 (t, J = 7.6 Hz, 1H), 7.21 (t, J = 7.6 Hz, 1H), 6.74 (s, 1H), 3.83 (s, 3H).

1H and 13C Spectra of Compounds

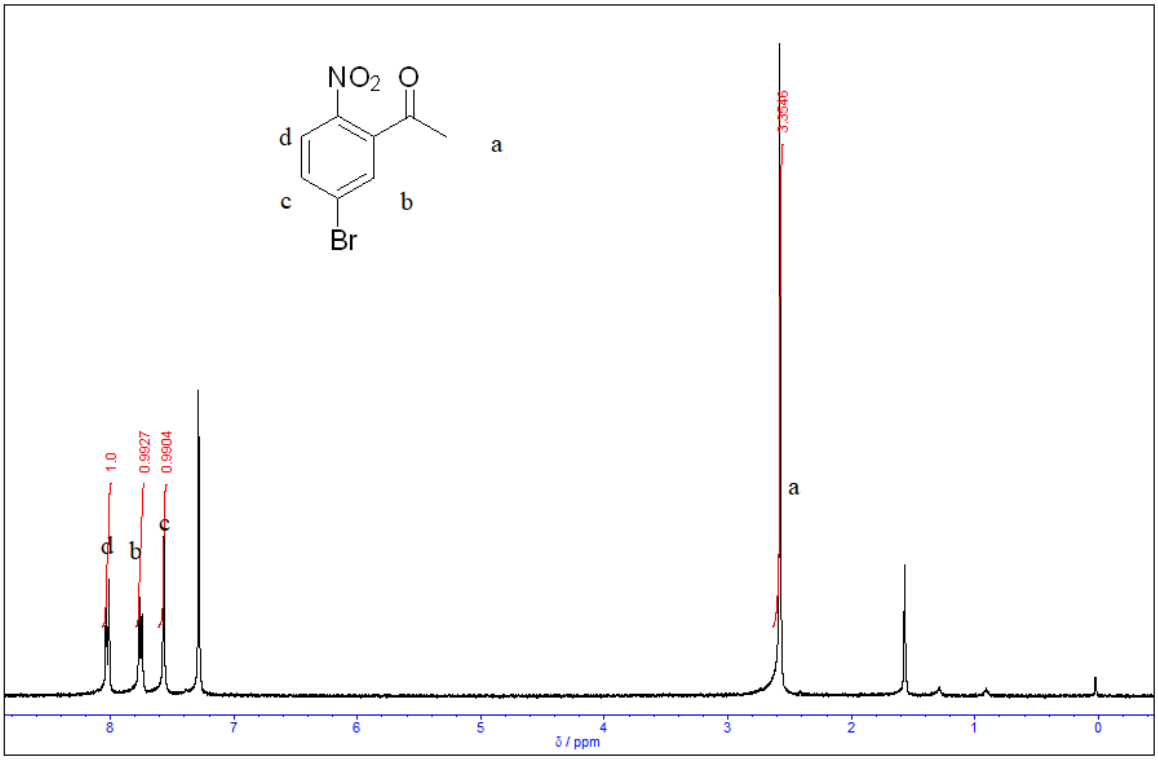

Figure S1: ^{1}H NMR spectrum of compound 6 (400 MHz, $CDCl_3$)

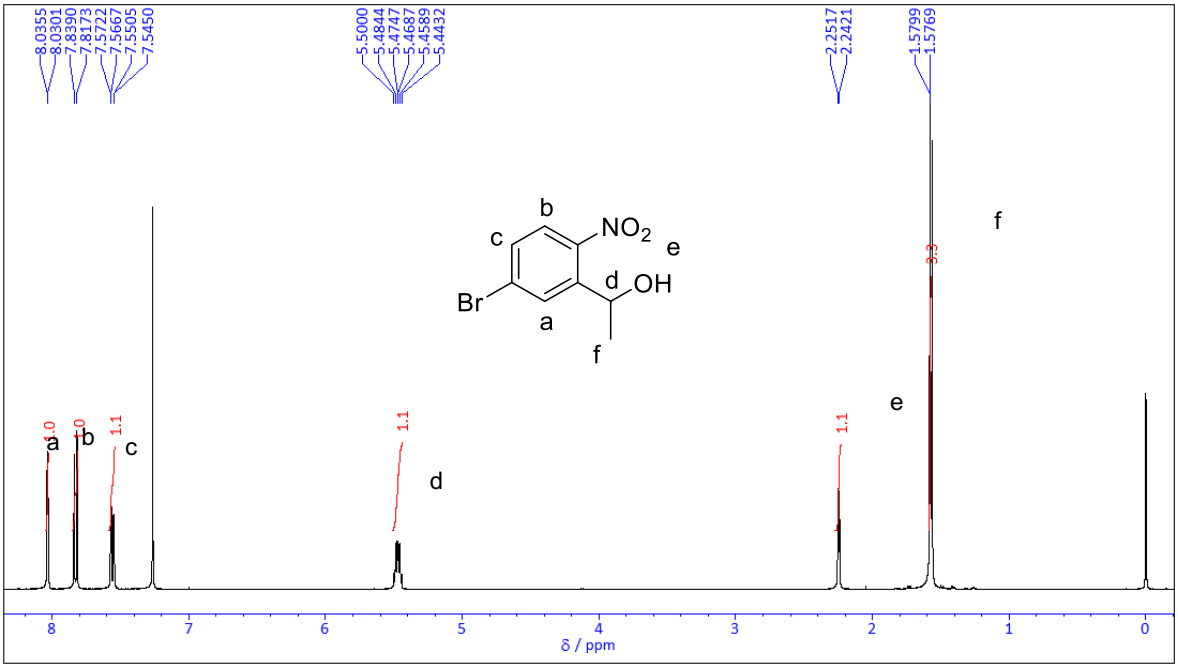

Figure S2: ^{1}H NMR spectrum of compound 7 (400 MHz, $CDCl_3$)

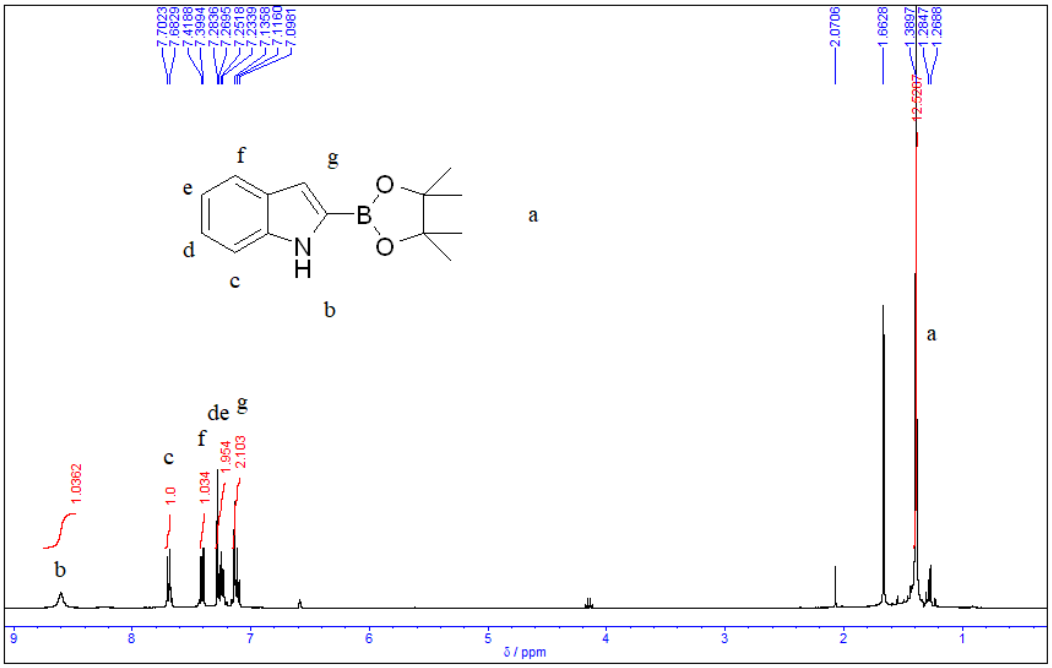

Figure S3: ^{1}H NMR spectrum of compound 9 (400 MHz, $CDCl_3$)

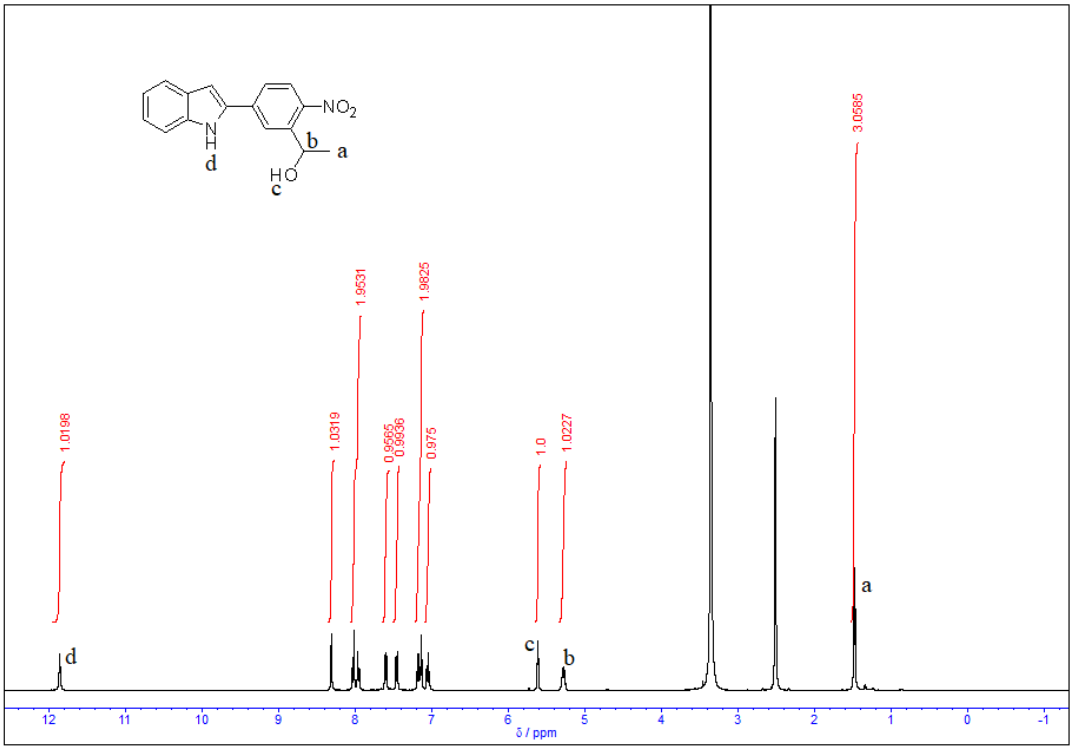

Figure S4: ^{1}H NMR spectrum of compound 10 (400 MHz, DMSO-d_6)

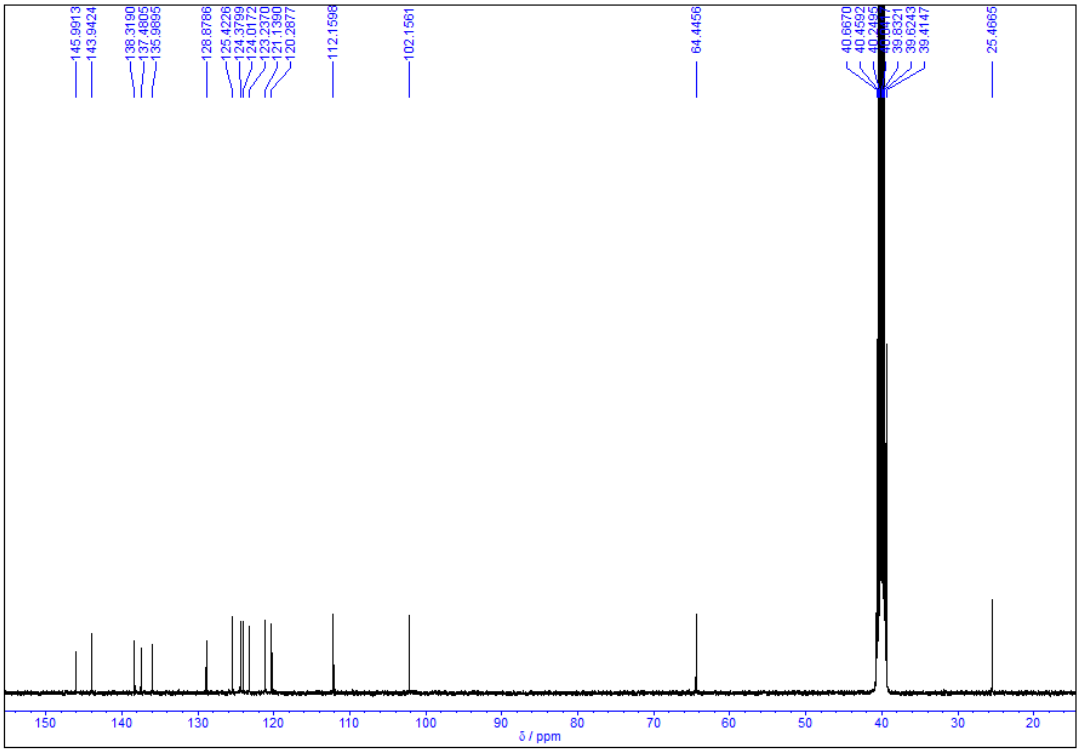

Figure S5: ^{13}C NMR spectrum of compound 10 (100 MHz, DMSO-d_6)

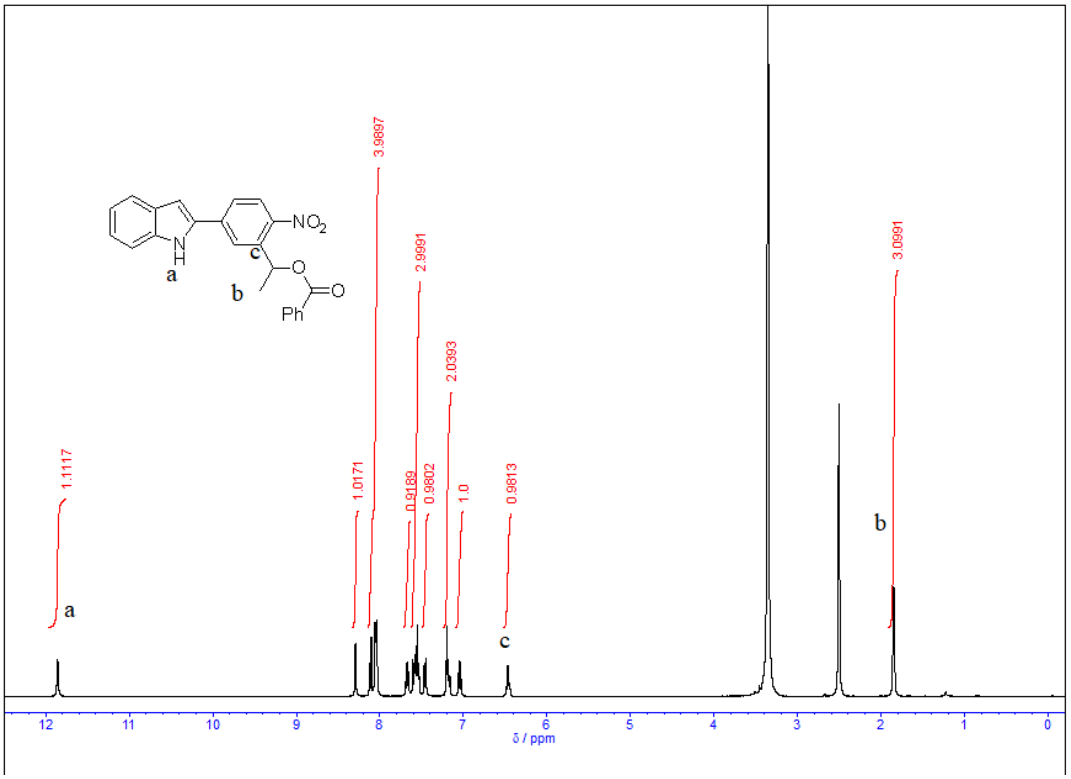

Figure S6: ^{1}H NMR spectrum of compound 1 (400 MHz, DMSO-d_6)

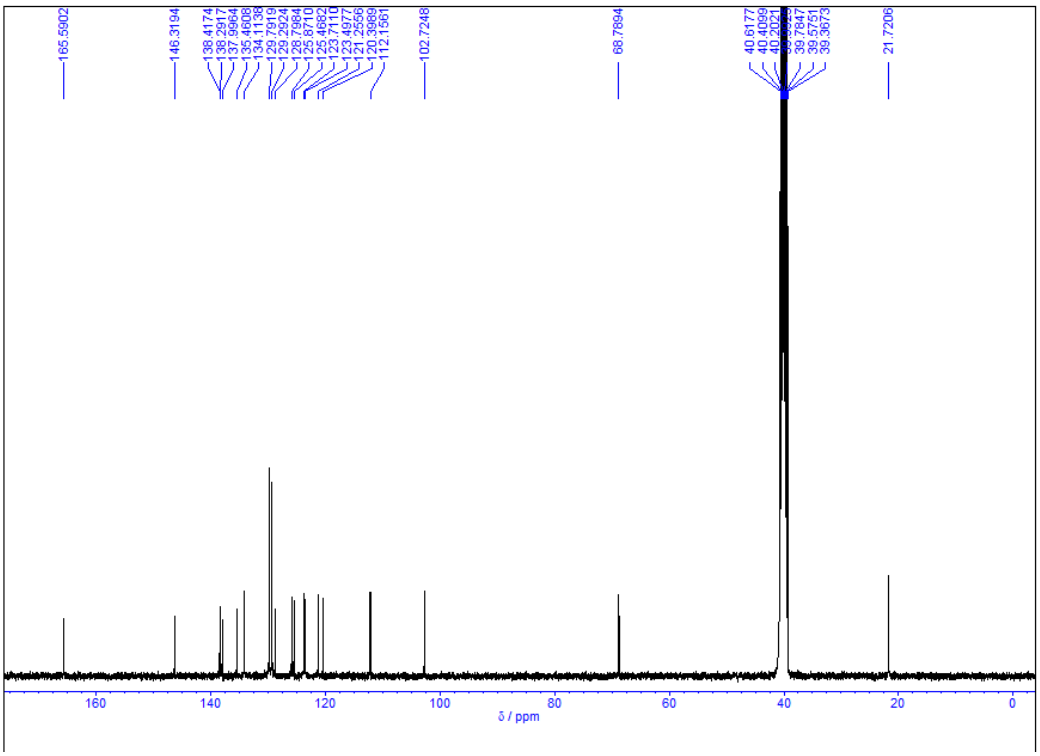

Figure S7: ^{13}C NMR spectrum of compound 1 (100 MHz, DMSO-d_6)

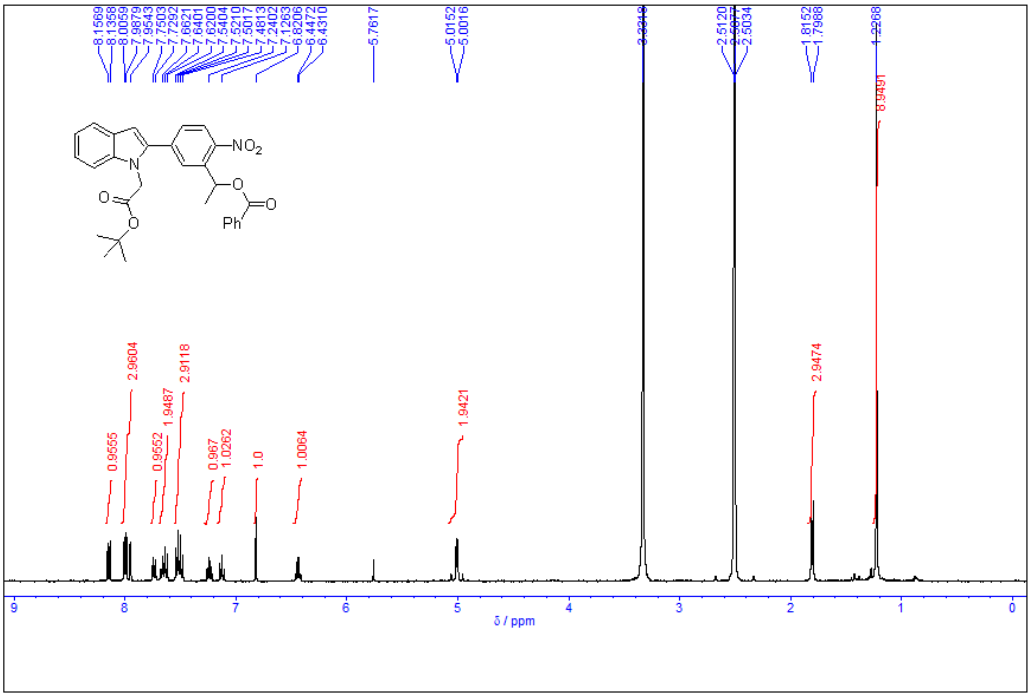

Figure S8: ^{1}H NMR spectrum of compound 12 (400 MHz, DMSO-d_6)

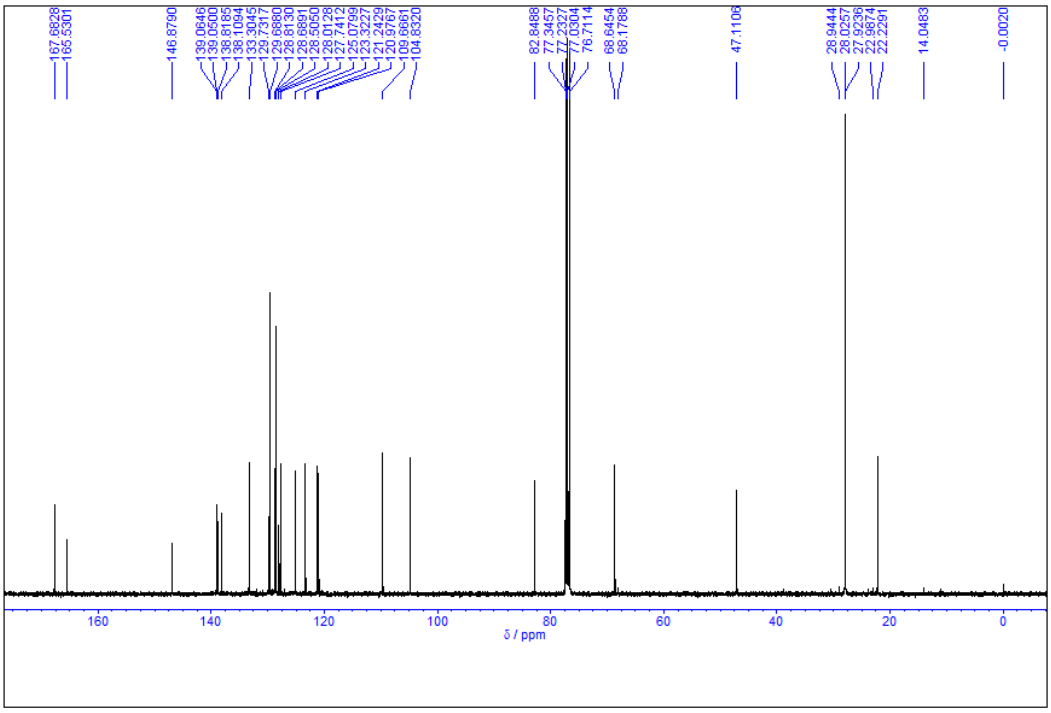

Figure S9: ^{13}C NMR spectrum of compound 12 (100 MHz, $CDCl_3$)

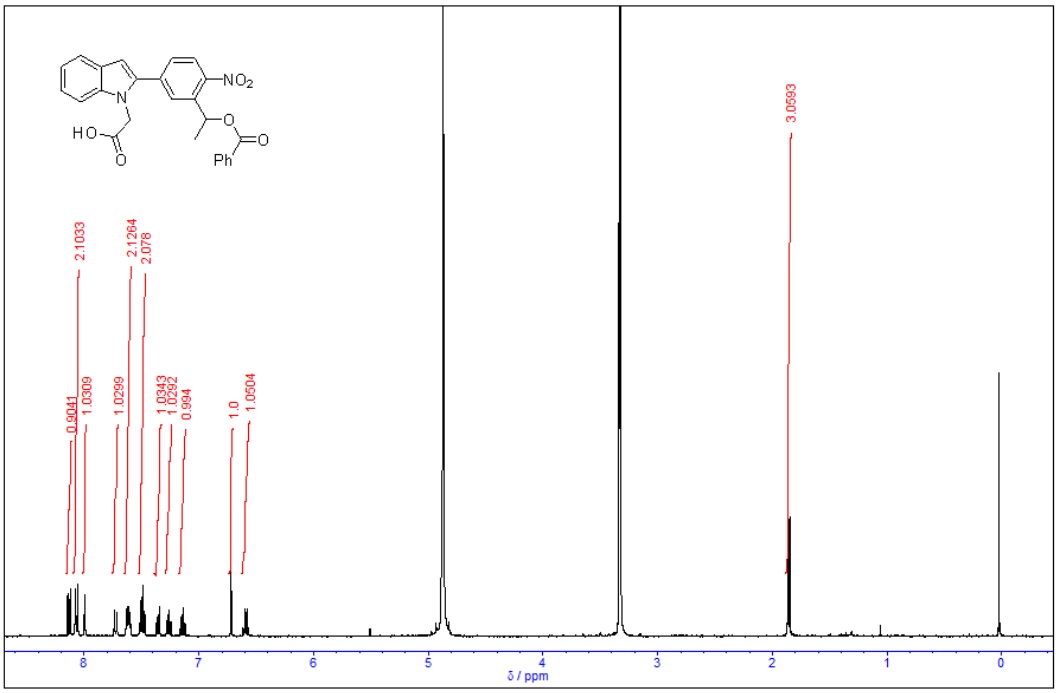

Figure S10: ^{1}H NMR spectrum of compound 2 (400 MHz, CD_3OD)

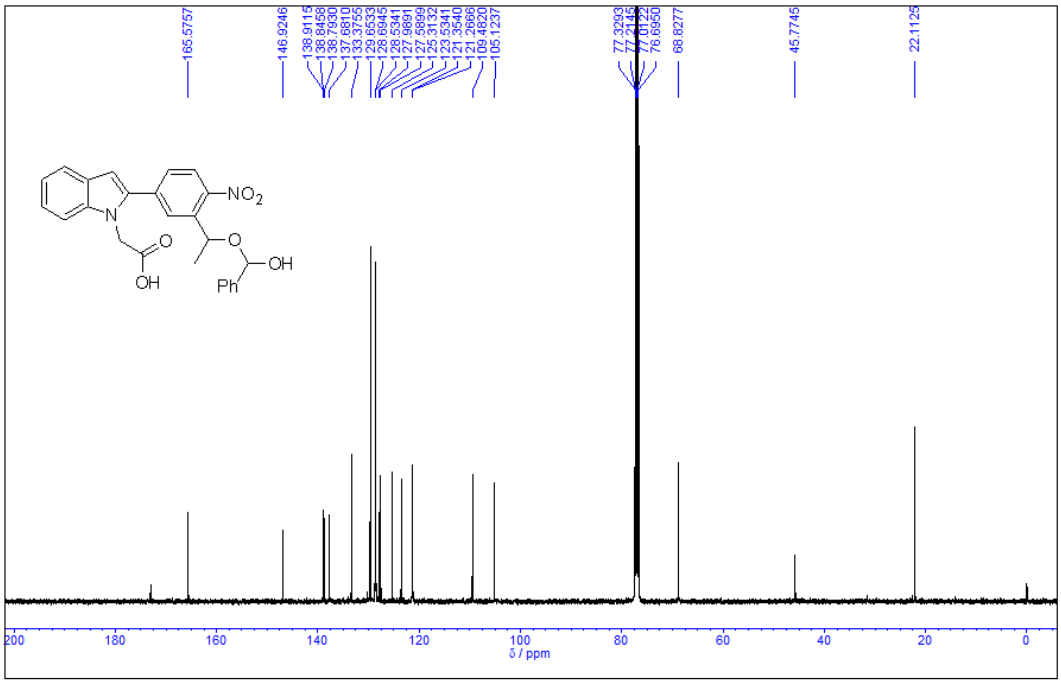

Figure S11: ^{13}C NMR spectrum of compound 2 (100 MHz, $CDCl_3$)

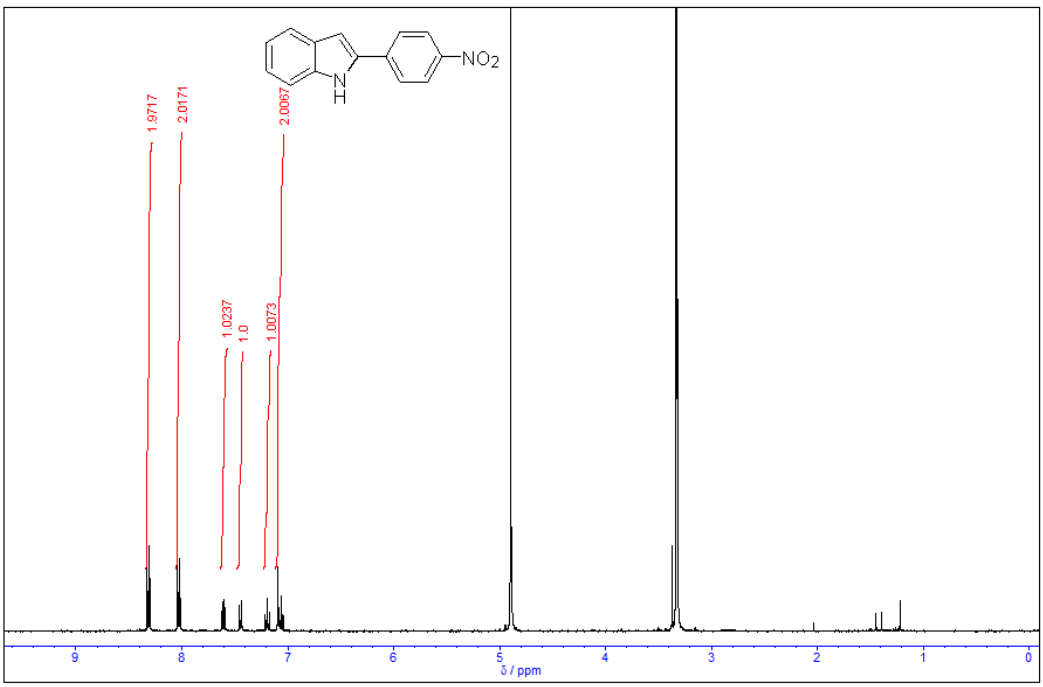

Figure S12: ^{1}H NMR spectrum of compound 14 (400 MHz, CD_3OD)

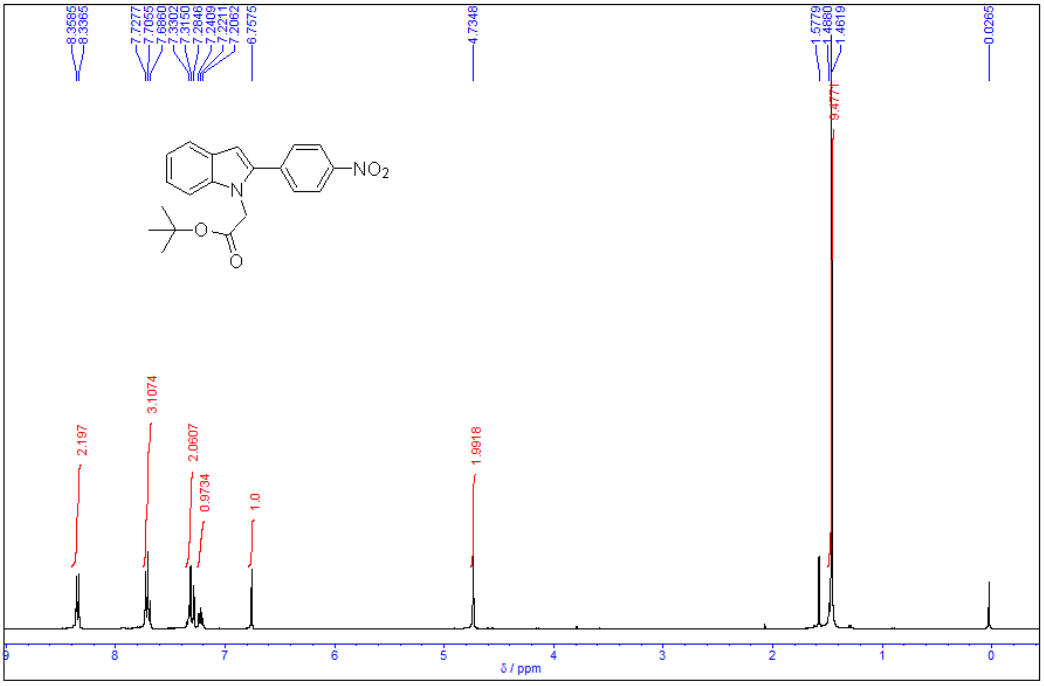

Figure S13: ^{1}H NMR spectrum of compound 15 (400 MHz, $CDCl_3$)

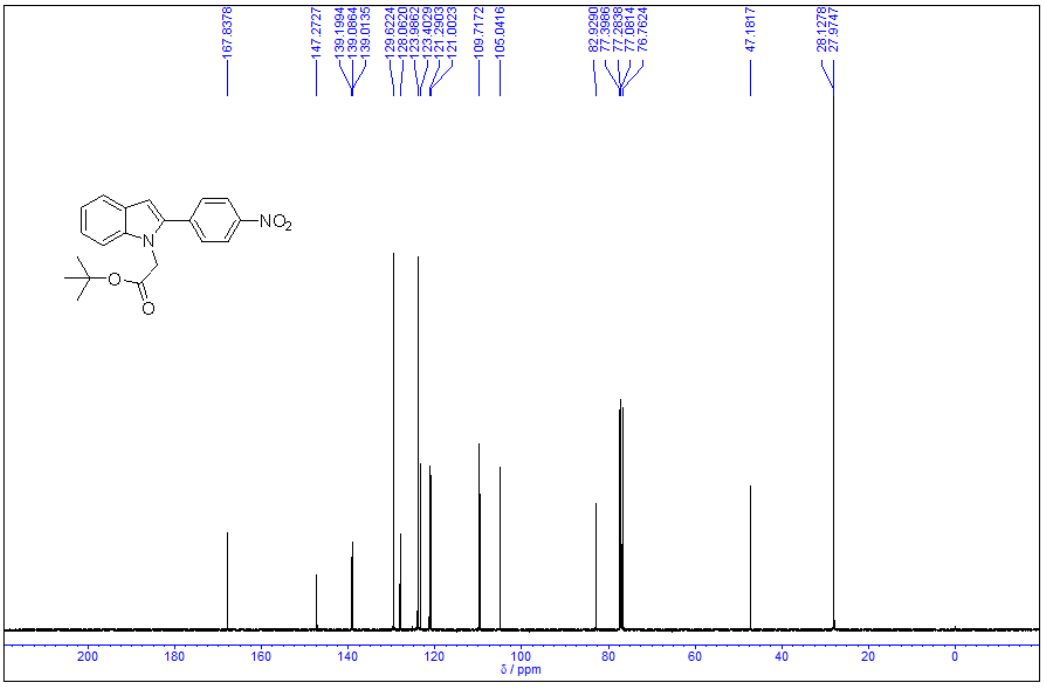

Figure S14: ^{13}C NMR spectrum of compound 15 (100 MHz, $CDCl_3$)

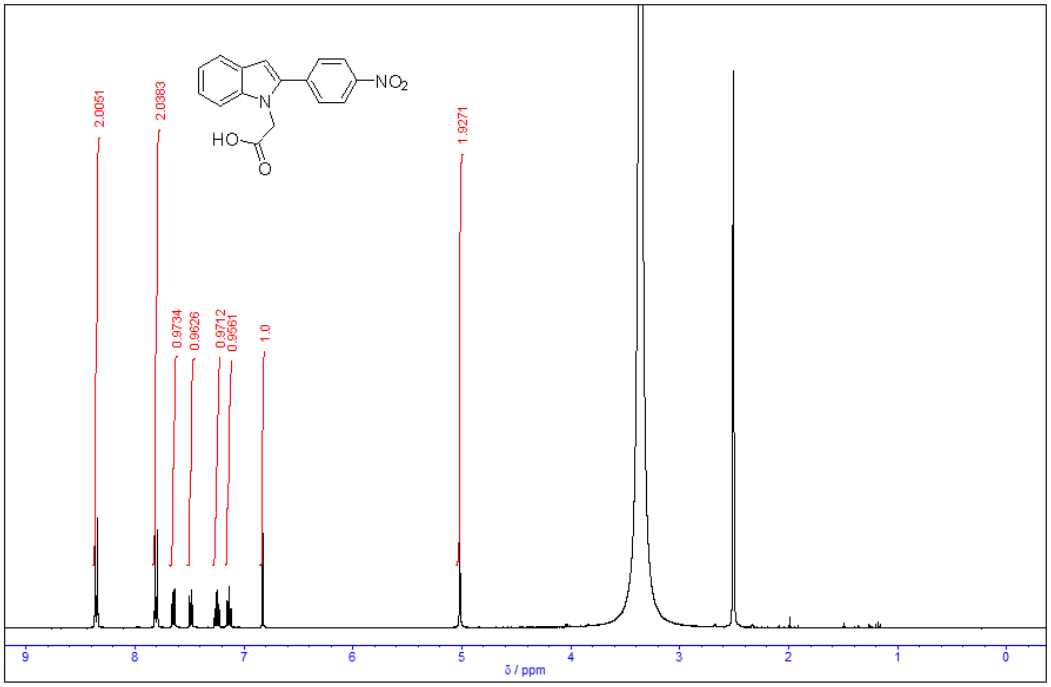

Figure S15: ^{1}H NMR spectrum of compound 3 (400 MHz, DMSO-d_6)

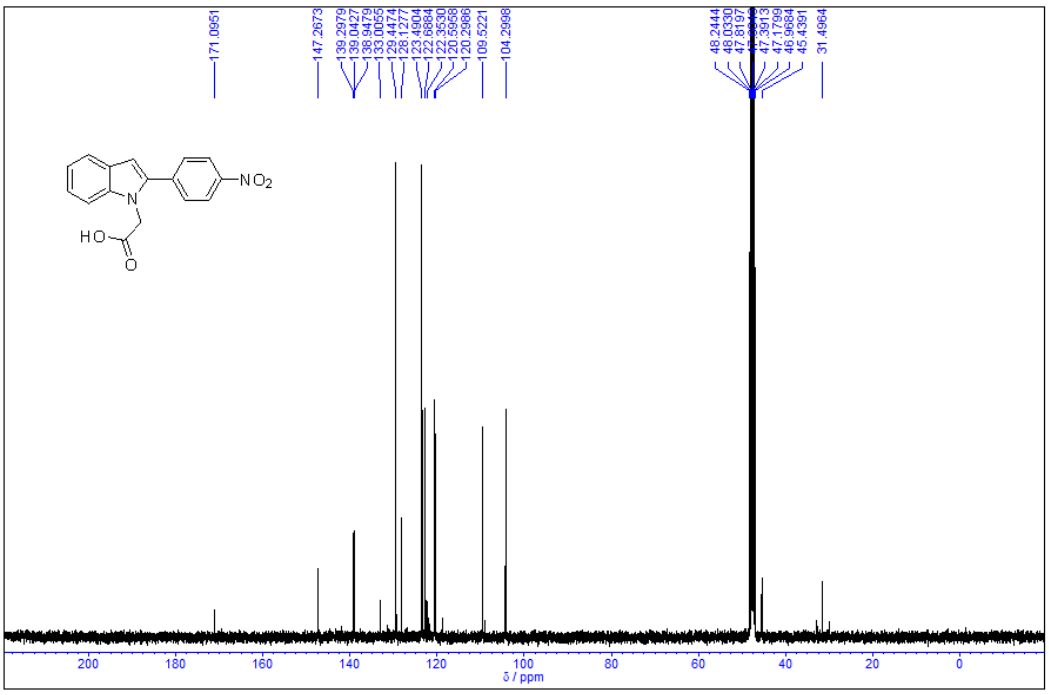

Figure S16: ^{13}C NMR spectrum of compound 3 (100 MHz, CD_3OD)

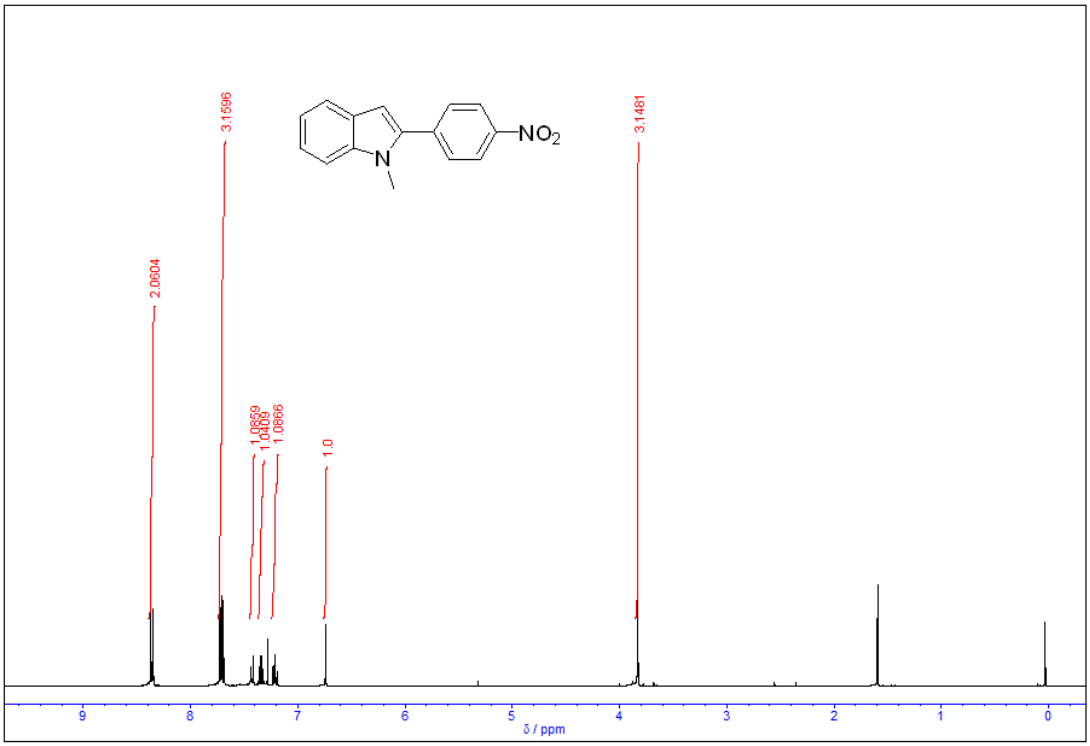

Figure S17: ^{1}H NMR spectrum of compound 4 (400 MHz, $CDCl_3$)

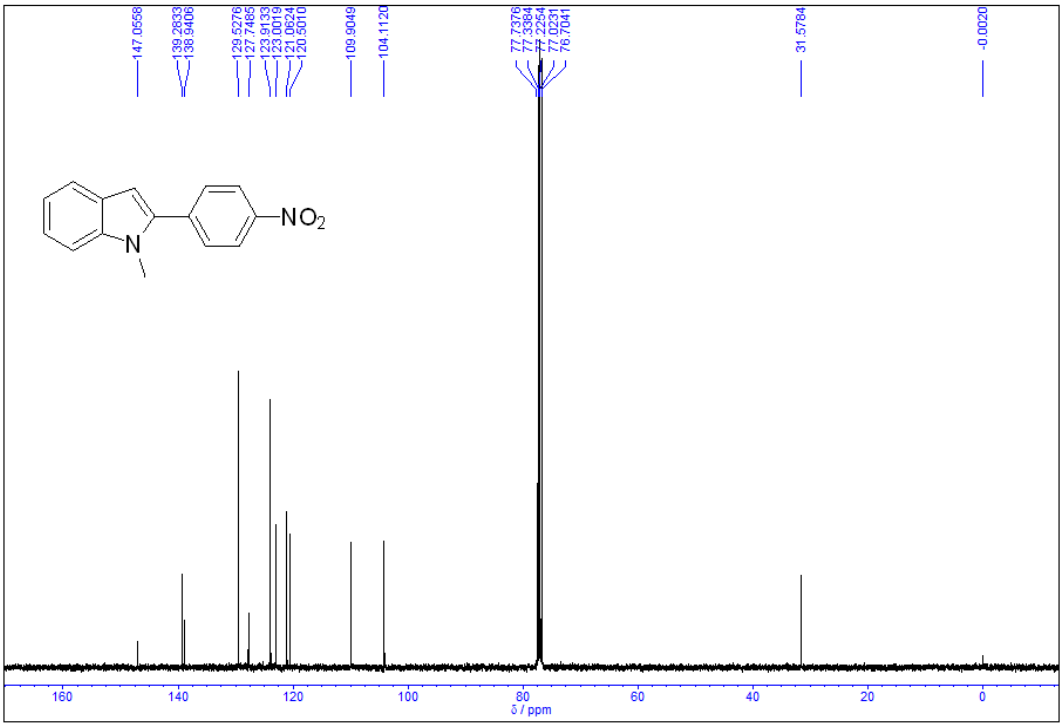

Figure S18: ^{13}C NMR spectrum of compound 4 (100 MHz, $CDCl_3$)

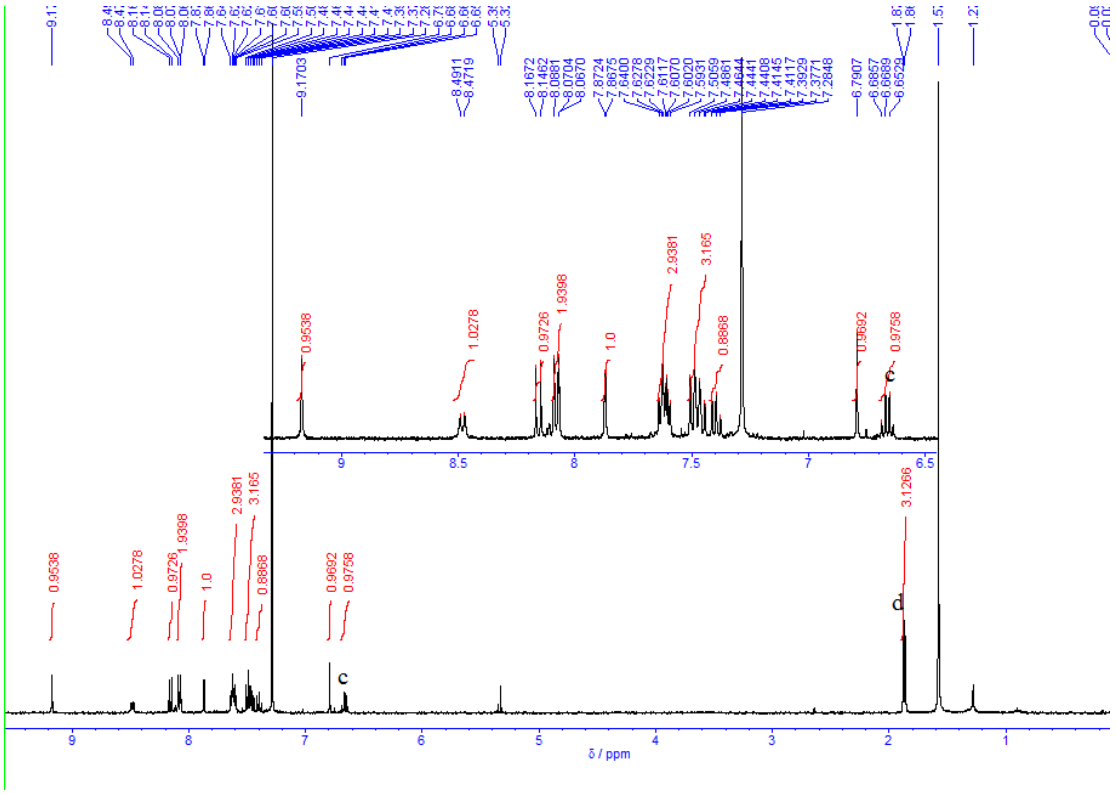

Figure S19: ^{1}H NMR spectrum of compound 16 (400 MHz, $CDCl_3$)

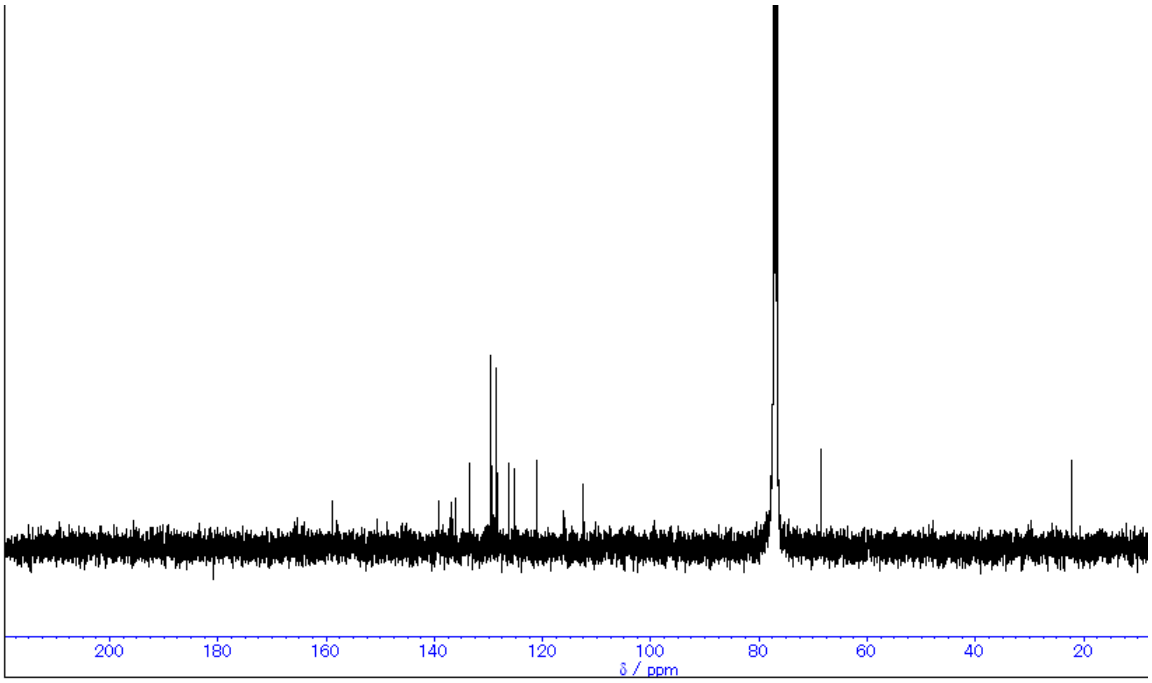

Figure S20: ^{13}C NMR spectrum of compound 16 (100 MHz, $CDCl_3$)

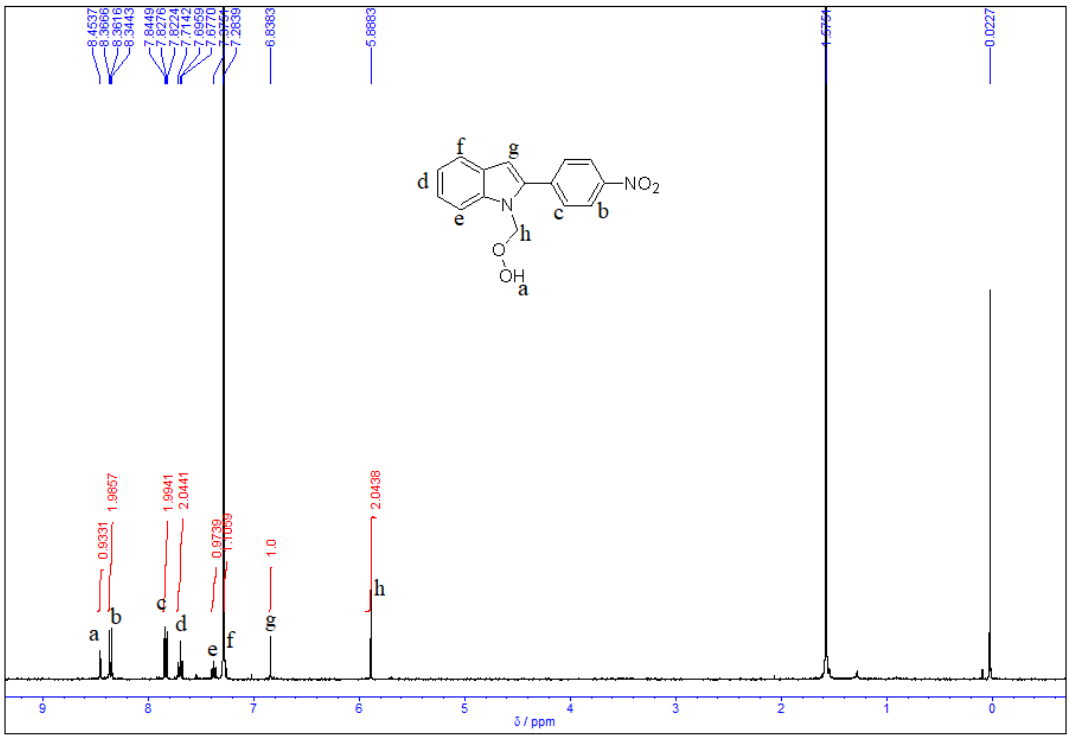

Figure S21: ^{1}H NMR spectrum of compound 17 (400 MHz, $CDCl_3$)

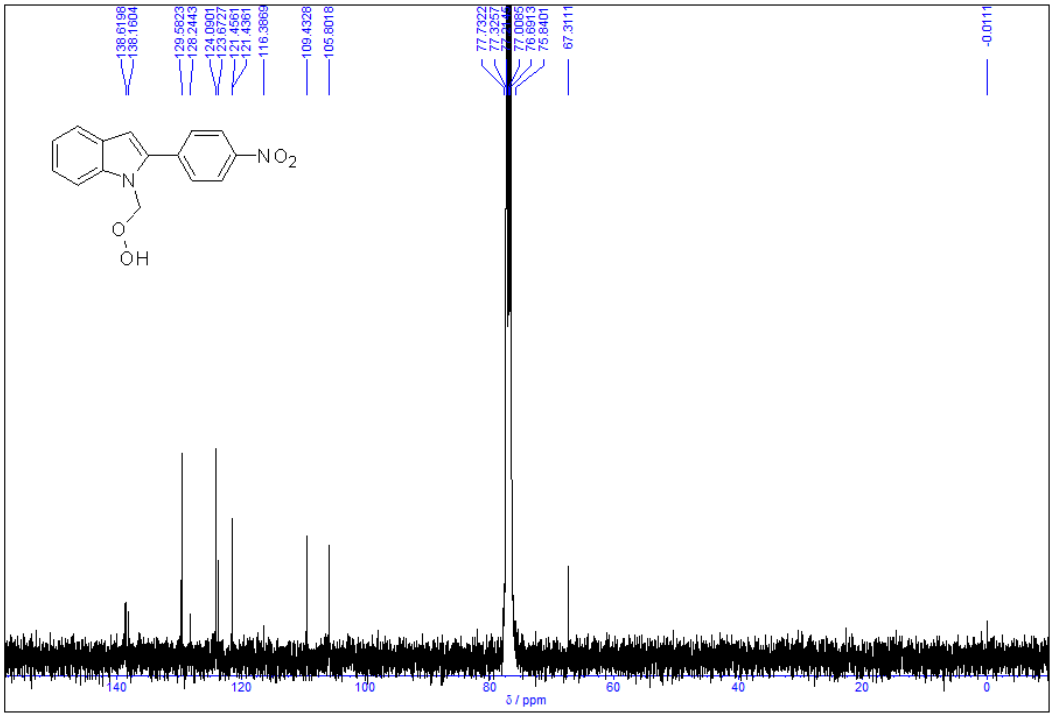

Figure S22: ^{13}C NMR spectrum of compound 17 (100 MHz, $CDCl_3$)

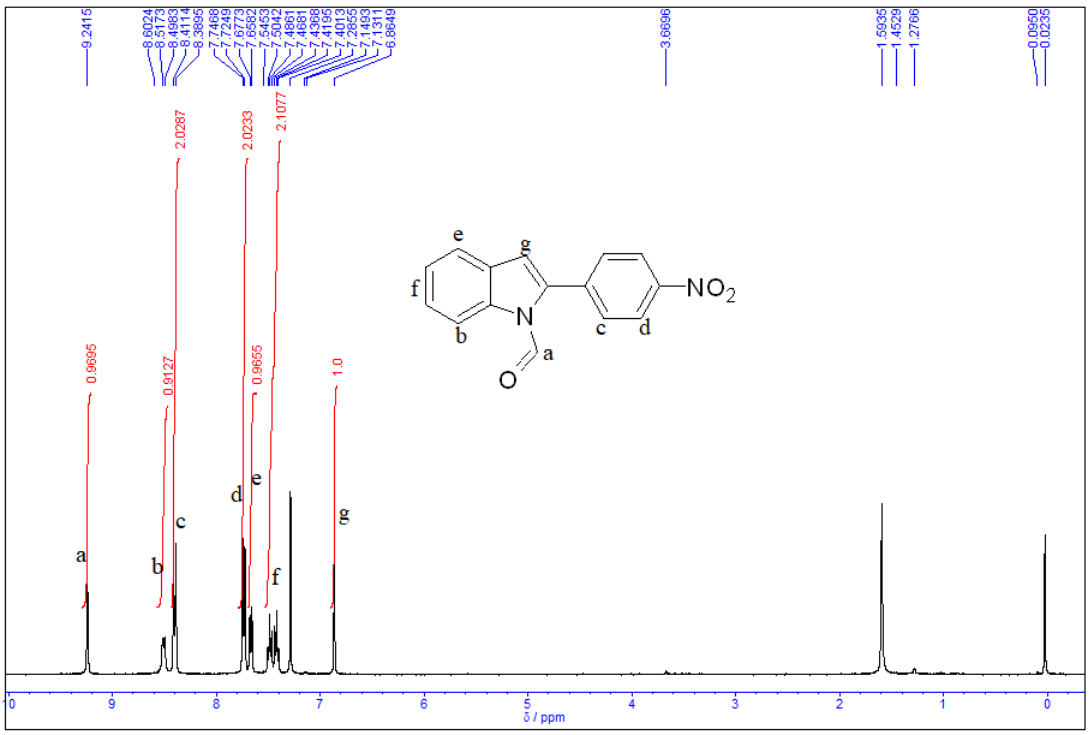

Figure S23: ^{1}H NMR spectrum of compound 18 (400 MHz, $CDCl_3$)

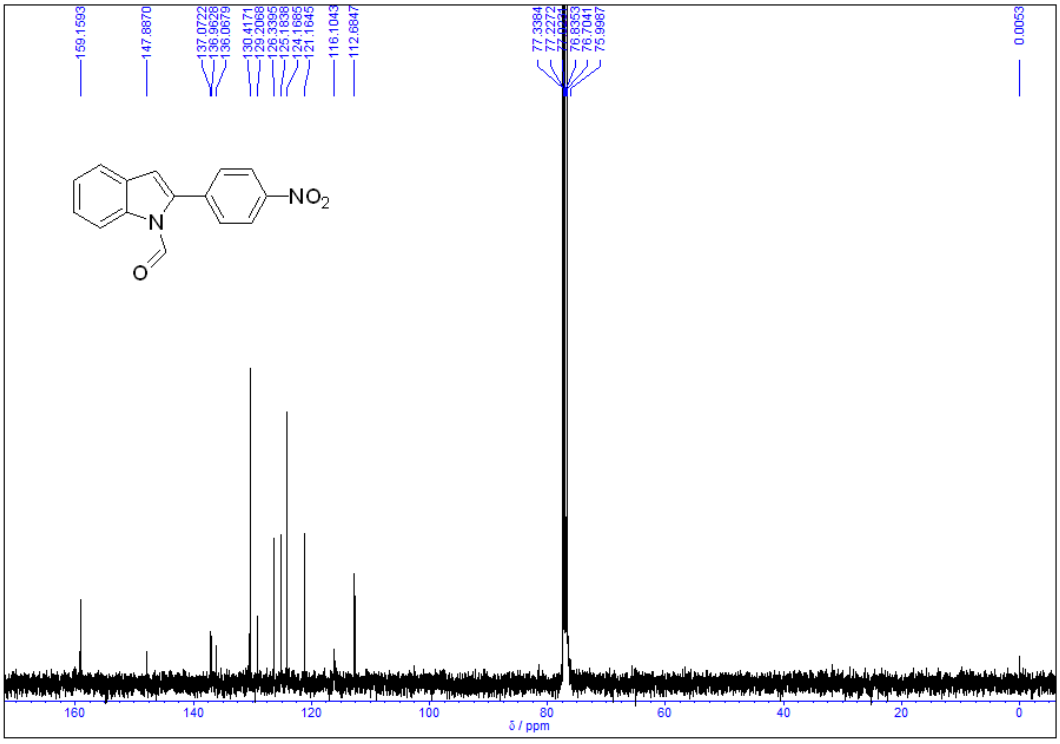

Figure S24: ^{13}C NMR spectrum of compound 18 (100 MHz, $CDCl_3$)

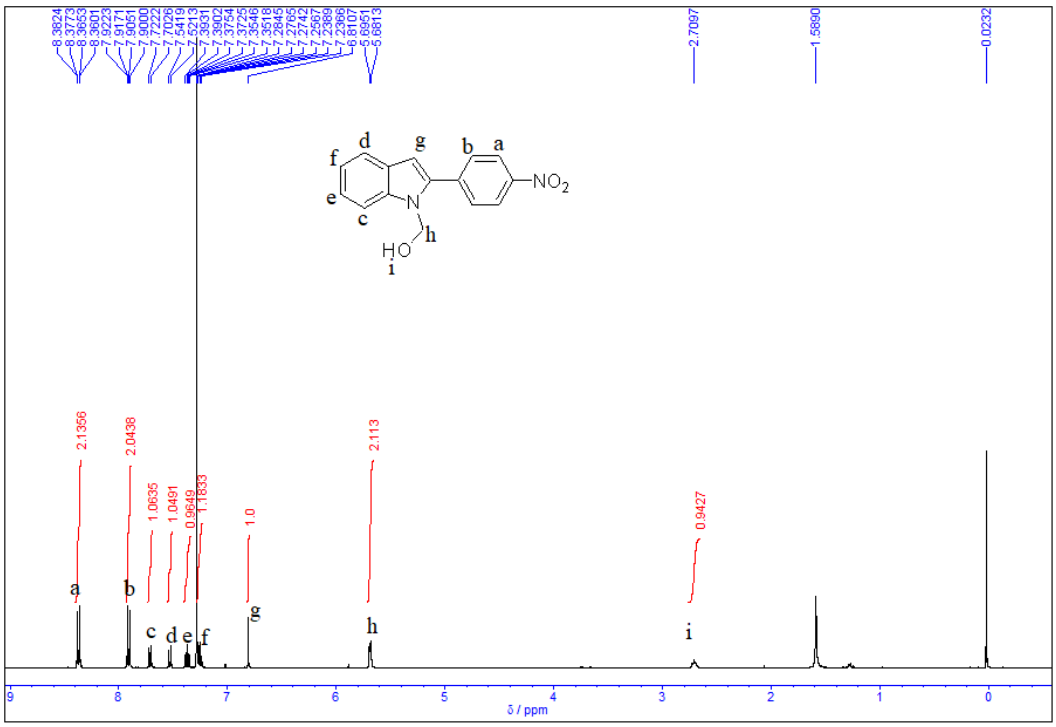

Figure S25: ^{1}H NMR spectrum of compound 19 (400 MHz, $CDCl_3$)

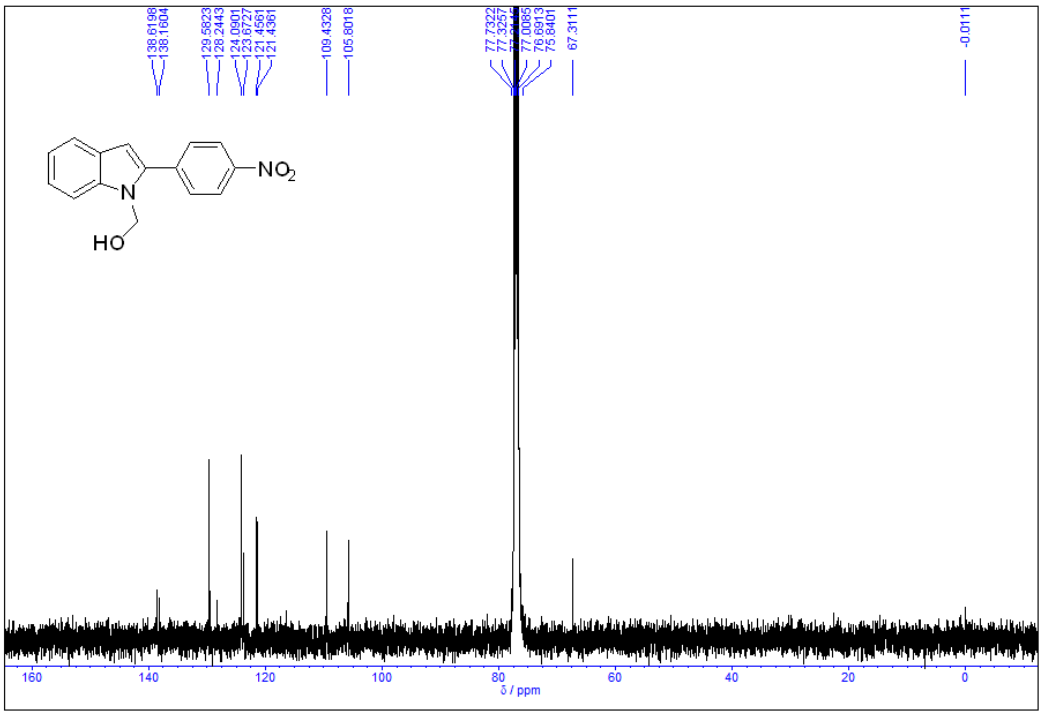

Figure S26: ^{13}C NMR spectrum of compound 19 (100 MHz, $CDCl_3$)

Fluorescence and phosphorescence emission spectra

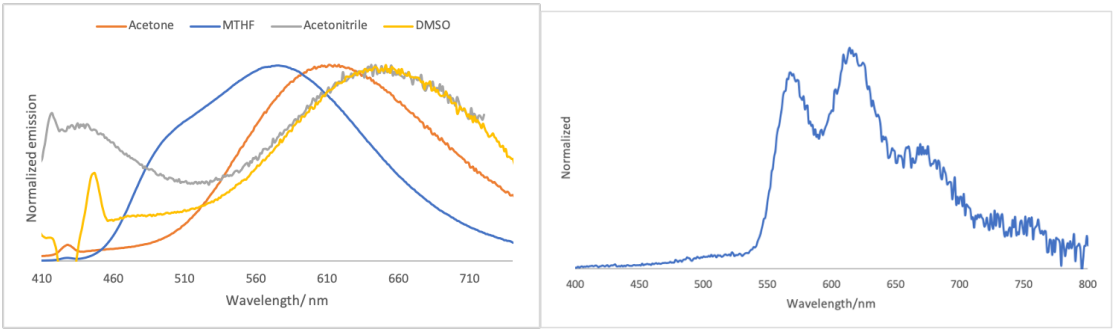

Figure S27: Fluorescence emission of 1 in different solvent and phosphorescence in 2-MTHF.

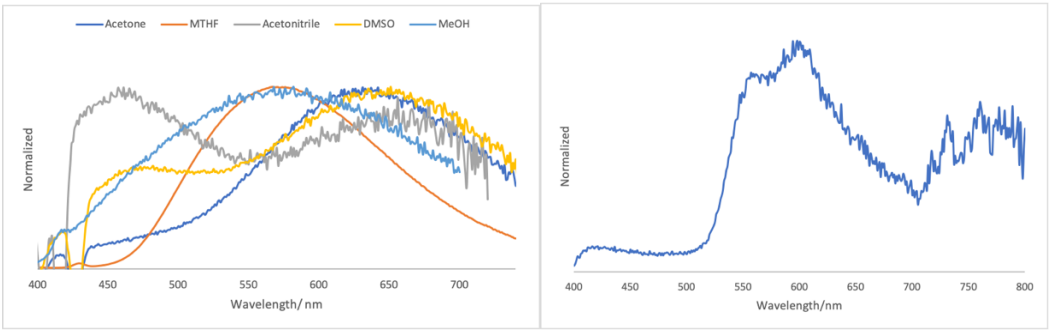

Figure S28: Fluorescence emission of 2 in different solvent and phosphorescence in 2-MTHF.

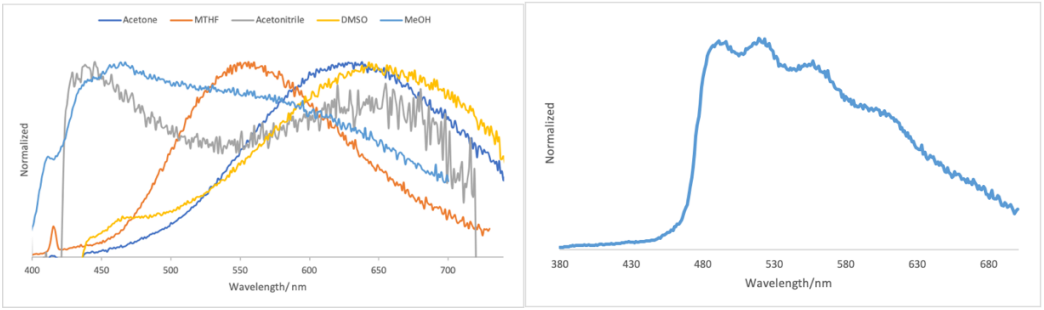

Figure S29: Fluorescence emission of 3 in different solvent and phosphorescence in

2-MTHF.

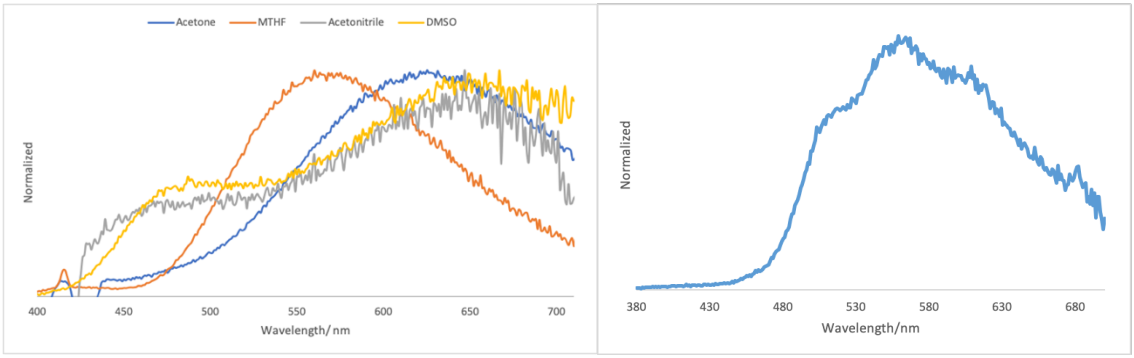

Figure S30: Fluorescence emission of 4 in different solvent and phosphorescence in 2-MTHF.

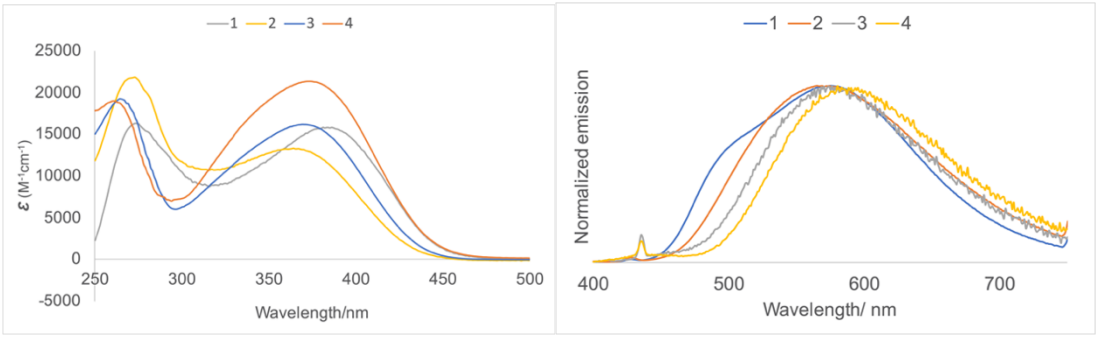

Figure S31. UV-vis absorption and fluorescence emission spectra of compound 1-4 in 2-MTHF at 298K

Transient absorption spectra of 3 in nanosecond time window

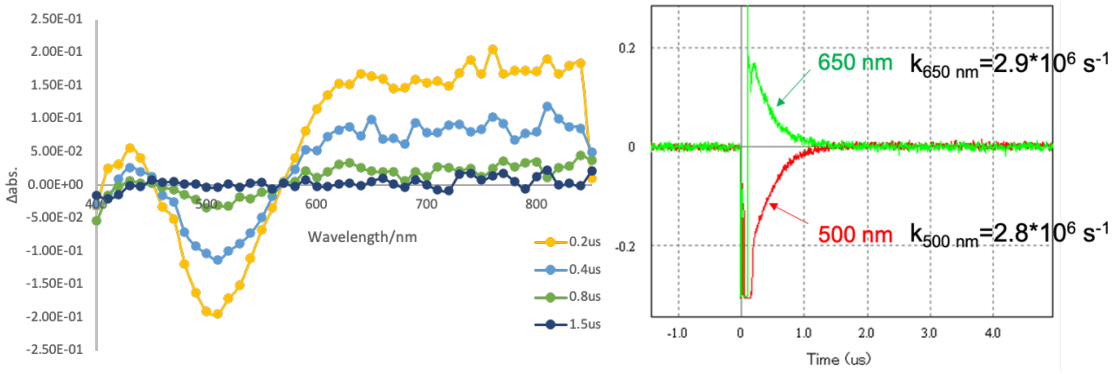

Figure S32: Transient absorption spectra of compound 3 after excitation with a 355 nm nanosecond laser pulse.

General procedures of photoreactions of compounds 1-4: Compound **X** (X = 1-4) was dissolved in CD_3OD or DMSO-d_6 and transferred to NMR tube. The reaction solution was irradiated using LED lamp (365 nm). The distance between light source and sample was 10 cm. After irradiation, the solvent was removed by evaporation. The products were subjected to silica gel column chromatography to isolated products.

Quantum yield of uncaging reaction

Chemical actinometer for quantum yield measurement: The rate of photo uncaging reaction can be quantified by quantum yield (Φ).

$$\Phi = \frac{\text{number of reacted molecules per time unit}}{\text{number of photons absorbed per time unit}}$$

Chemical actinometers are widely used to measure photon fluxes, one of the most popular and reliable one i.e., ferrioxalate, during the photo irradiation the potassium ferrioxalate decomposes according to the following equations.

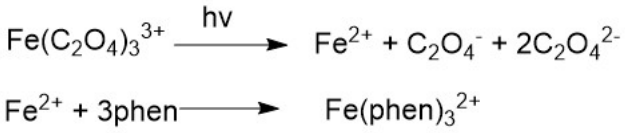

The number of ferrous ions formed during a photoirradiation is measured by conversion to the colored tris-phenanthroline compound at 510 nm (ε = 11100 M^{-1} cm^{-1}). The original ferric ions are not substantially complexed by phenanthroline and the complex does not absorb at 510 nm.

$$I\ (mol/s) = \frac{\text{moles of } Fe^{2+}}{\Phi_\lambda \times t \times F} = \frac{V_1 \times V_3 \times \Delta A(510\ nm)}{10^3 \times V_2 \times l \times \varepsilon\ (510\ nm) \times \Phi_\lambda \times t}$$

V_1: the irradiated volume (mL)

V_2: the aliquot of the irradiated solution taken for the determination of the ferrous ions (mL)

V_3: the final volume (mL)

ΔA: the optical difference in absorbance between the irradiated solution and that taken in the dark

l: optical pathlength of the irradiation cell

ε (510 nm): ε of the complex $Fe(phen)_3^{2+}$

Φ_λ: the quantum yield of ferrous ion production at the irradiation wavelength

t: the irradiation time

F: mean function of light absorbed by the ferrioxalate solution

Experiment procedures,

117.7 mg of $K_3[Fe(C_2O_4)_3] \cdot 3H_2O$ was dissolved in 20 mL of 0.05 M H_2SO_4. (0.012 M Ferrioxalate was prepared)-①

10.2 mg of 1,10-phenanthroline monohydrate and 1.78 g of CH_3COONa were dissolved in

10 mL of 0.5 M H_2SO_4-②

3 mL solution of ① irradiated at 370 nm for 0, 10, 20 and 30 seconds, 0.5 mL of solution ② was added each time then measured the absorption spectra at 510 nm to measure the change in absorbance with respect to an irradiation time was used to calculate the light amount.

Calculated number of photons from Xe-lamp at 370 nm= 3.95×10^{-7} mol/min.

Number of reacted molecules per time unit was confirmed by HPLC:

1. Compound 1 dissolved in MeOH (0.324mM);

2. Irradiated with 370nm Xe-lamp for 0, 0.5, 1, 2min, injected 5uL of irradiated solution to HPLC for analysis;

3. Measure the change of compound 1 peak area with respect to an irradiation time to calculate the conversion rate, then calculate quantum yield:

Time /min	Peak area			Inject /μL	Conversion of 1	Φ
	Benzoic acid	Photo product	Compound 8			
0	3767.037	1781.93	985949.4	5	0	0
0.5	3898.224	3806.28	952279	5	0.034150225	0.167951079
1	4667.865	5730.7	927097.8	5	0.059690257	0.146778578
2	4755.738	9678.602	911013.7	5	0.076003597	0.093446573

Same procedures for compound 2 to get quantum yield:

Time /min	Peak area			Inject /μL	Conversion of 8	Φ
	Benzoic acid	Photo product	Compound 8			
0	37021.62	-	694136.29	2.5	0	0
1	47169.44	-	680900.5	2.5	0.019068042	0.021696356
3	46288.31	-	663455.1	2.5	0.044200531	0.016764358
5	47288.4	-	639628.1	2.5	0.078526672	0.017870137

Photochemical reaction of 3 in different solvent

In CD_3CN:

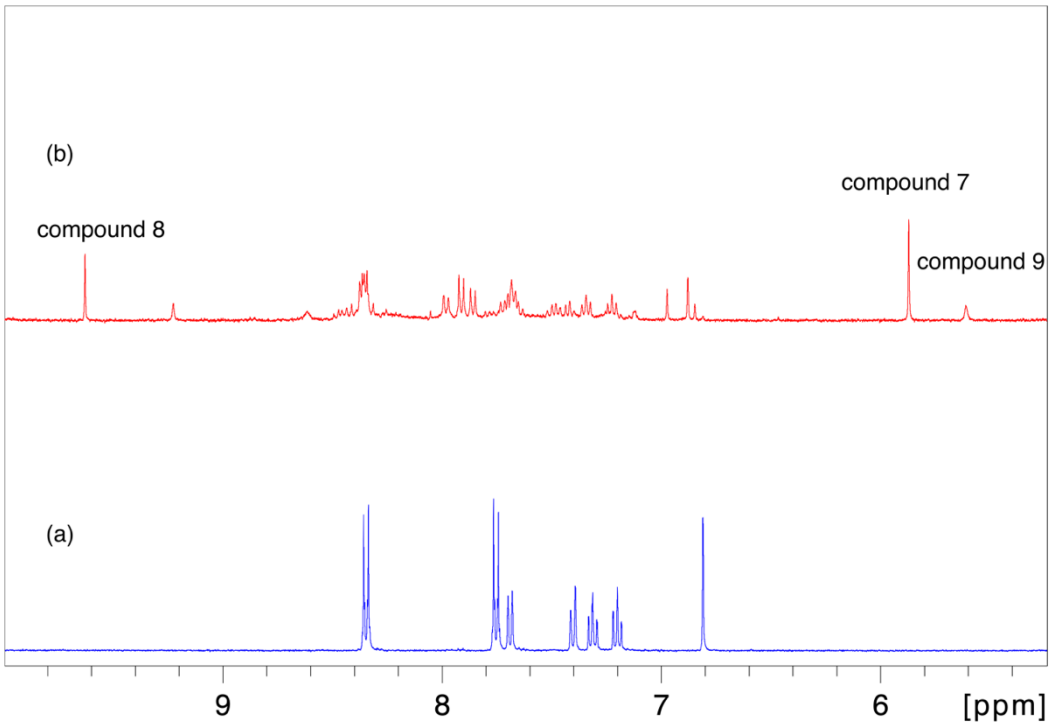

Figure S33: ^{1}H NMR spectroscopy analysis during the photolysis of compound 3 (7.4 mM) at 370 nm in CD_3CN; (a) before irradiation; (b) after 1h irradiation, δ 6-9 ppm.

In DMSO-d6:

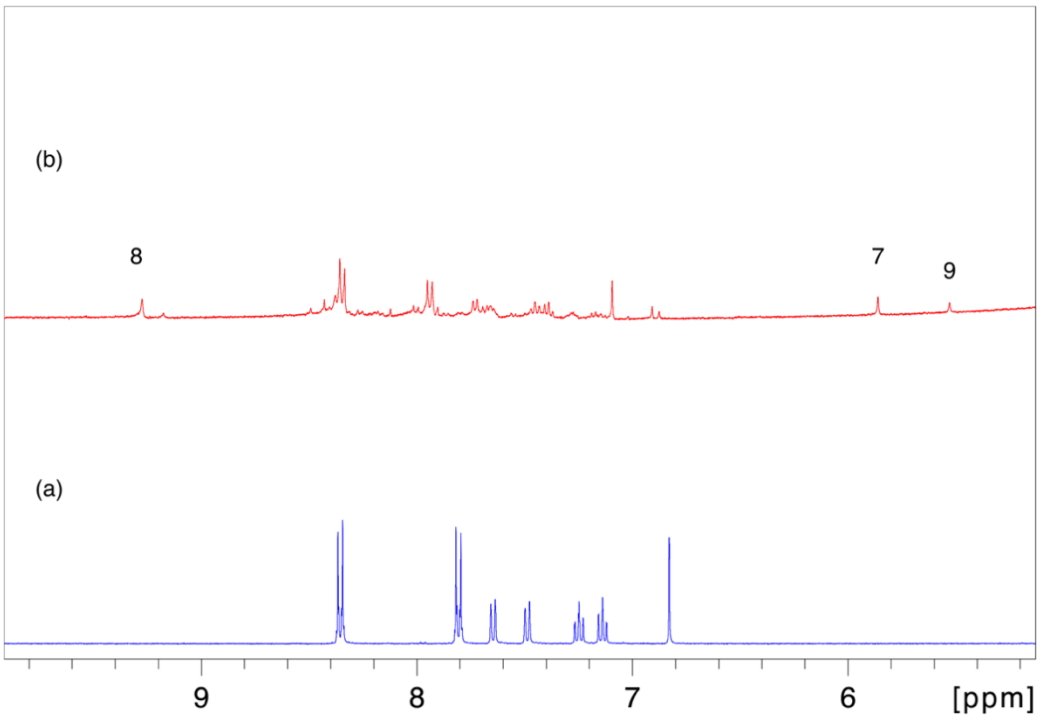

Figure S34: ^{1}H NMR spectroscopy analysis during the photolysis of compound 3 (3.7 mM) at 370 nm in DMSO-d6; (a) before irradiation; (b) after 1h irradiation, δ 6-9 ppm.

Computational details

We used density functional theory (DFT) and time-dependent (TD) DFT approaches, as implemented in the Gaussian 03 and 09 packages, to model molecule 3,4 and transient states. The predicted UV-vis absorption of triplet 3, 4 and 20, 21, 23, 24 was calculated as TD-B3LYP/6-31G(d) scrf=(smd,solvent=acetonitrile) level.

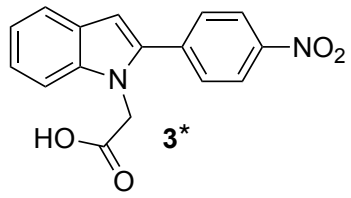

3*

H	3.66878	-3.56824	0.45297
C	3.75598	-2.50167	0.26904
C	3.96467	0.30467	-0.21783
C	2.59219	-1.70781	0.11861
C	5.00365	-1.89014	0.16844
C	5.11137	-0.51486	-0.07357
C	2.73215	-0.30217	-0.12034
H	5.90514	-2.4848	0.28057
H	6.09367	-0.05798	-0.14607
H	4.07296	1.37198	-0.38211
C	1.2259	-1.9871	0.14659
H	0.76208	-2.93947	0.35822
C	0.48549	-0.73345	-0.04886
N	1.4479	0.25939	-0.23318
C	-0.90381	-0.57301	-0.00038
C	-3.72869	-0.36302	0.00951
C	-1.56798	0.68462	0.25967
C	-1.75434	-1.72959	-0.18635
C	-3.1201	-1.62363	-0.19958
C	-2.93367	0.78339	0.2665

H	-0.98055	1.545	0.55645
H	-1.30088	-2.69707	-0.37357
H	-3.75539	-2.48384	-0.36923
H	-3.43283	1.71691	0.49416
N	-5.15088	-0.25008	-0.00598
O	-5.82	-1.28518	-0.19549
O	-5.65023	0.87968	0.16748
C	1.25537	1.54852	-0.85748
H	0.27571	1.57803	-1.34372
H	2.00473	1.68861	-1.64485
C	1.34026	2.72114	0.11621
O	1.22997	2.65406	1.31617
O	1.53147	3.87354	-0.56381
H	1.52722	4.59356	0.09555

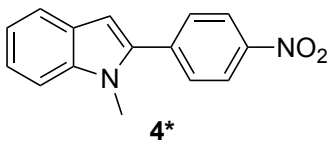

4*

H	-4.07741700	-2.77860300	-0.30059900
C	-4.10353000	-1.69788200	-0.19804600
C	-4.14079100	1.14863100	0.06897100
C	-2.89974600	-0.96350700	-0.09456600
C	-5.31212300	-1.00438700	-0.16562500

C	-5.33146000	0.39114600	-0.03361300
C	-2.94831300	0.45717000	0.04106400
H	-6.24891700	-1.54731400	-0.24543400
H	-6.28317600	0.91367700	-0.01306200
H	-4.18536800	2.22859100	0.15874800
C	-1.54831900	-1.32553900	-0.09945400
H	-1.14285400	-2.31956700	-0.22094800
C	-0.74905800	-0.10998600	0.02279400
N	-1.62483100	0.93679500	0.12696200
C	0.67338600	-0.05751600	0.00306800
C	3.51461000	-0.10718700	-0.02680800
C	1.41081100	-1.26026300	0.27692900
C	1.44005100	1.11221400	-0.31736500
C	2.81311200	1.08950700	-0.33849300
C	2.78334400	-1.28570000	0.27702100
H	0.87603300	-2.17081000	0.52500800
H	0.94071700	2.02909000	-0.60262700
H	3.37940100	1.97338100	-0.60341300
H	3.32486200	-2.19477200	0.50619600
C	-1.32177900	2.33032000	0.43589100
H	-1.13776800	2.91018100	-0.47401300
H	-0.44843600	2.38034500	1.08759700

H	-2.17241700	2.76214300	0.96509400
N	4.91470600	-0.12685300	-0.03277800
O	5.54253300	0.94452000	-0.30162900
O	5.51559700	-1.21427900	0.23257600

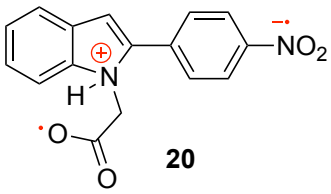

20

H	-3.77813	-2.63521	1.50382
C	-3.75586	-1.94514	0.66642
C	-3.7153	-0.12195	-1.5226
C	-2.57871	-1.21202	0.3805
C	-4.87086	-1.76963	-0.14231
C	-4.86383	-0.87744	-1.23012
C	-2.61845	-0.31579	-0.71478
H	-5.7746	-2.33333	0.07031
H	-5.75056	-0.76138	-1.84409
H	-3.70923	0.58151	-2.35048
C	-1.30524	-1.17165	0.97125
H	-0.99955	-1.68748	1.86904
C	-0.44257	-0.28138	0.21981
C	0.95536	-0.24323	0.08543
C	3.76788	-0.26395	-0.12399
C	1.76833	-1.00057	0.99067

C	1.63662	0.50755	-0.92582
C	3.01137	0.49185	-1.03186
C	3.14146	-1.00788	0.88987
H	1.29371	-1.57493	1.77837
H	1.08274	1.10871	-1.64169
H	3.52416	1.05295	-1.80327
H	3.75365	-1.57957	1.5764
N	5.20998	-0.2794	-0.2385
O	5.72588	0.3873	-1.14555
O	5.84766	-0.96132	0.57381
C	-1.45486	1.90536	-0.57337
H	-0.51994	2.36995	-0.8943
H	-2.27721	2.26832	-1.19012
N	-1.31816	0.39963	-0.8063
H	-0.90897	0.25985	-1.73764
C	-1.6904	2.22501	0.92377
O	-2.2032	3.30795	1.18248
O	-1.2564	1.33784	1.73926

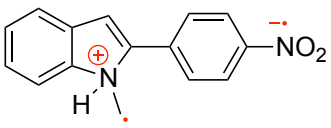

21

H	4.21369	-2.65715	0.00845
C	4.17288	-1.5743	-0.04418

C	4.08958	1.25949	-0.18886
C	2.94848	-0.90711	-0.03292
C	5.33966	-0.81866	-0.12665
C	5.30741	0.57523	-0.19904
C	2.95796	0.48352	-0.10981
H	6.29903	-1.32652	-0.13589
H	6.23362	1.13579	-0.26337
H	4.04192	2.34177	-0.24186
C	1.57699	-1.35635	0.02114
H	1.26742	-2.39158	0.0532
C	0.72401	-0.29639	-0.01937
N	1.5548	0.96246	-0.06646
H	1.34785	1.47723	-0.93414
C	-0.69947	-0.18437	-0.02467
C	-3.52605	-0.06743	-0.05214
C	-1.49245	-1.34669	0.19048
C	-1.38646	1.03703	-0.25911
C	-2.75678	1.09866	-0.27334
C	-2.8599	-1.29638	0.17924
H	-1.00337	-2.29706	0.37952
H	-0.83642	1.95357	-0.44799
H	-3.26935	2.03359	-0.45818

H	-3.45309	-2.18518	0.3508
N	-4.90922	-0.00989	-0.06282
O	-5.48016	1.10204	-0.2635
O	-5.57397	-1.07036	0.12767
C	1.32035	1.84487	1.0668
H	1.39504	1.38086	2.04002
H	1.3804	2.90646	0.87563

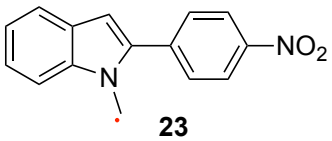

23

H	-4.14121	-2.6533	-0.63754
C	-4.13983	-1.59267	-0.40124
C	-4.15022	1.18603	0.22256
C	-2.9279	-0.91142	-0.20056
C	-5.3316	-0.88873	-0.28853
C	-5.33578	0.4865	0.02113
C	-2.95367	0.47424	0.10294
H	-6.27678	-1.40223	-0.44033
H	-6.28256	1.0129	0.10117
H	-4.16755	2.24632	0.45413
C	-1.55248	-1.30087	-0.23298
H	-1.16269	-2.27853	-0.48153
C	-0.78279	-0.18685	0.02719

N	-1.633	0.91586	0.25173
C	0.68098	-0.1048	0.02819
C	3.47165	-0.08272	-0.03745
C	1.38016	0.97205	-0.55448
C	1.42577	-1.17169	0.5707
C	2.81412	-1.16951	0.53789
C	2.76947	0.98907	-0.58656
H	0.82971	1.78894	-1.00869
H	0.90122	-1.99894	1.03785
H	3.39324	-1.98213	0.95884
H	3.31494	1.80791	-1.0393
N	4.93872	-0.06753	-0.067
O	5.49141	0.91103	-0.57117
O	5.53119	-1.03451	0.4137
C	-1.26966	2.1828	0.64778
H	-0.25786	2.34768	0.98252
H	-2.06056	2.87231	0.89997

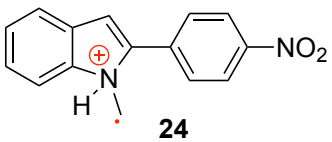

24

H	-4.21542	-2.66425	0.16675
C	-4.18403	-1.57976	0.14355
C	-4.12406	1.27458	0.09468

C	-2.9671	-0.89732	0.09344
C	-5.3625	-0.82724	0.16665
C	-5.33768	0.57273	0.1443
C	-2.98233	0.49968	0.07356
H	-6.31868	-1.33924	0.20452
H	-6.26899	1.12889	0.16577
H	-4.10212	2.35956	0.07432
C	-1.58305	-1.34147	0.08377
H	-1.27049	-2.37694	0.13055
C	-0.7305	-0.29518	0.04993
N	-1.56292	0.98134	0.01587
H	-1.35972	1.52969	0.86132
C	0.72356	-0.18744	0.0392
C	3.50104	-0.07124	0.05651
C	1.48975	-1.31991	-0.3045
C	1.389	1.00464	0.3861
C	2.77818	1.06778	0.39457
C	2.87717	-1.26702	-0.29226
H	0.99903	-2.24115	-0.60071
H	0.83854	1.89796	0.66786
H	3.30452	1.97574	0.66234
H	3.47966	-2.12732	-0.55741

N	4.97918	-0.00769	0.06323
O	5.58254	-1.03299	-0.23557
O	5.48969	1.06605	0.36722
C	-1.29967	1.80291	-1.1659
H	-1.35125	1.28613	-2.11354
H	-1.35341	2.87644	-1.0502

Transition state from 20 to 21

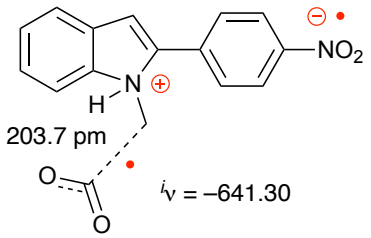

H	3.640553	-2.965676	-1.063550
C	3.646799	-2.114203	-0.390367
C	3.691895	0.129459	1.368817
C	2.456890	-1.382611	-0.157537
C	4.813241	-1.724215	0.251949
C	4.851913	-0.621585	1.128865
C	2.546938	-0.272861	0.716546
H	5.726824	-2.284859	0.074510
H	5.779899	-0.346231	1.618100
H	3.711531	0.987444	2.034514
C	1.124937	-1.529102	-0.592380
H	0.762142	-2.304615	-1.250903

C	0.296952	-0.537716	-0.007344
C	-1.099472	-0.351962	0.018255
C	-3.919798	-0.142458	0.078184
C	-1.934663	-1.190941	-0.791749
C	-1.765220	0.603361	0.853510
C	-3.138949	0.699440	0.889009
C	-3.306799	-1.086881	-0.764002
H	-1.475009	-1.921263	-1.448944
H	-1.195273	1.275129	1.490561
H	-3.637017	1.416861	1.529562
H	-3.931396	-1.720136	-1.382054
H	-5.354401	-0.031520	0.109350
H	-5.856612	0.820865	0.859192
H	-6.013855	-0.795325	-0.612066
H	1.257977	1.799009	0.414227
H	0.312346	2.164207	0.029291
H	1.734976	2.394740	1.187179
H	1.194792	0.358416	0.805373
H	0.861234	0.325016	1.779842
C	2.369076	2.082276	-1.268843
O	3.055938	3.019519	-0.987048
O	1.941133	1.247466	-2.014293

Reference

1 S. Boinapally, B. Huang, M. Abe, C. Katan, J. Noguchi, S. Watanabe, H. Kasai, B. Xue and T. Kobayashi, Caged Glutamates with π-Extended 1,2-Dihydronaphthalene Chromophore: Design, Synthesis, Two-Photon Absorption Property, and Photochemical Reactivity, *J. Org. Chem.*, 2014, **79**, 7822–7830.

2 M. MARONCELLI, J. MACINNIS and G. R. FLEMING, Polar Solvent Dynamics and Electron-Transfer Reactions, *Science (80-.).*, 1989, **243**, 1674–1681.

3 V. Coropceanu, X.-K. Chen, T. Wang, Z. Zheng and J.-L. Brédas, Charge-transfer electronic states in organic solar cells, *Nat. Rev. Mater.*, 2019, **4**, 689–707.

4 J. Kroon, J. W. Verhoeven, M. N. Paddon-Row and A. M. Oliver, Solvent Dependence of Photoinduced Intramolecular Electron Transfer: Criteria for the Design of Systems with Rapid, Solvent-Independent Charge Separation, *Angew. Chemie Int. Ed. English*, 1991, **30**, 1358–1361.

5 S. R. Greenfield, W. A. Svec, D. Gosztola and M. R. Wasielewski, Multistep Photochemical Charge Separation in Rod-like Molecules Based on Aromatic Imides and Diimides, *J. Am. Chem. Soc.*, 1996, **118**, 6767–6777.

6 L. Mencaroni, B. Carlotti, A. Cesaretti, F. Elisei, A. Grgičević, I. Škorić and A. Spalletti, Competition between fluorescence and triplet production ruled by nitro groups in one-arm and two-arm styrylbenzene heteroanalogues, *Photochem. Photobiol. Sci.*, 2020, **19**, 1665–1676.

7 H. Noda, H. Nakanotani and C. Adachi, Excited state engineering for efficient reverse

intersystem crossing, *Sci. Adv.*, 2018, **4**, 1–8.

8 T. Hosokai, H. Matsuzaki, H. Nakanotani, K. Tokumaru, T. Tsutsui, A. Furube, K. Nasu, H. Nomura, M. Yahiro and C. Adachi, Evidence and mechanism of efficient thermally activated delayed fluorescence promoted by delocalized excited states, *Sci. Adv.*, 2017, **3**, e1603282.

9 M. Saigo, K. Miyata, S. Tanaka, H. Nakanotani, C. Adachi and K. Onda, Suppression of Structural Change upon S1-T1 Conversion Assists the Thermally Activated Delayed Fluorescence Process in Carbazole-Benzonitrile Derivatives, *J. Phys. Chem. Lett.*, 2019, **10**, 2475–2480.

10 T. Matsushima, F. Bencheikh, T. Komino, M. R. Leyden, A. S. D. Sandanayaka, C. Qin and C. Adachi, High performance from extraordinarily thick organic light-emitting diodes, *Nature*, 2019, **572**, 502–506.

11 J. V. Morris, M. A. Mahaney and J. R. Huber, Fluorescence quantum yield determinations. 9,10-Diphenylanthracene as a reference standard in different solvents, *J. Phys. Chem.*, 1976, **80**, 969–974.

12 M. T. Feldmann, S. L. Widicus, G. A. Blake, D. R. Kent and W. A. Goddard, Aminomethanol water elimination: Theoretical examination, *J. Chem. Phys.*, 2005, **123**, 034304.

13 T. Nakagawa, K. Okamoto, H. Hanada and R. Katoh, Probing with randomly interleaved pulse train bridges the gap between ultrafast pump-probe and nanosecond flash photolysis, *Opt. Lett.*, 2016, **41**, 1498.

14 R. D. Bach, P. Y. Ayala and H. B. Schlegel, A Reassessment of the Bond Dissociation

Energies of Peroxides. An ab Initio Study, *J. Am. Chem. Soc.*, 1996, **118**, 12758–12765.

15 J. P. Hunt and H. Taube, The Photochemical Decomposition of Hydrogen Peroxide. Quantum Yields, Tracer and Fractionation Effects, *J. Am. Chem. Soc.*, 1952, **74**, 5999–6002.

16 R. Oyama and M. Abe, Reactivity and Product Analysis of a Pair of Cumyloxyl and tert-Butoxyl Radicals Generated in Photolysis of tert-Butyl Cumyl Peroxide, *J. Org. Chem.*, 2020, **85**, 8627–8638.

17 J. K. Kochi and T. W. Bethea, Photochemical decarboxylation of acids with thallium(III), *J. Org. Chem.*, 1968, **33**, 75–82.

18 L. Candish, M. Freitag, T. Gensch and F. Glorius, Mild, visible light-mediated decarboxylation of aryl carboxylic acids to access aryl radicals, *Chem. Sci.*, 2017, **8**, 3618–3622.

19 M. C. Fu, R. Shang, B. Zhao, B. Wang and Y. Fu, Photocatalytic decarboxylative alkylations mediated by triphenylphosphine and sodium iodide, *Science (80-.).*, 2019, **363**, 1429–1434.

20 A. Bhattacherjee, M. Sneha, L. Lewis-Borrell, O. Tau, I. P. Clark and A. J. Orr-Ewing, Picosecond to millisecond tracking of a photocatalytic decarboxylation reaction provides direct mechanistic insights, *Nat. Commun.*, 2019, **10**, 5152.

21 H. Yokoi, T. Nakano, W. Fujita, K. Ishiguro and Y. Sawaki, In-Cage Formation of Carbanions in Photoinduced Electron-Transfer Reaction of Carboxylate Ions, *J. Am. Chem. Soc.*, 1998, **120**, 12453–12458.

22 Y. Yoshimi, T. Itou and M. Hatanaka, Decarboxylative reduction of free aliphatic carboxylic acids by photogenerated cation radical, *Chem. Commun.*, 2007, 5244.

23 S. Kubosaki, H. Takeuchi, Y. Iwata, Y. Tanaka, K. Osaka, M. Yamawaki, T. Morita and Y. Yoshimi, Visible- and UV-Light-Induced Decarboxylative Radical Reactions of Benzoic Acids Using Organic Photoredox Catalysts, *J. Org. Chem.*, 2020, **85**, 5362–5369.

24 Y. Yoshimi, Photoinduced electron transfer-promoted decarboxylative radical reactions of aliphatic carboxylic acids by organic photoredox system, *J. Photochem. Photobiol. A Chem.*, 2017, **342**, 116–130.

25 X. Lai, X. Shu, J. Song and H. Xu, Electrophotocatalytic Decarboxylative C−H Functionalization of Heteroarenes, *Angew. Chemie*, 2020, **132**, 10713–10719.

26 T. Kodama, M. Kubo, W. Shinji, K. Ohkubo and M. Tobisu, Phenylene-bridged bis(benzimidazolium) (BBIm 2+): a dicationic organic photoredox catalyst, *Chem. Sci.*, , DOI:10.1039/D0SC03958F.

27 N. Komori, S. Jakkampudi, R. Motoishi, M. Abe, K. Kamada, K. Furukawa, C. Katan, W. Sawada, N. Takahashi, H. Kasai, B. Xue and T. Kobayashi, Design and synthesis of a new chromophore, 2-(4-nitrophenyl)benzofuran, for two-photon uncaging using near-IR light, *Chem. Commun.*, 2016, **52**, 331–334.

28 J. F. Hartwig, Regioselectivity of the borylation of alkanes and arenes, *Chem. Soc. Rev.*, 2011, **40**, 1992.

29 G. A. Kraus and H. Guo, One-Pot Synthesis of 2-Substituted Indoles from 2-Aminobenzyl Phosphonium Salts. A Formal Total Synthesis of Arcyriacyanin A,

Org. Lett., 2008, **10**, 3061–3063.

30 S. E. Denmark and J. D. Baird, Palladium-Catalyzed Cross-Coupling Reactions of 2-Indolyldimethylsilanols with Substituted Aryl Halides, *Org. Lett.*, 2004, **6**, 3649–3652.

Chapter 3. 2-(4-Nitrophenyl)-1*H*-indolyl-3-methyl chromophore: A versatile photocage that responds to visible-light one-photon and near-infrared-light two-photon excitations

3-1. Introduction

In the previous work, the leaving group (benzoic acid) was introduced to the ortho position on nitrobenzene and uncaged by intramolecular rearrangement.[1-4] Such caged compounds can release leaving group successfully but possess problems of low chemical yield and unable to detect remained chromophores.[5,6] In this study, we try to change the uncaging mechanism from rearrangement to bond-cleavage to generate clean photoreaction, which is inspired by a "breathing" type homolysis occurred with NPI chromophore.[7] A new type of caged compound was designed, in which the leaving group is introduced at C3 position of indole to avoid interference of amine and the ethyl moiety on nitrogen of indole is worked for increasing thermal stability. Thus, a new PPG: 2-(4-nitrophenyl)-1*H*-indolyl-3-methyl (NPIM) was designed for 1P and 2P uncaging. To test the uncaging performance of NPIM caged compounds, I have linked NPI with typical LGs: acid, alcohol and amine. These NPIM derivatives can conduct an efficient release of X–H with 57-98% chemical yields (carboxylic acids, alcohols, or amines) and their chromophore transform to a certain product 1-ethyl-2- (4-nitrophenyl)-1*H*-indole-3-carbaldehyde (**NPIM-Ald**). The donor-acceptor substitution of the stilbene core was designed to induce the 2P-response in the NIR region. Remarkably, in this study, poor leaving groups, such as alcohols (X = OR) and amines (X = NHR), which were directly attached to the PPG, were also released in moderate to high yields under air. In general, carbonate (OC(O)OR) or carbamate (OC(O)NHR) linkers are necessary to release alcohols (RO–H)) and amines (RNH–H) because of the low leaving group properties of OR and NHR.[8]

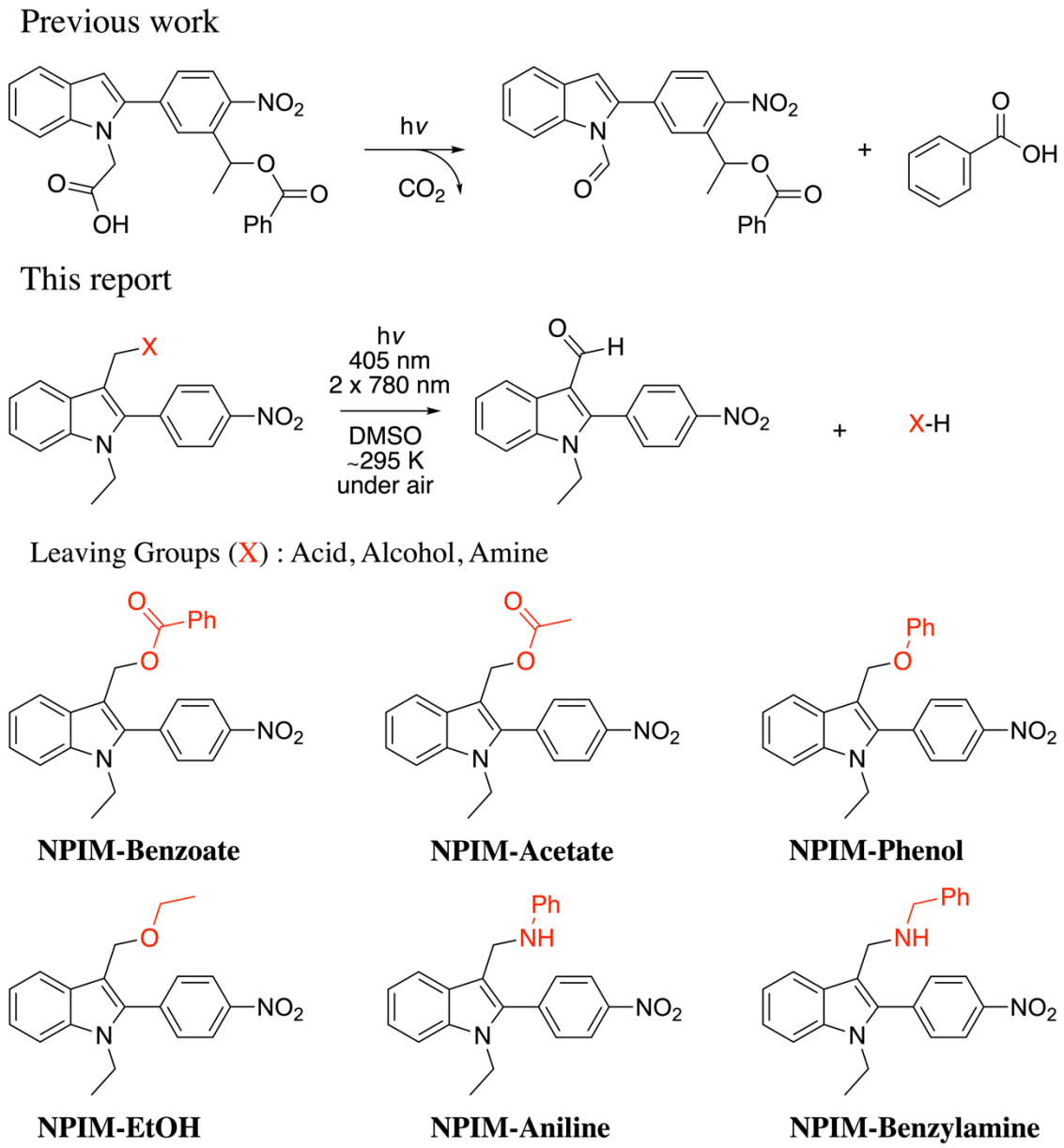

Figure 14. Photoreactions and structures of NPIM derivatives

3-2. Results and discussion

The syntheses of NPIM derivatives are shown in Scheme 3 and their photophysical properties are summarized in Table 3. The thermal stabilities were evaluated at 40 °C in

dimethyl sulfoxide (DMSO)-d_6 for 24 h. Thermal decomposition was not observed after heating, indicating that the caged compounds are thermally stable under these conditions (Figures S21–25). The absorption bands of NPIM derivatives are observed at approximately 300-450 nm (Figure 15), indicating that visible light 1P and NIR 2P photolysis are possible for these excitations.

Scheme 3. Synthesis of NPIM derivatives

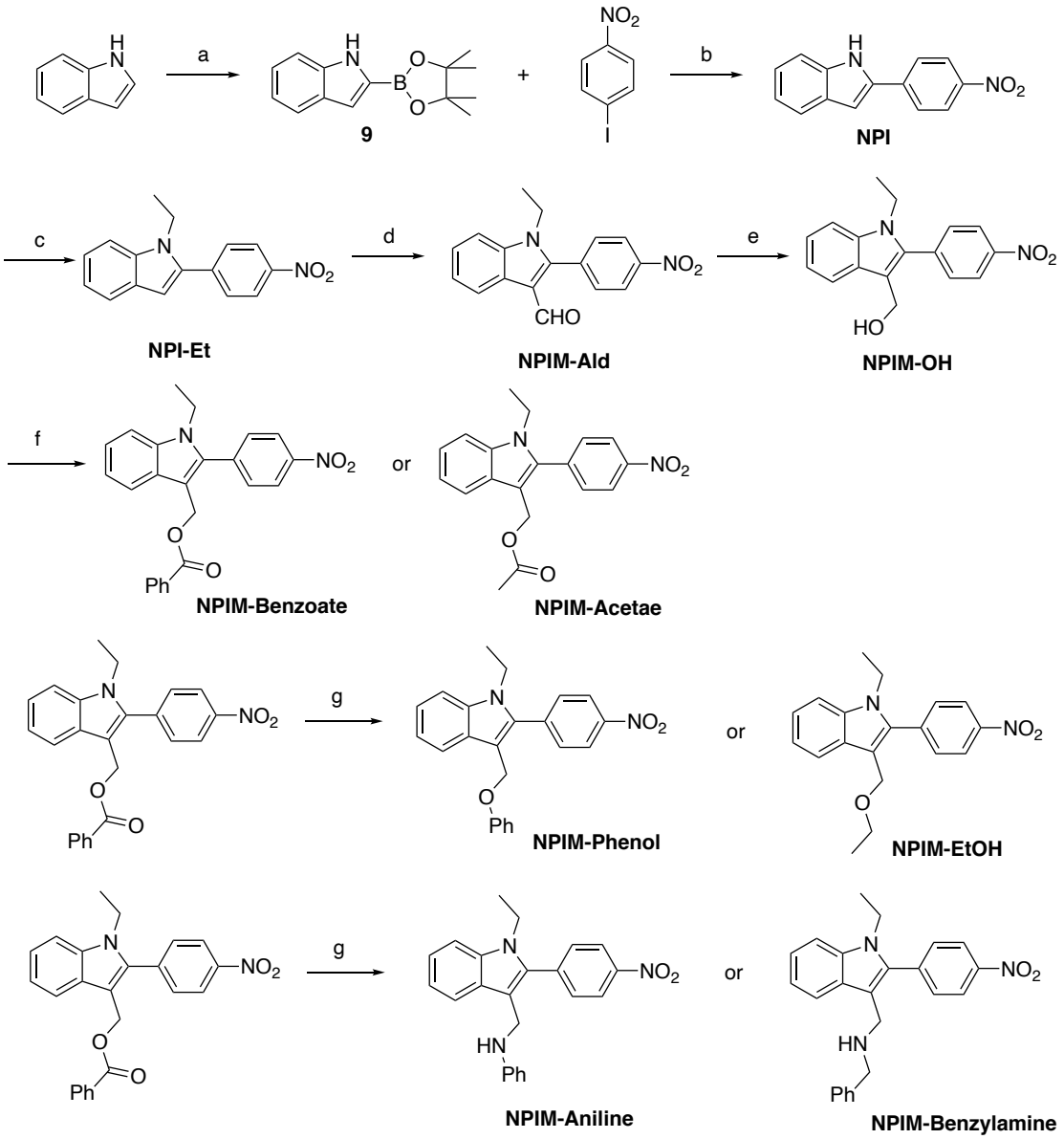

a. (1,5-Cyclooc- tadiene) (methoxy)iridium dimer, 4,4′-di-tert-buyl-2,2′-bipyridine, bis (pinacolato) diboron, RT, 18 h, 90%. b $Pd(PPh_3)_4$, K_2CO_3, THF/ H_2O, reflux, 15 h, 81%. c. KOH, iodoethane, RT, 3h, 95%. d. $POCl_3$, DMF, 3h, 83%. e. $NaBH_4$, MeOH, RT, 1h, 40%. f. Acetic anhydride or benzoic anhydride, DMAP, RT, 10 min, 95%. g. K_2CO_3, amine or alcohol, 50 °C, 24h, 95%.

Table 3. Photophysical properties and photoreactions of NPIM derivatives.

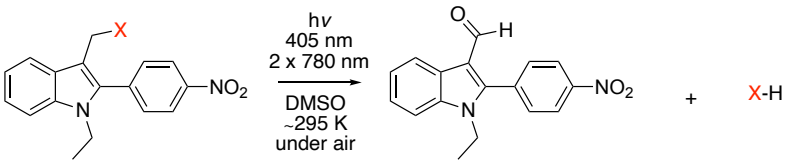

NPIM-X NPIM-Ald

Entry	NPIM-X	Abs. [a] λ_{max} /nm ε M^{-1} cm^{-1}	Emi. [b] λ_{max} / nm Φ_f	Products (yields, %) [c] reaction time
1	**NPIM-Benzoate**	345 9257	462 0.13	Benzoate (98) NPIM-Ald (36) 4 h
2	**NPIM-Acetate**	349 6926	462 0.09	Acetate (86) NPIM-Ald (35) 2.5 h
3	**NPIM-Phenol**	349 6488	462 0.08	Phenol (95) NPIM-Ald (48) 1 h
4	**NPIM-EtOH**	362 7709	475 0.05	EtOH (87) NPIM-Ald (65) 3 h
5	**NPIM-Aniline**	357 7450	465 0.03	Aniline (62) NPIM-Ald (59) 3 h
6	**NPIM-Benzylamine**	369 5085	469 0.14	Benzylamine (57) NPIM-Ald (-) 3 h

[a] Absorbance, molar extinction coefficient, and fluorescence determined in DMSO at ~25 °C.

[b] Fluorescence quantum yield (Φ_f) determined using 9,10-diphenylanthracene as a reference standard.

[c] Photolyses of NPI derivatives were conducted using a 405 nm LED lamp and yields were determined using ^{1}H NMR spectroscopy with triphenylmethane as a standard.

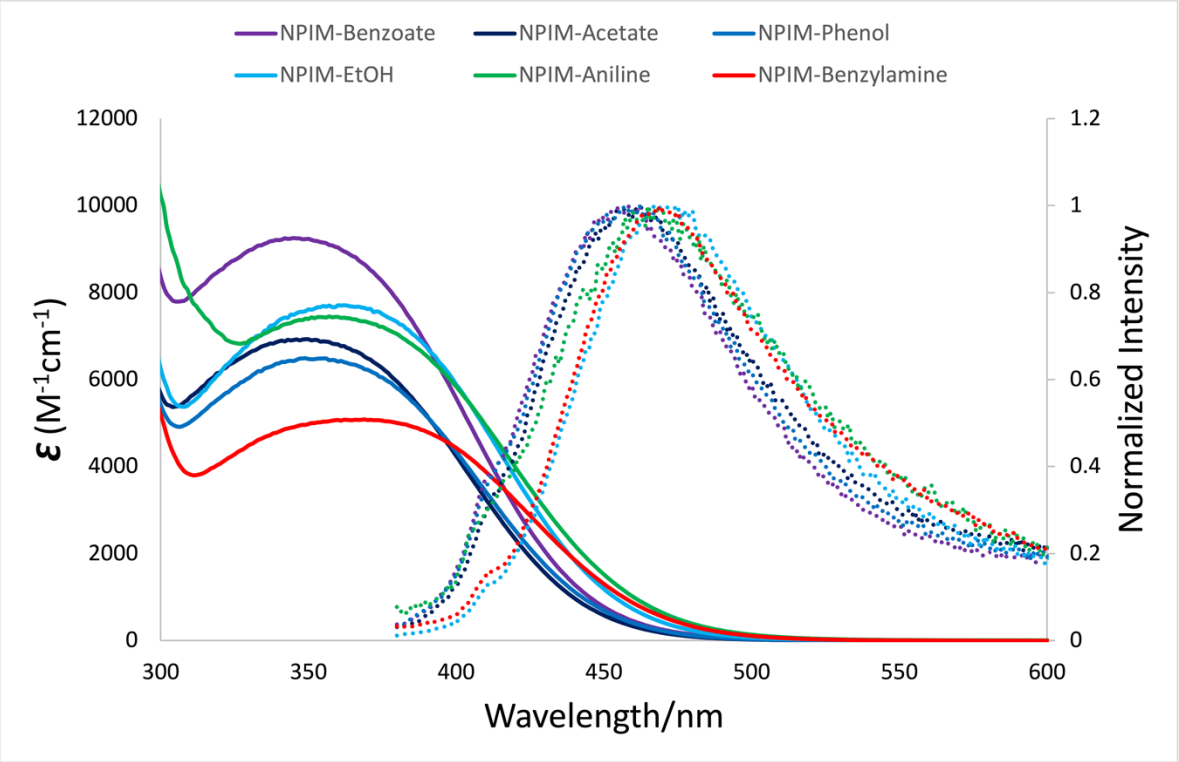

Figure 15. Absorption (solid) and fluorescence emission (dashed) spectra of the NPIM derivatives in DMSO.

First, the 1P uncaging reaction of **NPIM-Benzoate** was conducted in DMSO-d_6 under air using a 405 nm light-emitting diode (LED) lamp (entry 1, Figure 16). After 4 h irradiation, the reaction was almost complete, releasing benzoic acid in a 98% yield. Simultaneously, 1-ethyl-2-(4-nitrophenyl)-1*H*-indole-3-carbaldehyde (**NPIM-Ald**) was isolated in a 36% yield. Based on the ^{1}H NMR signals (Figure 16c), there are no isolable products other than Benzoate and **NPIM-Ald**. The low yield of **NPIM-Ald** is due to a secondary photoreaction, as the independent irradiation of **NPIM-Ald** produced a complex mixture (Figure S32). The quantum yield of the photochemical decomposition of **NPIM-Benzoate** was determined to be 2% in DMSO using potassium ferrioxalate as a chemical

actinometer (SI).

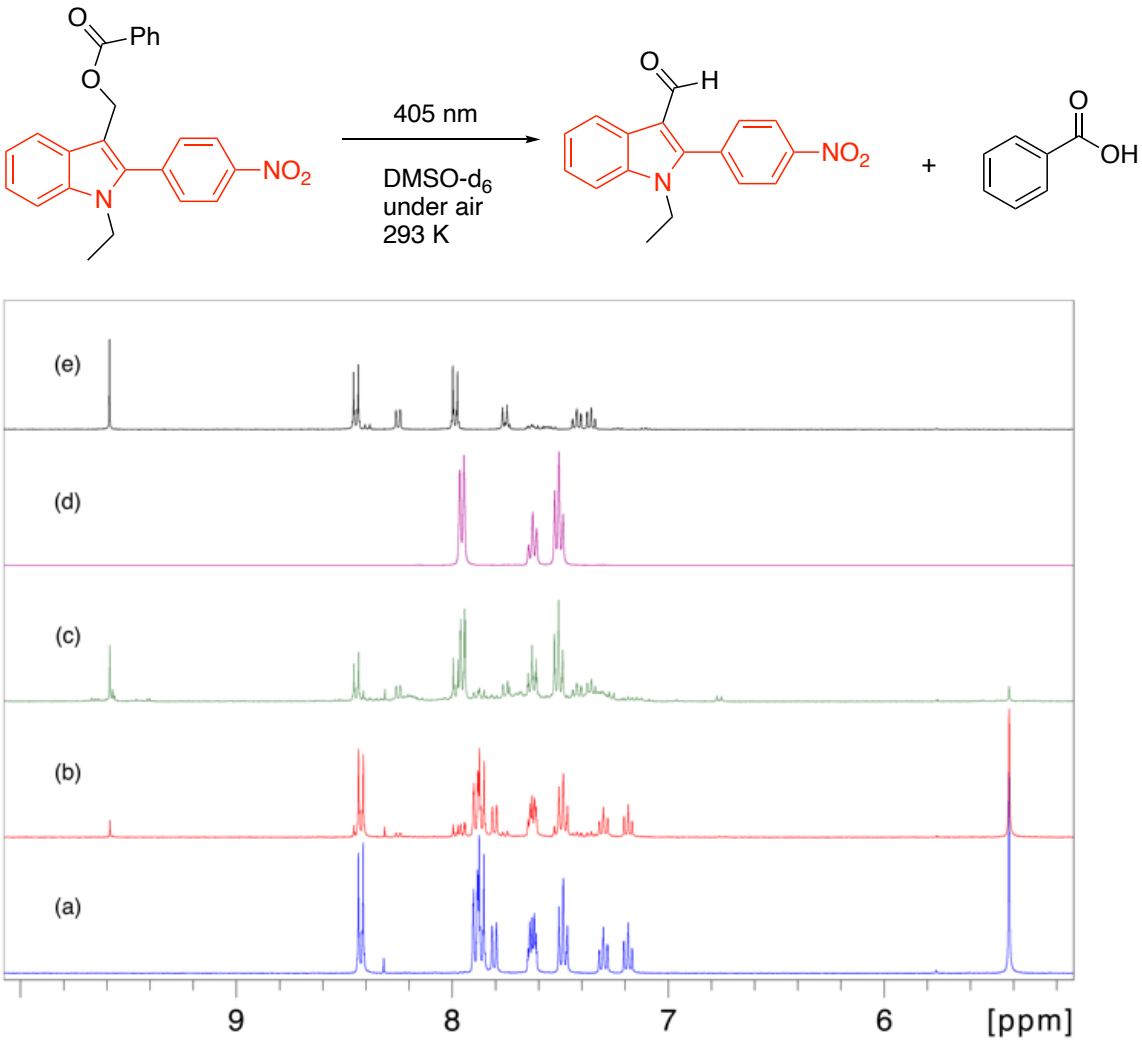

Figure 16. ^{1}H NMR spectral analysis of **NPIM-Benzoate** photolysis (12 mM) at 405 nm in DMSO-d_6; (a) before irradiation; (b) after 1 h irradiation; (c) after 4 h irradiation; ^{1}H NMR spectra in DMSO-d_6 of (d) benzoate and (e) 1-ethyl-2-(4-nitrophenyl)-1*H*-indole-3-carbaldehyde (**NPIM-Ald**), δ 6–9 ppm.

The photolysis of **NPIM-Benzoate** was also evaluated under different conditions (Table 4, Figures S33–35). In DMSO (entry 1 in Table 4), the yield of benzoic acid was high,

although the reaction rate was slow. Conversely, in benzene, the yield was low, but the reaction rate was much faster (entry 4) than that in DMSO. In acetonitrile (entry 2), the yield of benzoate was higher than that in benzene but lower than that in DMSO. The reaction rate was faster than that in DMSO but slower than that in benzene. The formation of benzoate is influenced by the water concentration in the solvent, which is the proton source for benzoate formation. The concentration of water in deuterated DMSO (<0.2%) and acetonitrile (<0.1%) should be higher than that in non-polar benzene (<0.05%). The chemical yield of benzoate can be improved to 64% by adding D_2O to C_6D_6, which indicates water can promote uncaging reaction.

To investigate the formation mechanism of **NPIM-Ald**, the photochemical reaction was conducted in acetonitrile under N_2 (entry 3). The yield of benzoate decreases, with a longer reaction time required to complete the photoreaction. Furthermore, the yield of **NPIM-Ald** decreases to 20%. The complete removal of O_2 is difficult from the reaction solution. Therefore, O_2 plays a role not only in the formation of **NPIM-Ald** but also in the photochemical decomposition of starting compound.

Subsequently, photochemical deprotections (uncaging) were conducted for other leaving groups (entries 2–6 in Table 3, Figures S27–31). Acetic acid is also cleanly released in an 86% yield from NPIM chromophore, along with the formation of **NPIM-Ald** (35%) under similar photoreaction conditions in DMSO (entry 2 in Table 3). Remarkably, alcohols such as phenol and ethanol in yields of 95% and 87%, respectively, are also efficiently produced upon irradiation at 405 nm under air in DMSO (entries 3 and 4 in Table 3).

Table 4. Photolysis of **NPIM-Benzoate** under different conditions.

entry	solvent	Conditions	reaction time (min)	yields of **Benzoate** and **NPIM-Ald** (%)	quantum yield (%)[a]
1	DMSO-d_6	under air	240	**Benzoate** (98) **NPIM-Ald** (36)	2
2	CD_3CN	under air	40	**Benzoate** (80) **NPIM-Ald** (26)	12
3	CD_3CN	under N_2[b]	90	**Benzoate** (55) **NPIM-Ald** (20)	5
4	C_6D_6	under air	10	**Benzoate** (51) **NPIM-Ald** (16)	45
5	C_6D_6/D_2O (29/1) v/v	under air	25	**Benzoate** (64) **NPIM-Ald** (9)	19

[a] Quantum yields of the consumption of **NPIM-Benzoate** were determined using a ferrioxalate actinometer.

[b] N_2 bubbling for 20 min.

Based on the results, we propose a mechanism for the photochemical decomposition of **NPIM-Benzoate** (Scheme 1). **NPIM-Benzoate** absorbs light, generating the singlet excited state **NPIM-Benzoate** *, followed by homolytic cleavage to produce the radical pair. Radical recombination regenerates **NPIM-Benzoate**. Alternatively, the oxygen trapping reaction produces the photolabile hydroperoxide **4** that decomposes to **NPIM-Ald**.[36] Alcohol **NPIM-OH** was not observed in the photolysate (Figure S26). Thus, homolysis and not heterolysis is proposed for the bond cleavage in the excited state.

Scheme 4. Proposed mechanism of the photochemical decomposition of **NPIM-Benzoate**.

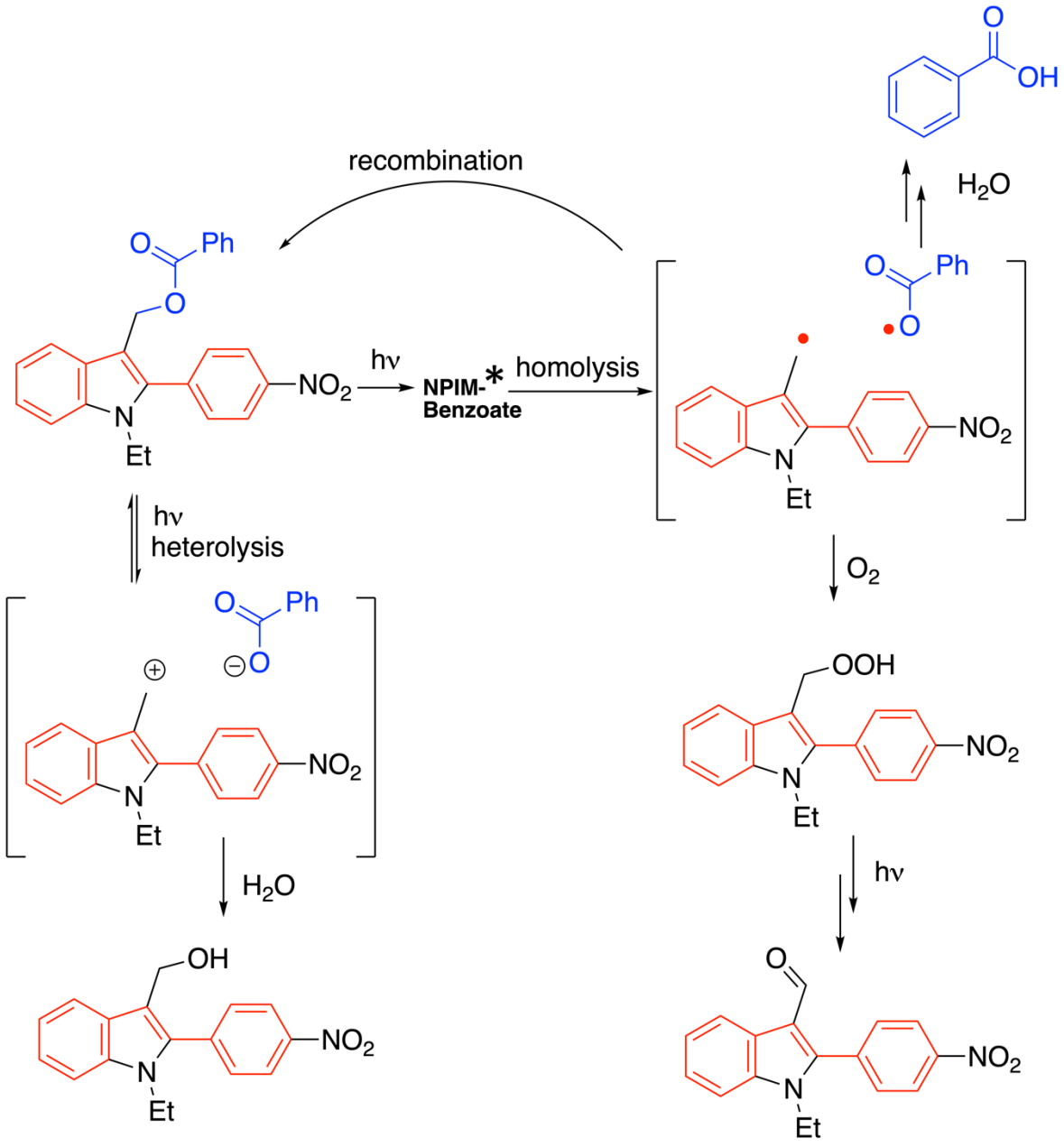

The amine functional group is crucial for the bioactivities of neurotransmitters, such as serotonin and dopamine. The direct release of amines is, thus, examined upon the photolyses of **NPIM-Aniline** and **NPIM-Benzylamine** (entries 5 and 6 in Table 3). The

release of aniline in a 62% yield was clearly observed, along with **NPIM-Ald** (59%), in the photolysis of **NPIM-Aniline** in DMSO under air (entry 5). Benzylamine was also successfully produced in a 57% yield in the photolysis of **NPIM-Benzylamine** (entry 6 in Table 3). Therefore, the NPIM chromophore is an excellent PPG, because the carbonate and carbamate linkers are not needed.

As the NPIM chromophore could now be used in biological studies, the cytotoxicity and NIR-2P-excitation of **NPIM-Benzoate** were studied (Figures 17 and 18). Incubating HeLa cells with different concentrations of **NPIM-Benzoate** for 12 h indicates that **NPIM-Benzoate** exhibits low cytotoxicity (Figure 17).

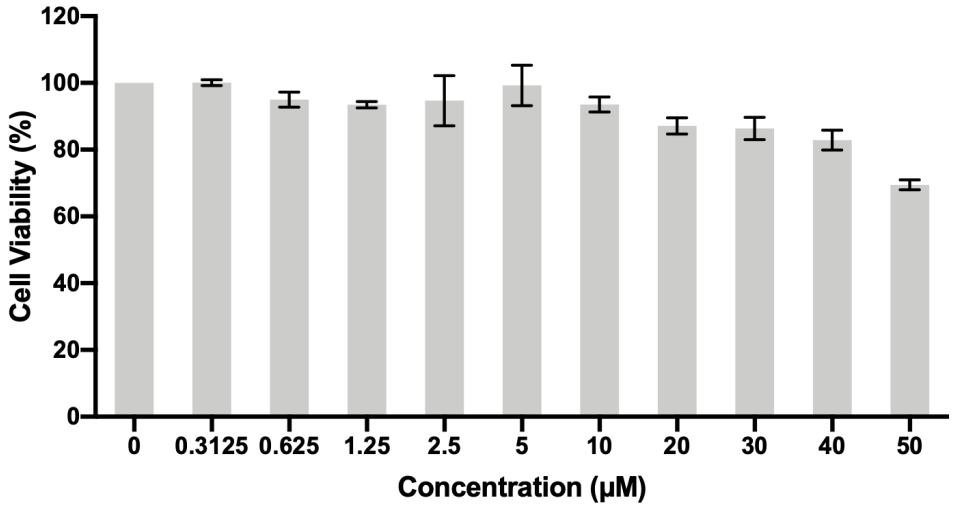

Figure 17. Cell viabilities of HeLa cells exposed to different concentrations of **NPIM-Benzoate**.

2P photolysis of **NPIM-Benzoate** was measured in DMSO using 700, 720, 750, and 780 nm light from a Ti: Sapphire laser. The consumption of **NPIM-Benzoate** during irradiation was determined using high performance liquid chromatography (SI). The 2P

uncaging rates differ according to excitation wavelength, with the fastest rate observed at 780 nm. By employing a standard reference NPBF, the 2P absorption cross section is estimated as 198 GM at 780 nm. This potentially reveals a 2P uncaging efficiency of ~4 GM (198 GM × 2%), which is sufficient to overcome the threshold (3 GM) of biological application.

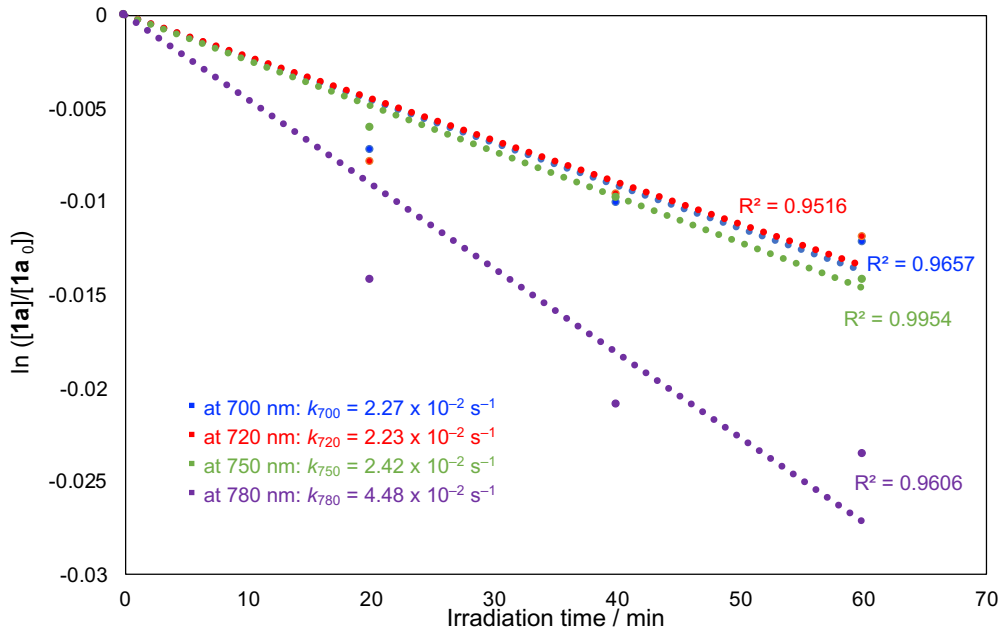

Figure 18. Time profile of the 2P uncaging of **NPIM-Benzoate** represented as ln([NPI]/[NPI]$_0$) as a function of irradiation time at wavelengths of 700, 720, 750, and 780 nm.

3-3. Conclusions

In summary, we developed a 1P- and 2P-responsive PPG, NPIM, which showed efficient photochemical release of carboxylic acids, alcohols, and amines. Also detected during

photolysis was **NPIM-Ald**, which was formed by the reaction of the intermediate radical with molecular oxygen. The photochemical release was accelerated by the presence of oxygen, suggesting that homolysis occurred in the excited state, releasing the X group. **NPIM-Benzoate** exhibited low cytotoxicity, indicating that the protected bioactive compounds based on NPIM could be used in further biological studies.

3-4. Supporting information

Experimental section

Dry acetonitrile (ACN, Spectro grade), DMSO, acetone (Spectro grade) and dimethylformamide (DMF, super dehydrated) were purchased from commercial suppliers and stored at least 24 h under nitrogen gas over activated 3 Å molecular sieves (3 Å MS), which were predried at 300 °C for 24 h before use.[79] ^{1}H NMR spectra were obtained at 400 MHz, chemical shifts are reported in ppm, and referenced to the $CHCl_3$ singlet at 7.26 ppm. ^{13}C NMR spectra were obtained at 100 MHz and referenced to the center peak of the $CDCl_3$ triplet at 77.02 ppm. The abbreviations s, d, t, and m stand for the resonance multiplicities singlet, doublet, triplet, and multiplet, respectively. UV-vis spectra were recorded on a SIMADZU UV-3600 Plus spectrophotometer. Mass-spectrometric data were measured with a mass spectrometric Thermo Fisher Scientific LTQ Orbitrap XL. HeLa cells (RCB0007) were procured from RIKEN BRC through the National Bio-Resource Project of MEXT/AMED, Japan. Cells were cultured in Dulbecco's

Modified Eagle's Medium (DMEM, 05919, NISSUI PHARMACEUTICAL CO., LTD, Tokyo, Japan) supplemented with 10% (v/v) fetal bovine serum (8048, Biological Industries) at 37 ℃ in a 5% CO_2 humidified atmosphere.

Cytotoxicity assay

The cell viability was assessed by Cell Counting Kit-8 (CK04, Dojindo, Kumamoto, Japan) according to the manufacturer's instructions. Briefly, HeLa cells were seeded in clear bottom 96-well plate at density of 10000 cells per well for 40 hours prior to compound treatment. Then the medium was replaced with 100 μL of fresh medium with different concentration of **NPIM-Benzoate** in DMSO. After treatment for 12 h, 10 μL of CCK-8 solution was added to each well and the plate was incubated at 37℃ for 1 hour. The absorbance of 450 nm was quantified on a microplate reader (SpectraMax iD3, Molecular Devices, CA, USA). The cell viability was calculated by the following formula:

Cell Viability (%) = $[(OD_{test} - OD_{blank})/ (OD_{control} - OD_{blank})] \times 100$

2-(4,4,5,5-tetramethyl-1,3,2-dioxaborolan-2-yl)-1*H*-indole (9)[78]

Inside a glove box, $[Ir(cod)OMe]_2$ (6.4 mg, 0.0096 mmol), dtbpy (5.2 mg, 0.019 mmol), bis(pinacolato)diboron (162.2 mg, 0.64 mmol), the indole (150.1 mg, 1.28 mmol), and THF (2 mL) were added consecutively to a dry vial with a magnetic stir bar. The vial was sealed and heated at 80 °C for 18 h. The reaction mixture was cooled to room temperature, concentrated and purified by column chromatography to give the product. (278.5 mg, 89.5%), EtOAc:hexane = 1:9 (Rf = 0.3). ^{1}H NMR (400 MHz, CDCl3): δ = 8.69 (br, 1 H),

7.73 (dd, J = 8 and 0.8 Hz, 1 H), 7.43 (dd, J = 8.4 and 1.2 Hz, 1 H), 7.29–7.25 (m, 1 H), 7.17–7.14(m, 2 H), 1.42 (s, 12 H).

2-(4-nitrophenyl)-1*H*-indole (NPI)[78]

To a solution of 1-iodo-4-nitrobenzene (1.0 g, 4.14 mmol) and **1** (1.0 g, 4.12 mmol), K_2CO_3 (74.1 mg, 0.44 mmol) in THF/H_2O (1:1) (10 mL) was added $Pd(PPh_3)_4$ (230.2 mg, 0.2 mmol) under N_2. The mixture was heated and reflux for 15 h. The reaction mixture was quenched with satu- rated NH_4Cl solution and extracted with ethyl acetate. The combined extracts were washed with water, dried (Na_2SO_4), and evaporated under reduced pressure. Flash chromatography on silica gel using hexane/ethyl acetate afforded target. (0.80 g, 81%). ^{1}H NMR (400 MHz, CD_3OD): δ = 8.32 (d, J = 9.1 Hz, 2 H), 8.03 (d, J = 9.1 Hz, 2 H), 7.61 (d, J = 7.9 Hz, 1 H), 7.45 (d, J = 7.9 Hz, 1 H), 7.19 (t, J = 8.5 Hz, 1 H), 7.09 (s, 1 H), 7.06 (t, J = 8.5 Hz, 1 H).

1-ethyl-2-(4-nitrophenyl)-1*H*-indole (NPI-Et)

Compound **2** (2.38 g, 0.01 mol), KOH (0.57 g, 0.01 mol) in 30 mL MeCN was stirred for 30 min at rt. To the mixture iodoethane (1.57 g, 0.01 mol) was added and stirred 12 h. Reaction stopped and poured mixture into water extracted with EtOAc three times, washed with brine, dried with $NaSO_4$, solvent removed to get crude product. Flash chromatography on silica gel afforded pure product (2.52 g, 95%). ^{1}H NMR (400 MHz, $CDCl_3$) δ = 8.36 (d, J = 9.0 Hz, 2 H), 7.7 (d, J = 8.9 Hz, 2 H), 7.68 (d, J = 8.5 Hz, 1 H), 7.45 (d, J = 8.5 Hz, 1 H), 7.31 (t, J = 6.8 Hz, 1 H), 7.19 (t, J = 6.8 Hz, 1 H), 6.69 (s, 1 H), 4.27 (q, J = 7.3 Hz,2 H), 1.37 (t, J =7.3 Hz, 3 H); ^{13}C NMR (100 MHz, $CDCl_3$) δ 147.2, 139.8, 138.4, 138.1, 129.5, 128.1, 123.9, 122.8, 121.2, 120.5, 110.3, 104.6, 39.1, 15.4. mp

113-115 °C; HRMS–ESI: calcd for $C_{16}H_{15}O_2N_2$: 267.11335, found 267.11039 $[M+H]^+$.

1-ethyl-2-(4-nitrophenyl)-1*H*-indole-3-carbaldehyde (NPIM-Ald)

$POCl_3$(4.8ml, 0.02 mol) was slowly added dropwise to DMF (8 mL) under ice bath. The mixture was stirred at ice bath for 30 min. Then, DMF (7 ml) solution of 3 (5.81 g, 0.02 mol) was added dropwise to the reaction system. Keeping the reaction at room temperature for 3 h, ice cold $NaHCO_3$ solution was added into the reaction system and continue to stir to a lot of yellow solid precipitation. The solid was recrystallized from ethyl acetate and petroleum ether to obtain **NPIM-Ald** (4.89 g, 0.017 mol) in yields of 97.6%.^{1}H NMR (400 MHz, $CDCl_3$) δ = 9.74 (s, 1 H), 8.46 (d, J = 9.2 Hz, 3 H), 7.74 (d, J = 9.2 Hz, 2 H), 7.38-7.5 (mult, 3 H), 4.15 (q, J = 7.4 Hz, 2 H), 1.38 (t, J = 7.4 Hz, 3 H); ^{13}C NMR (100 MHz, $CDCl_3$) δ 185.4, 148.6, 147.1, 136.4, 135.7, 131.8, 125.5, 124.7, 123.8, 123.7, 122.5, 116.7, 110.2, 39.3, 15.3; mp 115-116 °C; HRMS–ESI: calcd for $C_{17}H_{14}N_2O_3Na$: 317.09021, found 317.08978 $[M+Na]^+$.

(1-ethyl-2-(4-nitrophenyl)-1*H*-indol-3-yl)methanol (NPIM-OH)

To a solution of **NPIM-Ald** (2.91g, 10 mmol) in MeOH (20ml) was added $NaBH_4$ (0.5 g, 13.5 mmol) under ice bath, mixture was stirred for 1 h at room temperature. Solvent remove to get crude and purified by silica gel chromatography (EtOAc : hexane = 1:3, rf = 0.3) to gather **NPIM-OH** (1.2 g, 0.004 mmol) in yield of 40%. ^{1}H NMR (400 MHz, $CDCl_3$) δ = 8.41 (d, J = 8.9 Hz, 2 H), 7.83 (d, J = 8.1 Hz, 1 H), 7.71 (d, J = 8.9 Hz, 2 H), 7.45 (d, J = 8.1 Hz, 1 H), 7.36 (t, J = 7.7 Hz, 1 H), 7.26 (t, J = 7.7 Hz, 1 H), 4.76 (d, J = 4.7 Hz, 2 H), 4.16 (q, J = 7.3 Hz,2 H), 1.30 (t, J = 7.3 Hz, 3 H); ^{13}C NMR (100 MHz, $CDCl_3$) δ 147.66, 138.08, 136.75, 136.64, 131.27, 127.4, 123.73, 123.1, 120.54, 119.38,

114.67, 110.12, 55.9, 39.2, 15.4; mp 145-147 °C; HRMS–ESI: calcd for $C_{17}H_{16}O_2N_3$: 296.11069, found 296.11591 $[M+H]^+$.

(1-ethyl-2-(4-nitrophenyl)-1*H*-indol-3-yl)methyl acetate (NPIM-Acetate)

To a solution of **NPIM-OH** (296 mg, 1 mmol) in 10 ml of DCM and 3 ml of acetone containing 100 mg DMAP was added acetic anhydride (102 mg, 1 mmol). The solution was stirred for 10 min and directly flash-chromatograghed with EtOAc as eluent. The eluted solution was washed with $NaHCO_3$ solution, dried with Na_2SO_4, evaporate solvent to get crude. silica gel chromatography (EtOAc : hexane = 1:3, rf = 0.4) to gather **NPIM-Acetate** (330.2 mg, 1 mol) in yields of 97%. ^{1}H NMR (400 MHz, $CDCl_3$) δ = 8.41 (d, *J* = 8.3 Hz, 2 H), 7.79 (d, *J* = 8.3 Hz, 1 H), 7.67 (d, *J* = 8.3 Hz, 2 H), 7.45 (d, *J* = 8.3 Hz,1 H) 7.36 (t, *J* = 8.3 Hz, 1 H) 7.26 (t, *J* = 8.3 Hz, 1 H) 5.21 (s, 2 H) 4.14 (q, *J* = 7.2 Hz, 2 H), 2.1 (s, 3 H), 1.29 (t, *J* = 7.2 Hz, 3H); ^{13}C NMR (100 MHz, CDCl3) δ 171.04, 147.85, 137.81, 137.72, 136.54, 131.35, 127.5, 123.79, 123.23, 120.71, 119.66, 110.07, 109.83, 57.79, 39.04, 21.07, 15.31; mp 136-138°C; HRMS–ESI: calcd for $C_{19}H_{18}N_2O_4$: 361.11643, found 361.11600 $[M+Na]^+$.

(1-ethyl-2-(4-nitrophenyl)-1*H*-indol-3-yl)methyl benzoate (NPIM-Benzoate)

Same procedure with **NPIM-Acetate** to obtain **NPIM-Benzoate** in yield of 95%. ^{1}H NMR (400 MHz, $CDCl_3$) δ = 8.41 (d, *J* = 9.1 Hz, 2 H), 8.03 (d, *J* = 7.8 Hz, 2 H), 7.87 (d, *J* = 7.8 Hz, 1 H), 7.71 (d, *J* = 9.1 Hz, 2 H), 7.56 (t, *J* = 7.8 Hz, 1 H), 7.33-7.48 (mult, 4 H), 7.27 (t, *J* = 8.0 Hz, 1 H), 5.46 (s, 2 H), 4.15 (q, *J* = 7.2 Hz, 2 H), 1.32 (t, *J* = 7.2 Hz, 3 H); ^{13}C NMR (100 MHz, CDCl3) δ 166.5, 147.9, 137.8, 137.7, 136.5, 133.0, 131.4, 130.3, 129.6, 128.4, 127.7, 123.8, 123.2, 120.8, 119.8, 110.1, 109.9, 58.5, 39.1, 15.5; mp

146-148°C; HRMS–ESI: calcd for $C_{24}H_{20}N_2NaO_4$: 423.13208, found 423.13135 $[M+Na]^+$.

1-ethyl-2-(4-nitrophenyl)-3-(phenoxymethyl)-1*H*-indole (NPIM-Phenol)

To a solution of **NPIM-benzoate** (40 mg, 0.1 mmol) in MeCN (5 ml) was added phenol (15 mg, 0.16 mmol), K_2CO_3 (30mg, 0.2 mmol), reflux for 12h. Solvent was removed by vacuum after cooling and extracted with EtOAc, washed with brine, dired with Na_2SO_4. The concentrated crude was purified by silica gel chromatography (EtOAc : hexane = 1:3, rf = 0.35) to obtain **NPIM-Phenol** (32 mg, 0.08 mmol) in yield of 85%. ^{1}H NMR (400 MHz, $CDCl_3$) δ = 8.36 (d, J = 8.8 Hz, 2 H), 7.78 (d, J = 8.4 Hz, 1 H), 7.69 (d, J = 8.8 Hz, 2 H), 7.46 (d, J = 8.4 Hz, 1 H) 7.36 (t, J = 7.8 Hz, 1 H) 7.31 (mlt, 3 H) 7.25 (t, J = 7.8 Hz, 1 H) 6.99 (mlt, 3 H) 5.07 (s, 2 H) 4.18 (q, J = 7.2 Hz, 2 H) 1.32 (t, J = 7.2 Hz, 3 H); ^{13}C NMR (100 MHz, CDCl3) δ 158.84, 147.72, 137.93, 137.45, 136.73, 131.26, 129.46, 127.78, 123.75, 123,21, 120.99, 120.69, 119.55, 114.98, 110.54, 110.12, 61.67, 39.10, 15.37; mp 152-153°C; HRMS–ESI: calcd for $C_{23}H_{20}N_2NaO_3$: 395.13716, found 395.13672 $[M+Na]^+$.

3-(ethoxymethyl)-1-ethyl-2-(4-nitrophenyl)-1*H*-indole (NPIM-EtOH)

Same procedure with **NPIM-Phenol** to obtain **NPIM-EtOH** in yield of 95%. ^{1}H NMR (400 MHz, $CDCl_3$) δ = 8.4 (d, J = 8.56 Hz, 2 H), 7.8 (d, J = 7.85 Hz, 1 H), 7.71 (d, J = 8.6 Hz, 2 H), 7.42 (d, J = 7.8 Hz, 1 H) 7.33 (t, J = 7.8 Hz, 1 H) 7.23 (t, J = 7.8 Hz, 1 H) 4.54 (s, 2 H) 4.15 (q, J = 7.2 Hz, 2 H) 3.57 (q, J = 6.8 Hz, 2 H) 1.27 (mlt, 6 H); ^{13}C NMR (100 MHz, CDCl3) δ 147.56, 138.33, 137.03, 136.75, 131.25, 128.08, 123.61, 122.99, 120.44, 119.65, 112.51, 109.96, 65.47, 63.27, 39.01, 15.34; mp 126-127°C; HRMS–ESI: calcd for

$C_{19}H_{20}N_2NaO_3$: 347.13716, found 347.13669 $[M+Na]^+$.

***N*-((1-ethyl-2-(4-nitrophenyl)-1*H*-indol-3-yl)methyl)aniline (NPIM-Aniline)**

Same procedure with **NPIM-Phenol** to obtain **NPIM-Aniline** in yield of 95%. ^{1}H NMR (400 MHz, $CDCl_3$) δ = 8.37 (d, J = 8.5 Hz, 2 H), 7.77 (d, J = 7.8 Hz, 1 H), 7.69 (d, j = 8.5 Hz, 2 H), 7.49 (d, J = 7.8 Hz, 1 H) 7.38 (t, J = 8.3 Hz, 1 H) 7.23 (mlt, 3 H) 6.67 (t, J = 7.4 Hz, 1 H) 6.65 (d, J = 7.7 Hz, 2 H) 4.35 (s, 2 H) 4.19 (q, J = 6.8 Hz, 2 H) 1.33 (t, J = 7.2 Hz, 3 H); ^{13}C NMR (100 MHz, CDCl3) δ 148.24, 147.66, 138.18, 136.82, 136.3, 131.11, 129.28, 127.55, 123.84, 123.15, 120.43, 119.54, 117.55, 112.79, 112.26, 110.17, 39.24, 39.07, 15.41; mp 131-133°C; HRMS–ESI: calcd for $C_{23}H_{20}N_3O_2$: 370.15555 found 370.15503 $[M-H]^-$.

***N*-benzyl-1-(1-ethyl-2-(4-nitrophenyl)-1*H*-indol-3-yl)methanamine (NPIM-Benzylamine)**

Same procedure with **NPIM-Phenol** to obtain **NPIM-Benzylamine** in yield of 95%. ^{1}H NMR (400 MHz, DMSO-d_6) δ = 8.31 (d, J = 8.2 Hz, 2 H), 7.78 (d, J = 8.2 Hz, 2 H), 7.75 (d, J = 8.1 Hz, 1 H), 7.55 (d, J = 8.1 Hz, 1 H) 7.2 (mlt, 7 H) 4.13 (q, J = 7.1 Hz, 2 H) 3.68 (s, 4 H) 1.11 (t, J = 7.1 Hz, 3 H); ^{13}C NMR (100 MHz, DMSO-d_6) δ 147.35, 138.60, 136.84, 136.27, 131.89, 128.43, 128.09, 126.95, 123.94, 122.86, 120.25, 119.96, 110.76, 52.93, 42.84, 38.85, 15.51; mp 124-125°C; HRMS–ESI: calcd for $C_{24}H_{24}N_3O_2$: 386.18685, found 386.18640 $[M+H]^+$.

1H and 13C Spectra of Compound

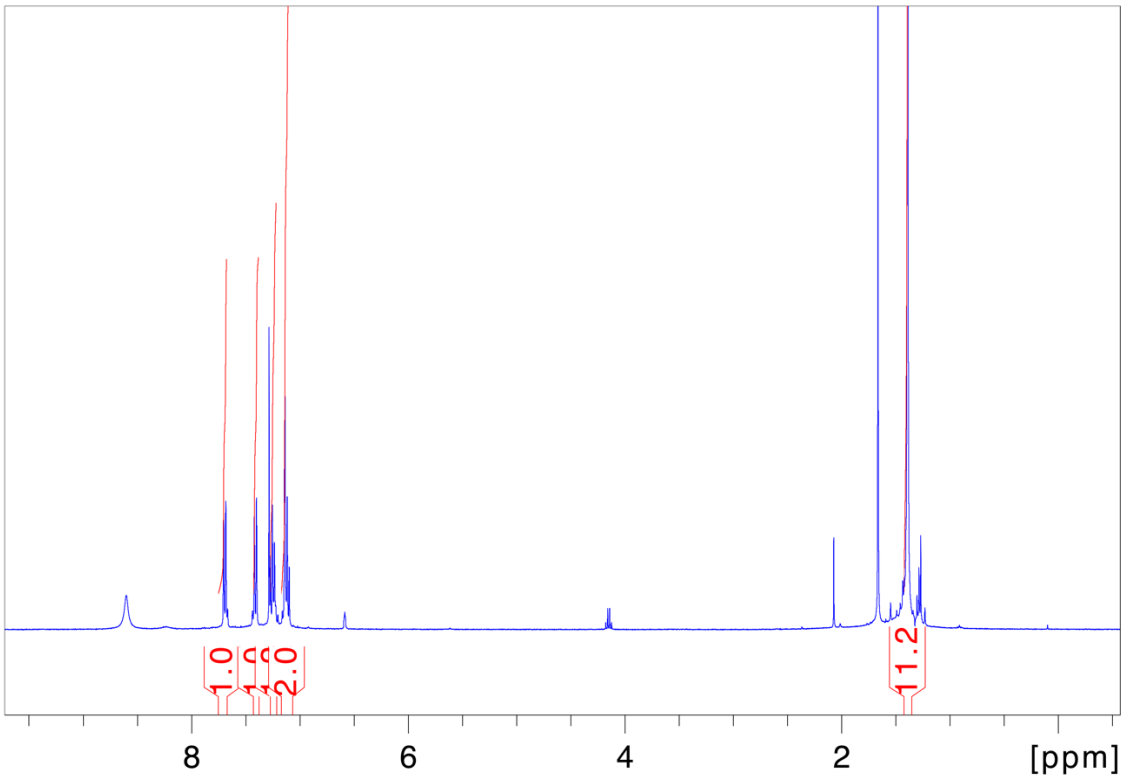

Figure S1. ^{1}H NMR of **9** in $CDCl_3$.

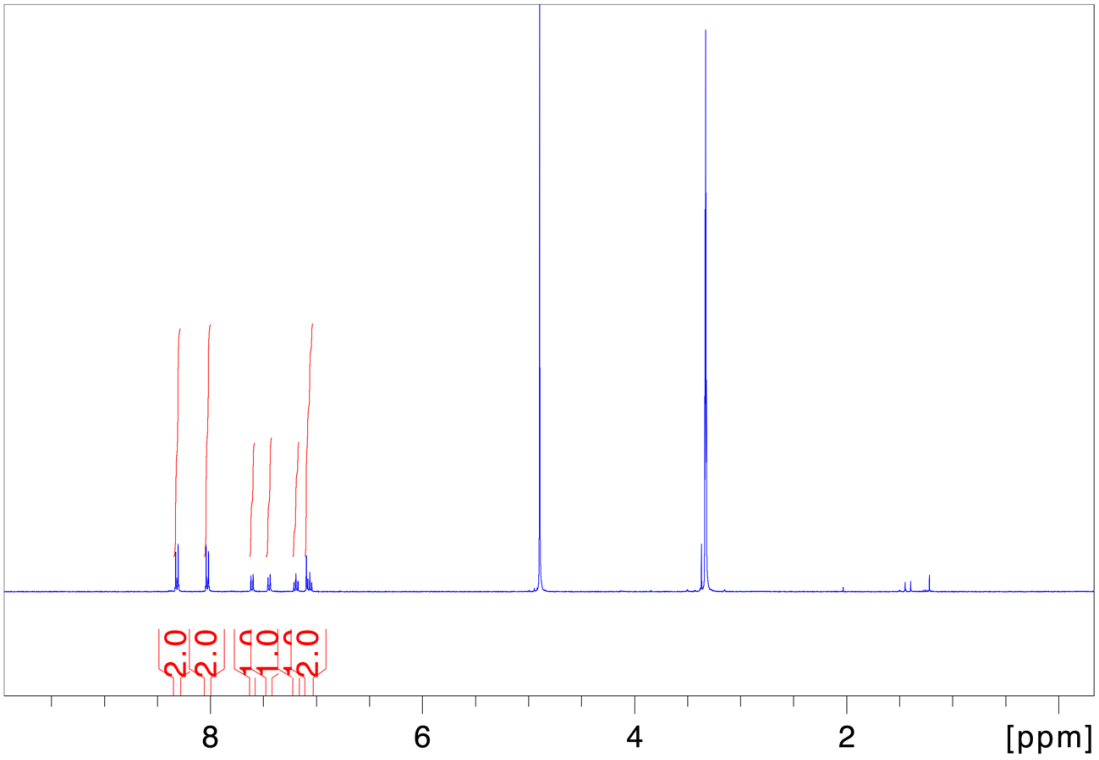

Figure S2. ^{1}H NMR of **NPI** in CD_3OD.

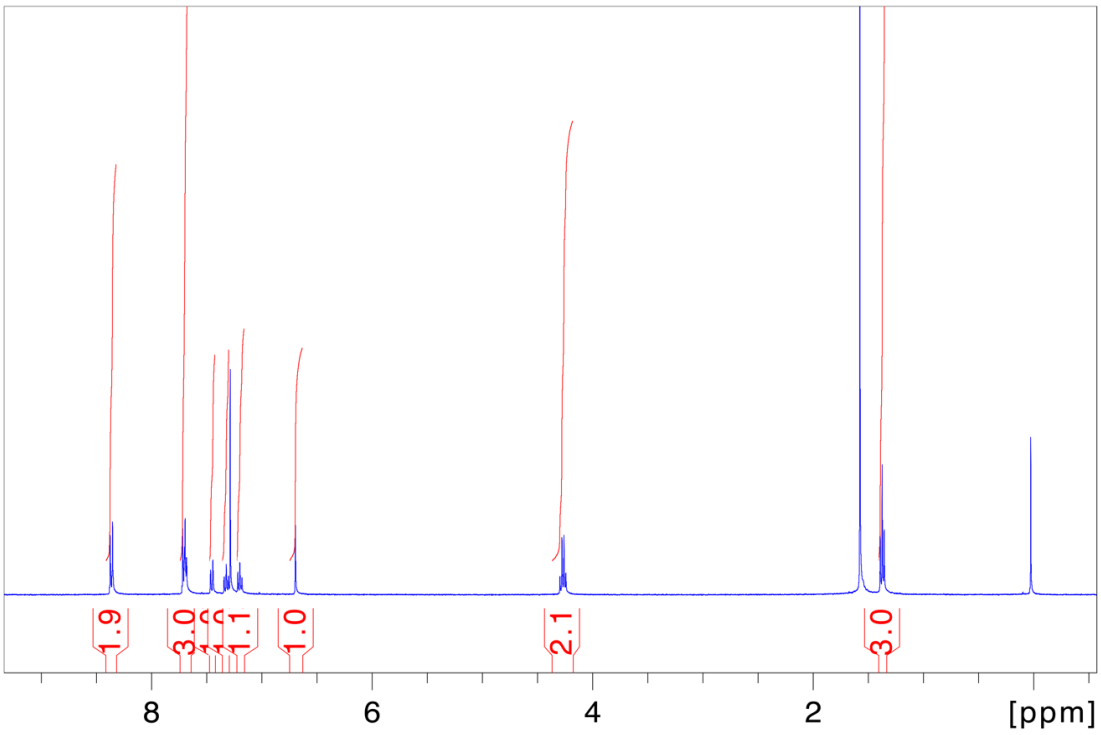

Figure S3. ^{1}H NMR of **NPI-Et** in $CDCl_3$.

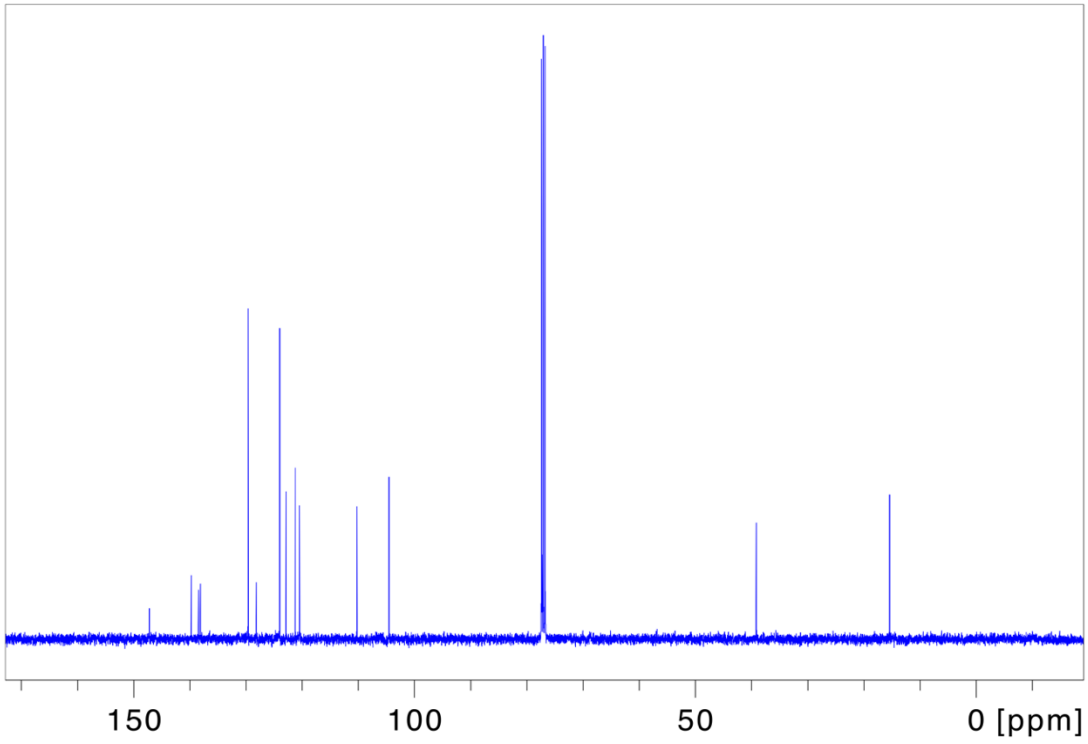

Figure S4. ^{13}C NMR of **NPI-Et** in $CDCl_3$.

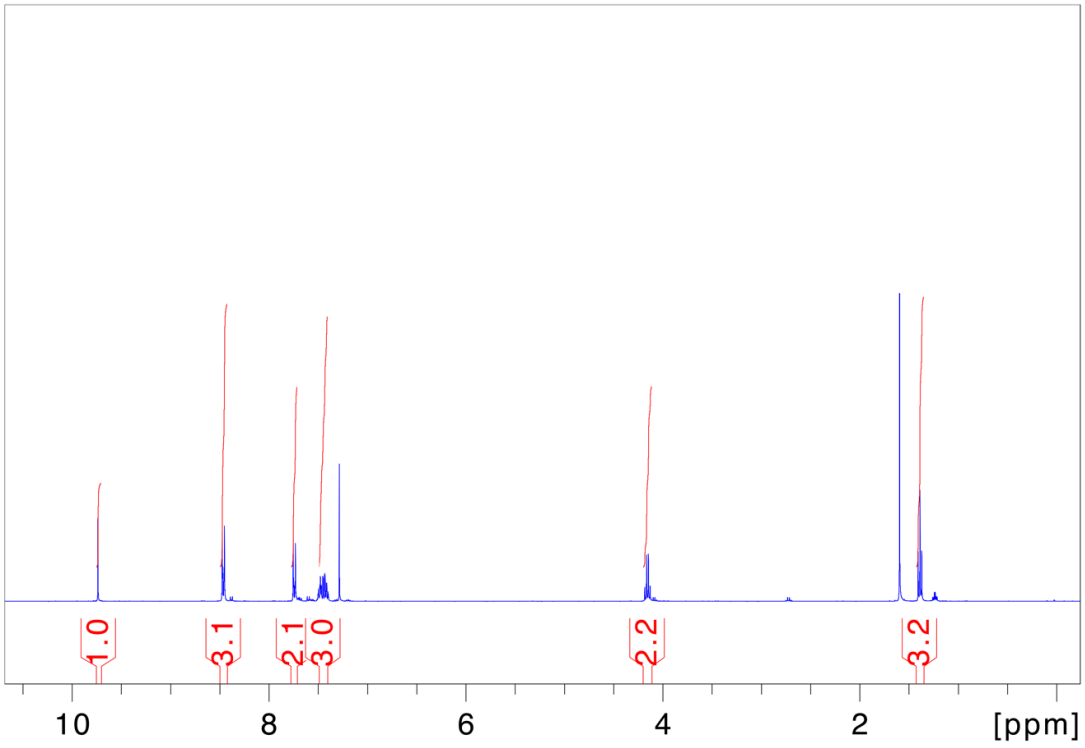

Figure S5. ^{1}H NMR of **NPIM-Ald** in $CDCl_3$.

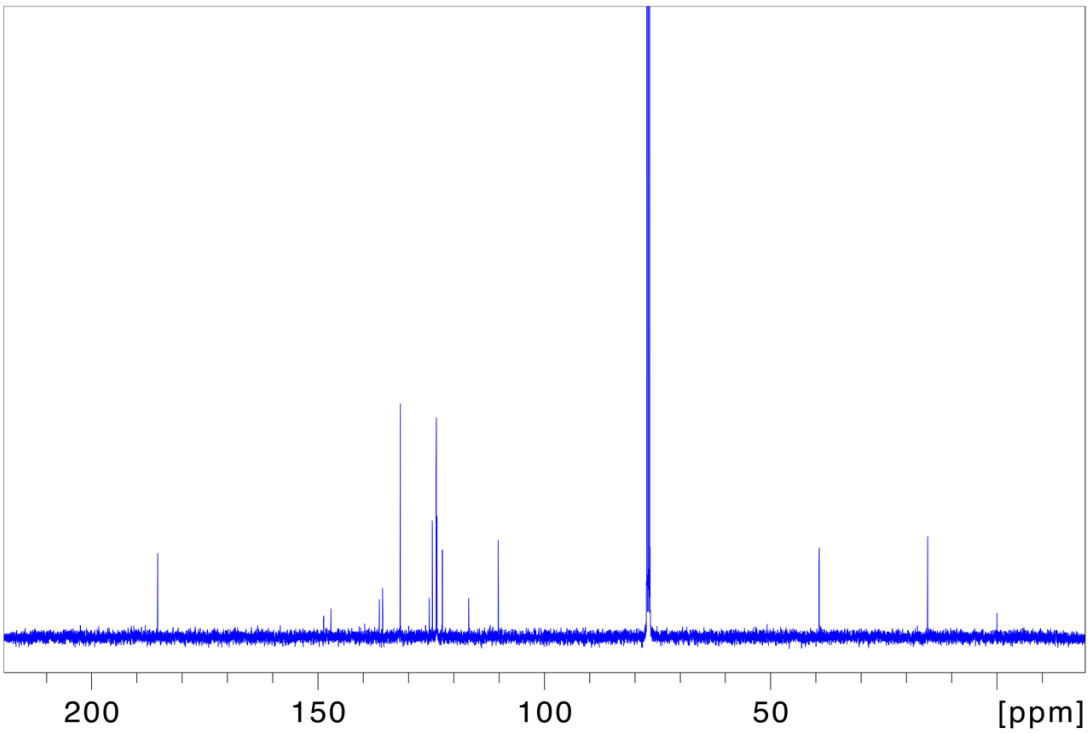

Figure S6. ^{13}C NMR of **NPIM-Ald** in $CDCl_3$.

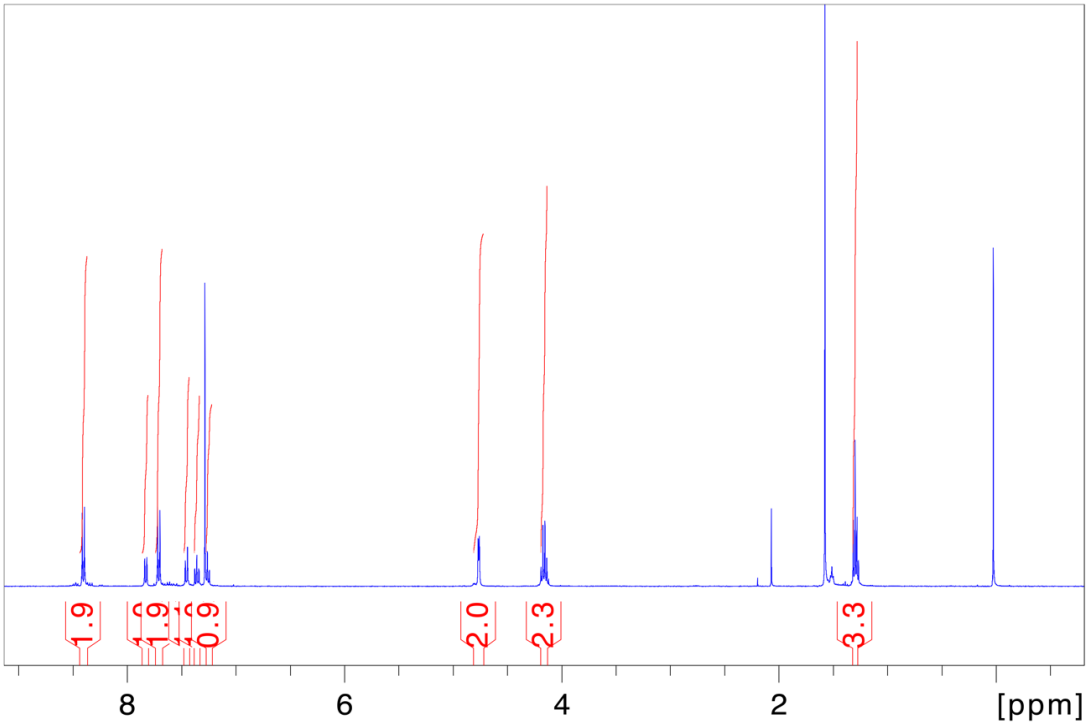

Figure S7. ^{1}H NMR of **NPIM-OH** in $CDCl_3$.

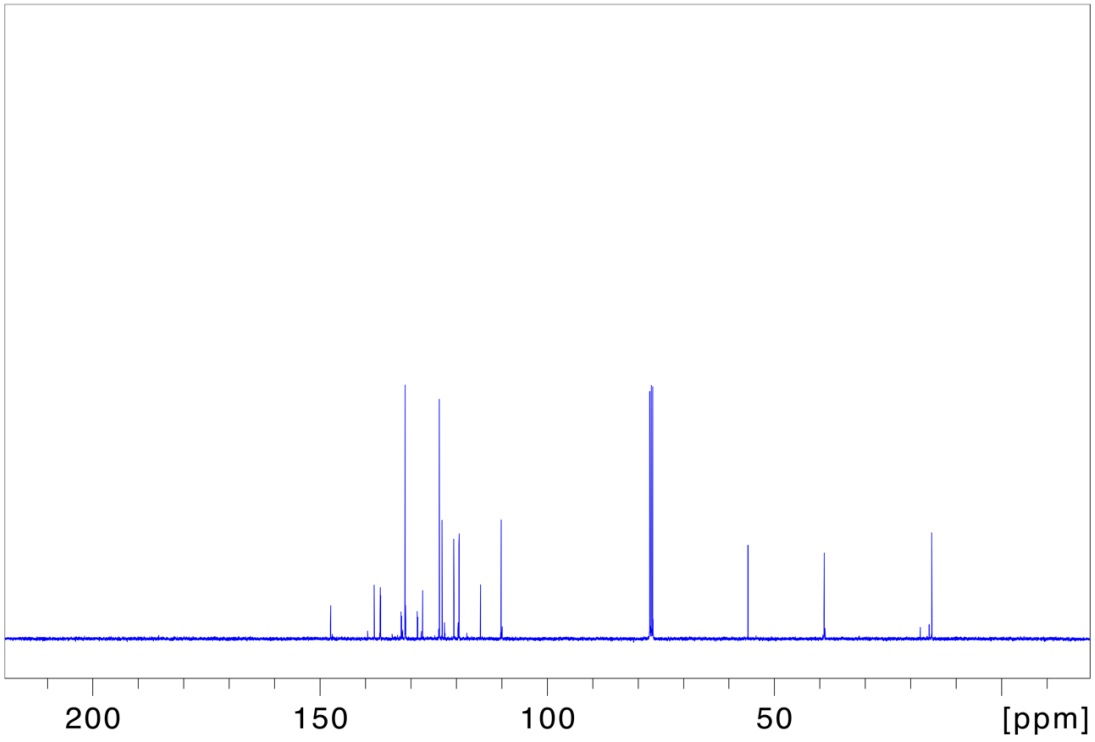

Figure S8. ^{13}C NMR of **NPIM-OH** in $CDCl_3$.

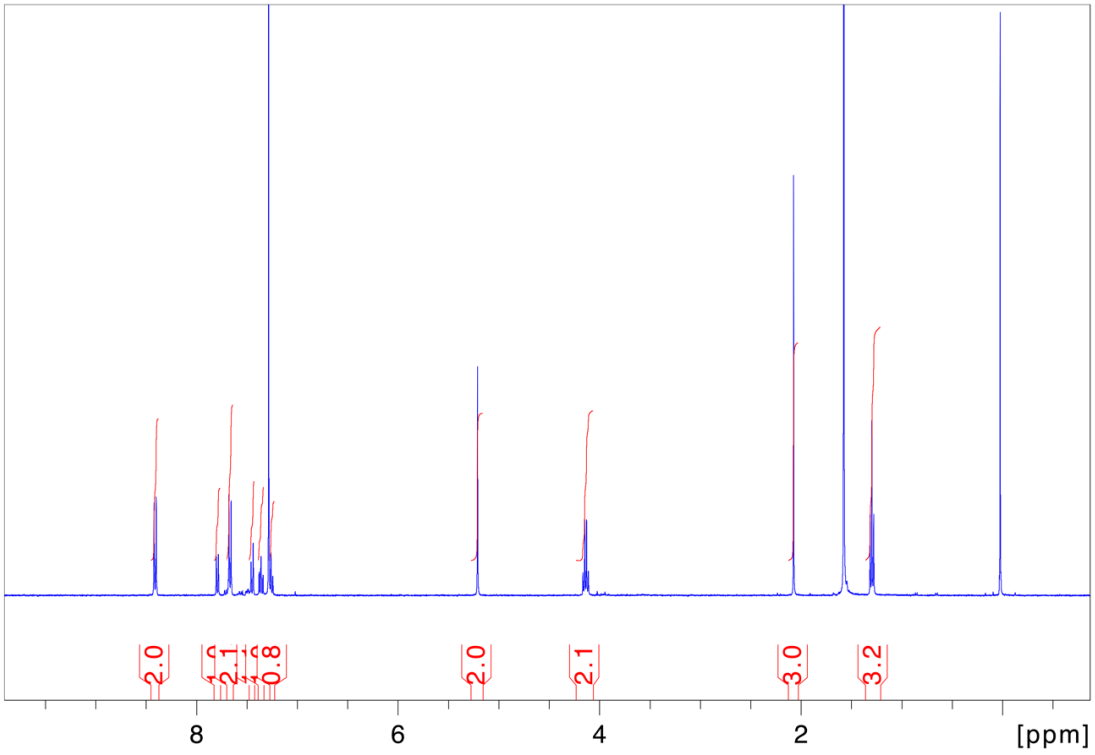

Figure S9. ^{1}H NMR of **NPIM-Acetate** in $CDCl_3$.

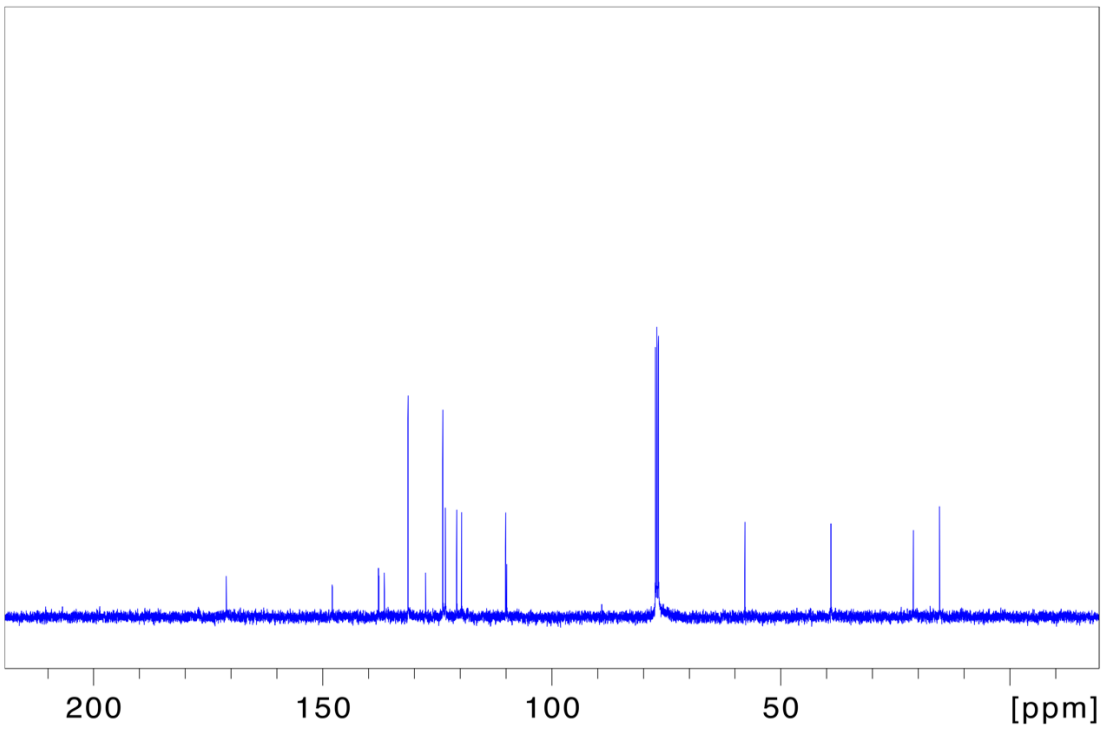

Figure S10. ^{13}C NMR of **NPIM-Acetate** in $CDCl_3$.

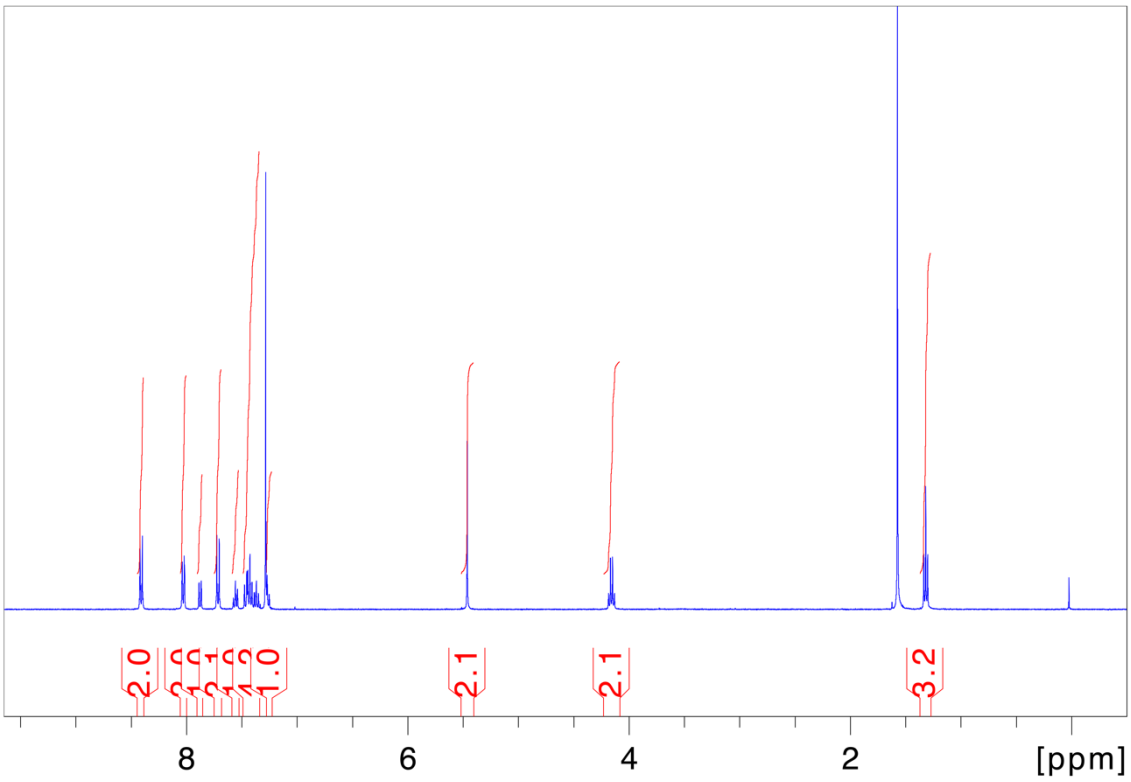

Figure S11. ^{1}H NMR of **NPIM-Benzoate** in $CDCl_3$.

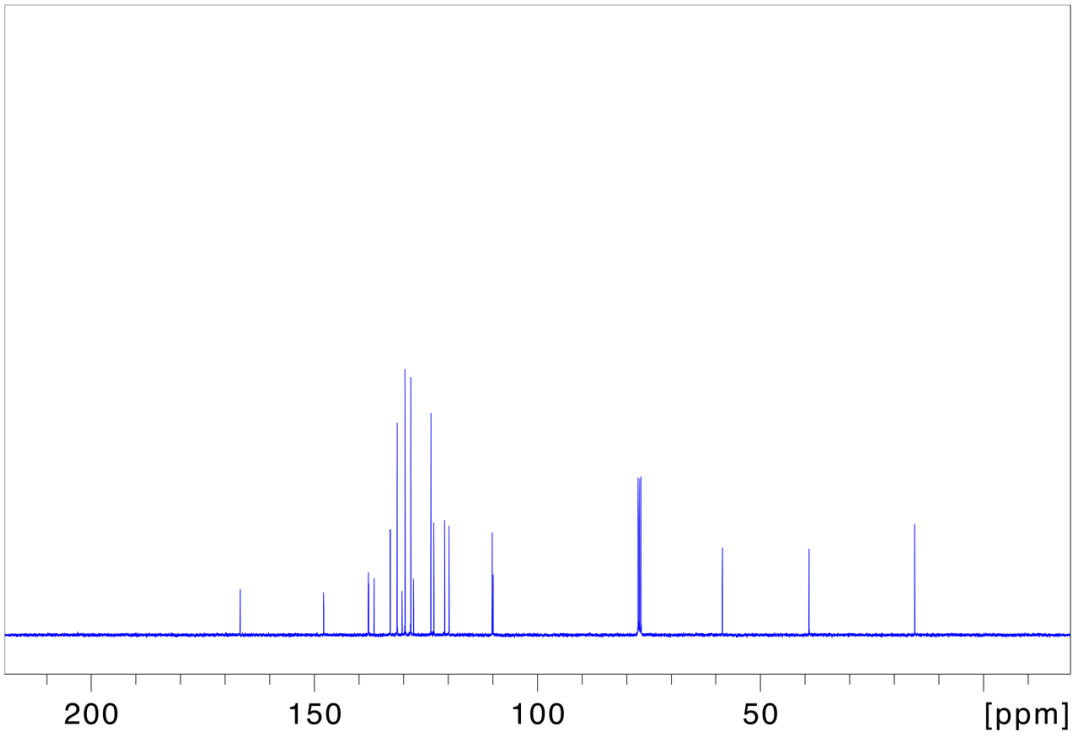

Figure S12. ^{13}C NMR of **NPIM-Benzoate** in $CDCl_3$.

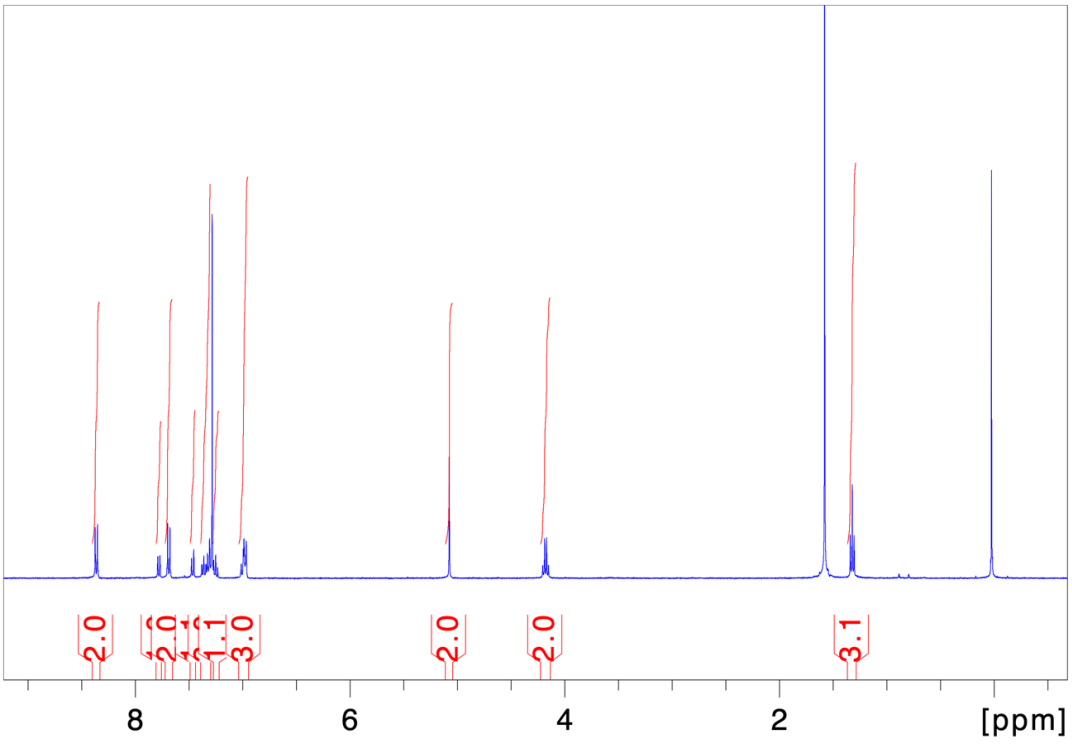

Figure S13. ^{1}H NMR of **NPIM-Phenol** in $CDCl_3$.

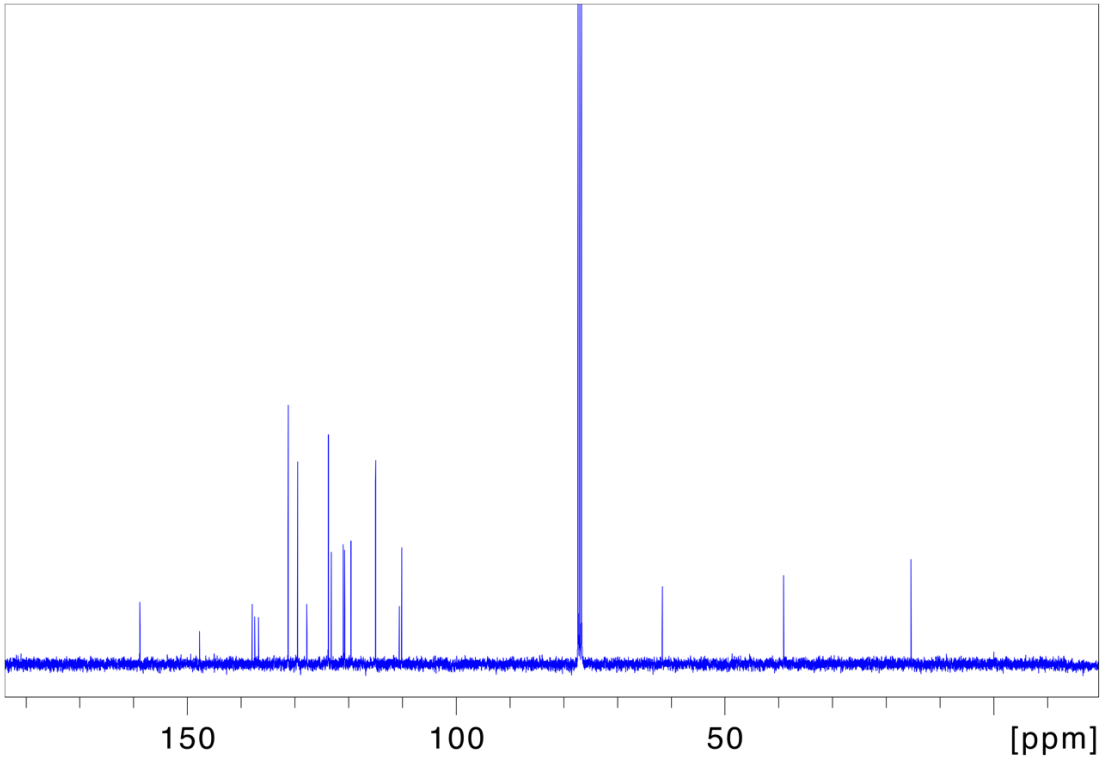

Figure S14. ^{13}C NMR of **NPIM-Phenol** in $CDCl_3$.

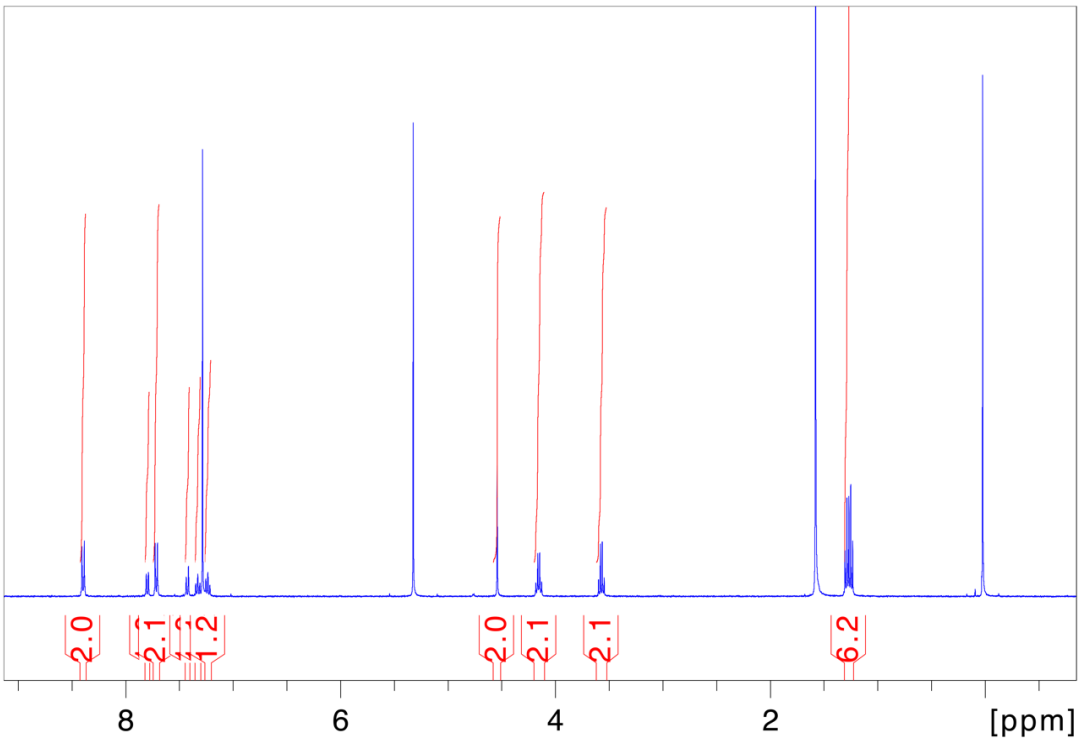

Figure S15. ^{1}H NMR of **NPIM-EtOH** in $CDCl_3$.

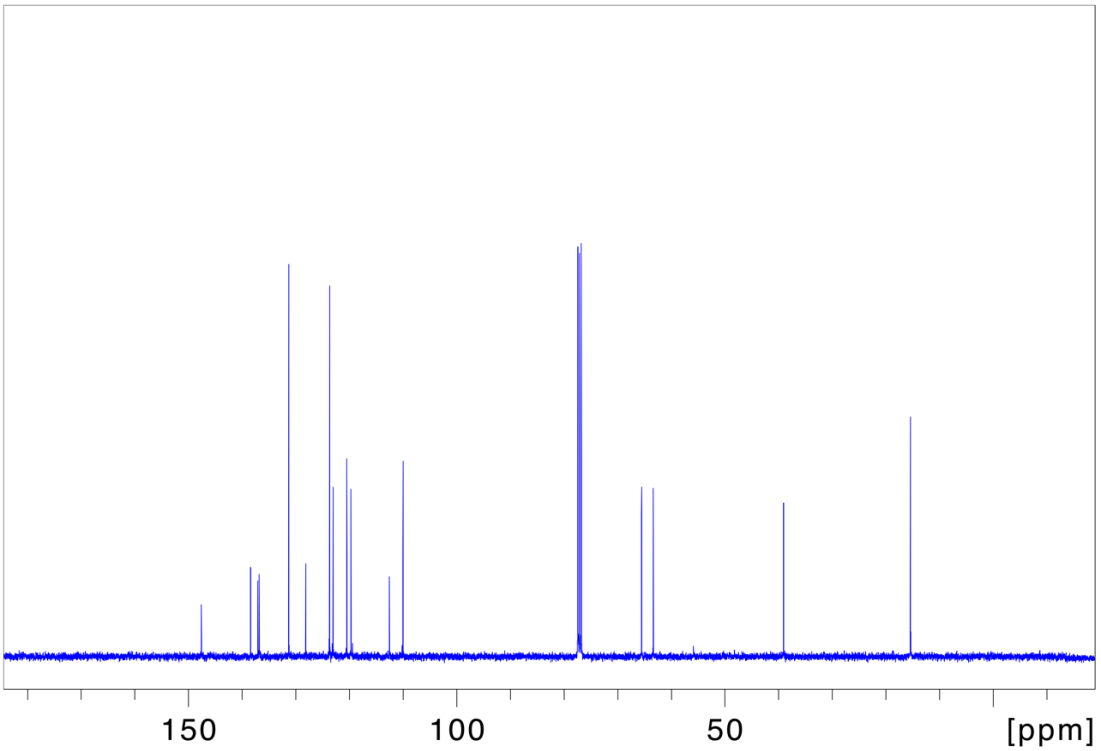

Figure S16. ^{13}C NMR of **NPIM-EtOH** in $CDCl_3$.

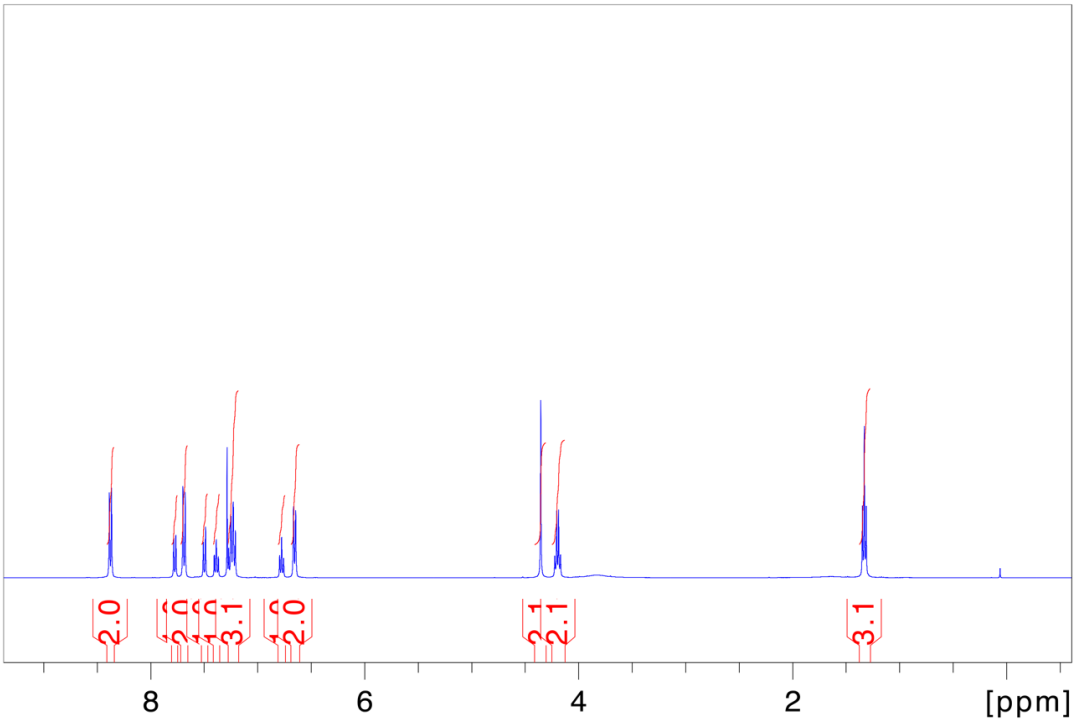

Figure S17. ^{1}H NMR of **NPIM-Aniline** in $CDCl_3$.

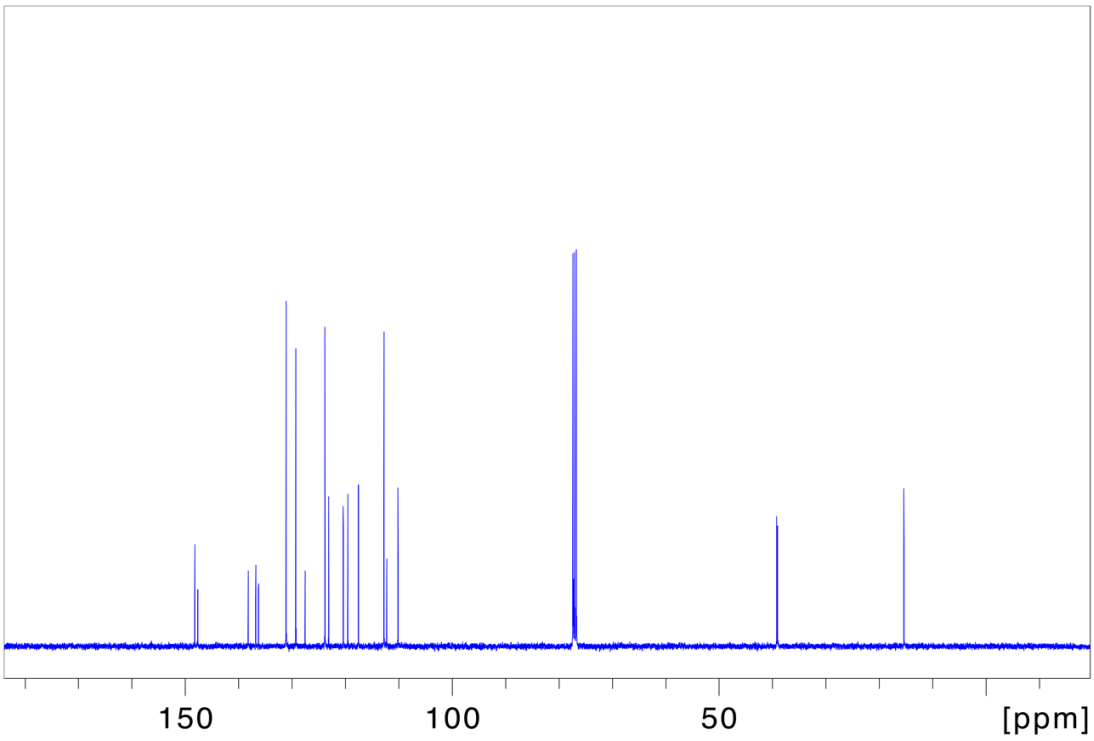

Figure S18. ^{13}C NMR of **NPIM-Aniline** in $CDCl_3$.

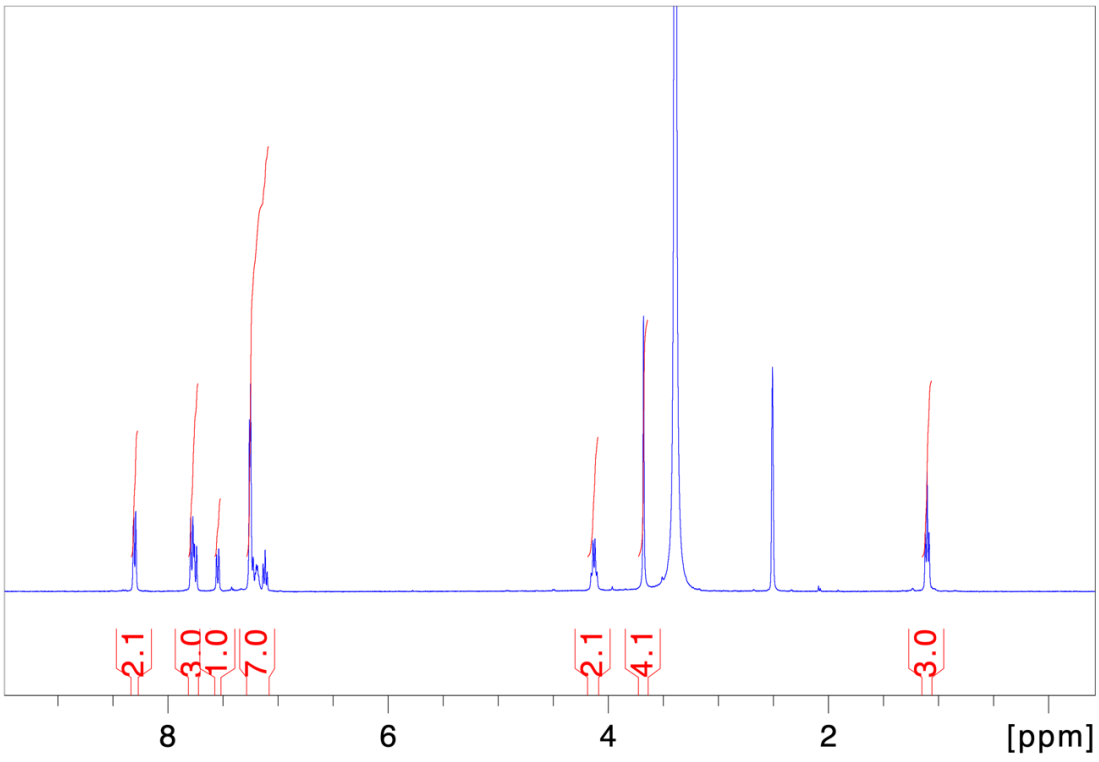

Figure S19. ^{1}H NMR of **NPIM-Benzylamine** in DMSO-d_6.

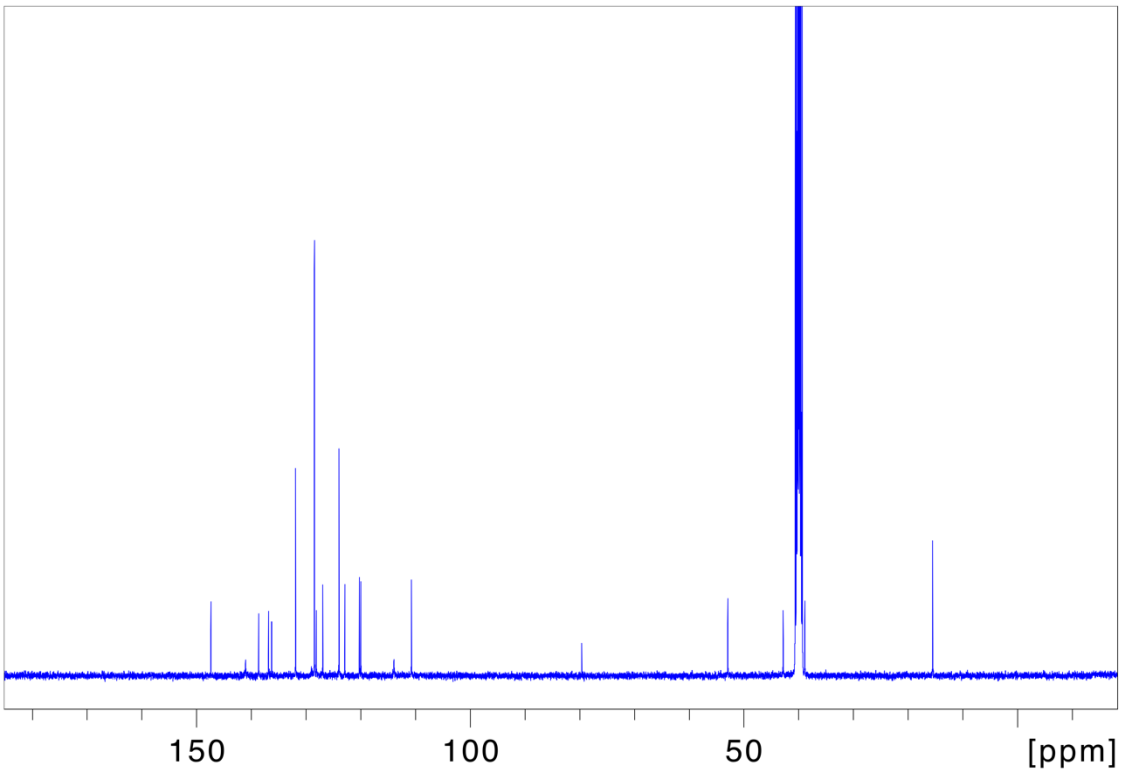

Figure S20. ^{13}C NMR of **NPIM-Benzylamine** in DMSO-d_6.

Thermal stability test

Procedures: dissolve NPI derivatives in DMSO-d_6, measure ^{1}H NMR before heating. Set NPI samples with 40°C oil bath for 24 h under dark condition. After cooling down the sample measure NMR again for comparison.

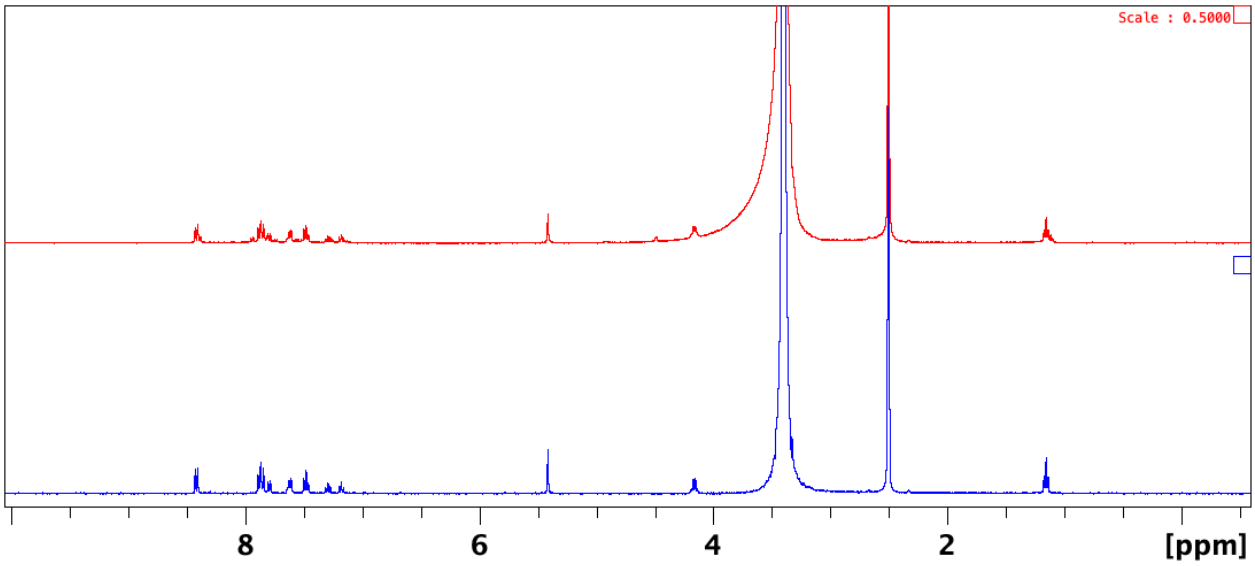

Figure S21. Thermal stability test of **NPIM-Benzoate**, ^{1}H NMR of **NPIM-Benzoate**, bot: before heatting; top: after heated 24h.

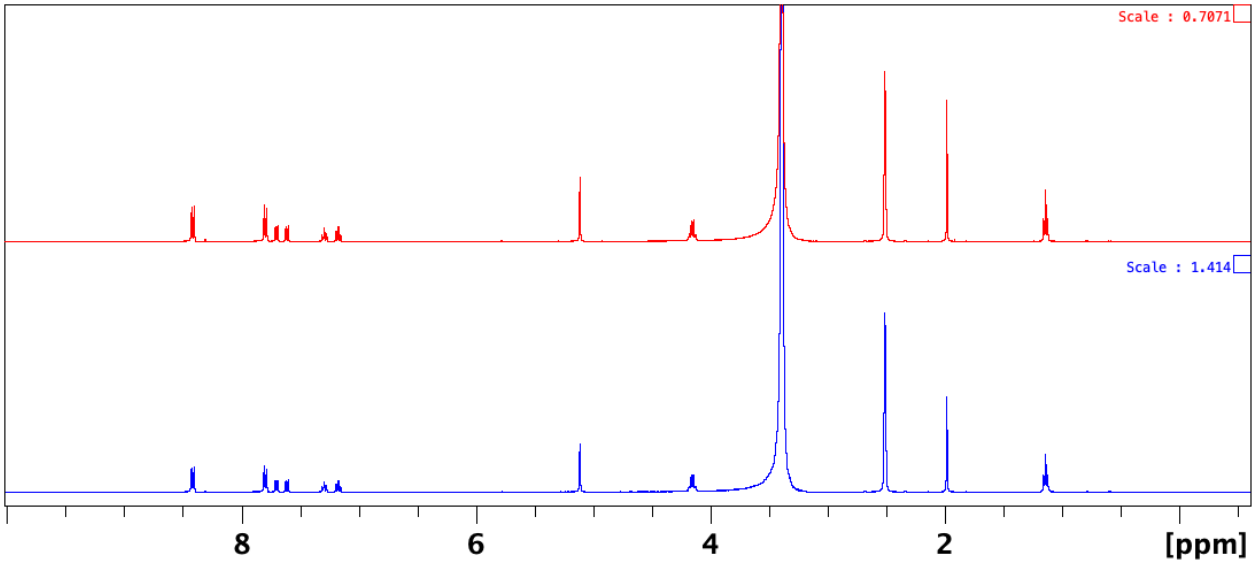

Figure S22. Thermal stability test of **NPIM-Acetate**, ^{1}H NMR of **NPIM-Acetate**, bot: before heatting; top: after heated 24h.

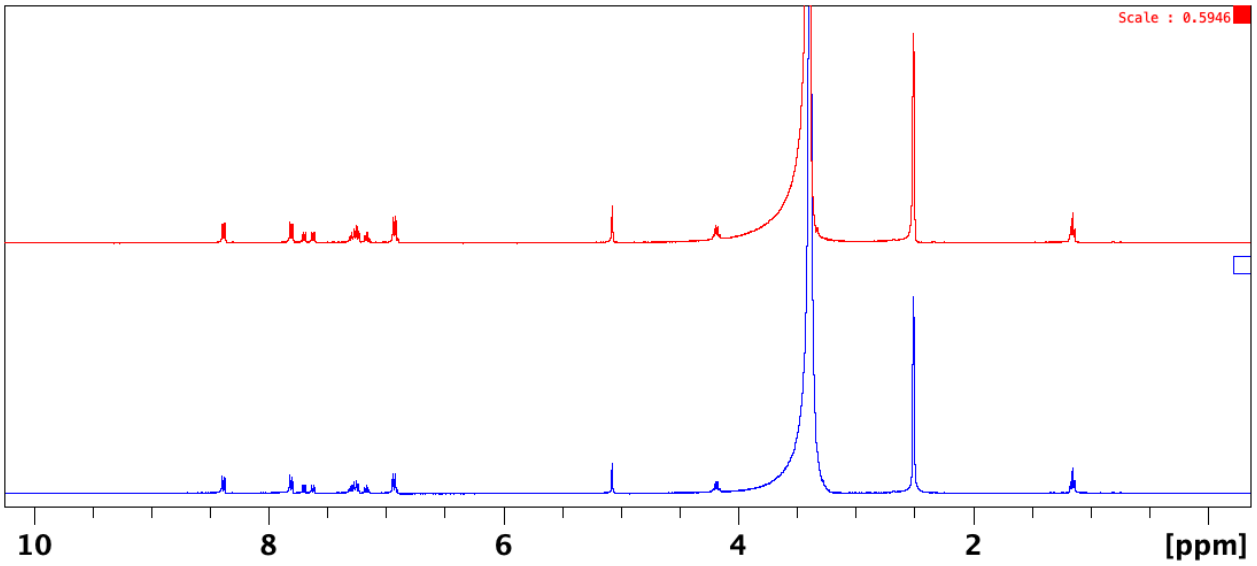

Figure S23. Thermal stability test of **NPIM-Phenol**, ^{1}H NMR of **NPIM-phenol**, bot: before heatting; top: after heated 24h.

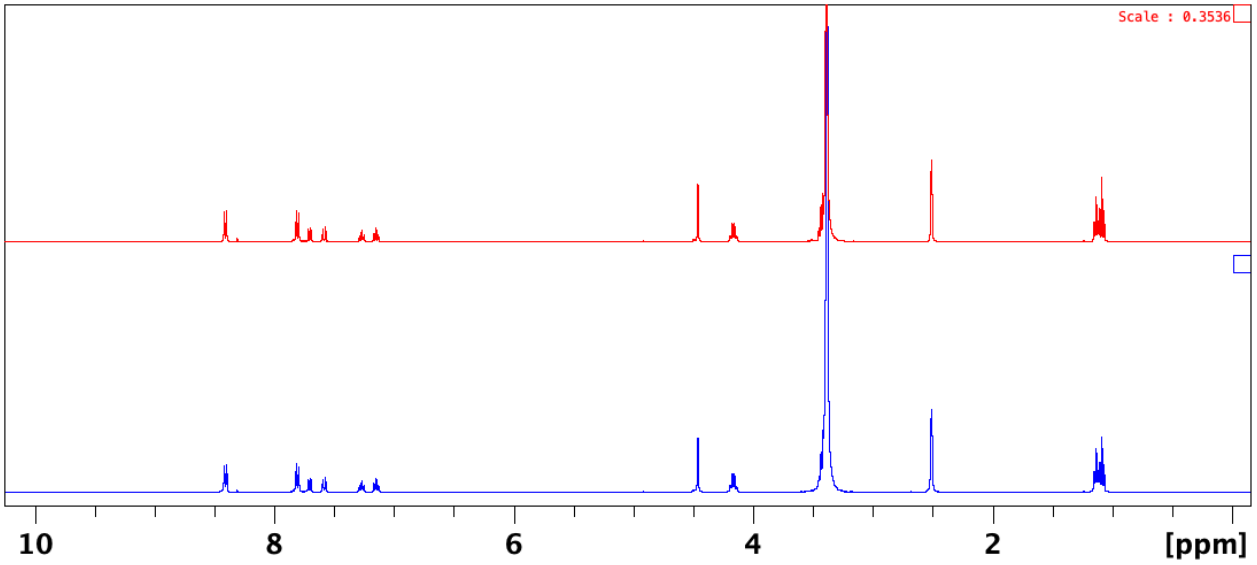

Figure S24. Thermal stability test of **NPIM-EtOH**, ^{1}H NMR of **NPIM-EtOH**, bot: before heatting; top: after heated 24h.

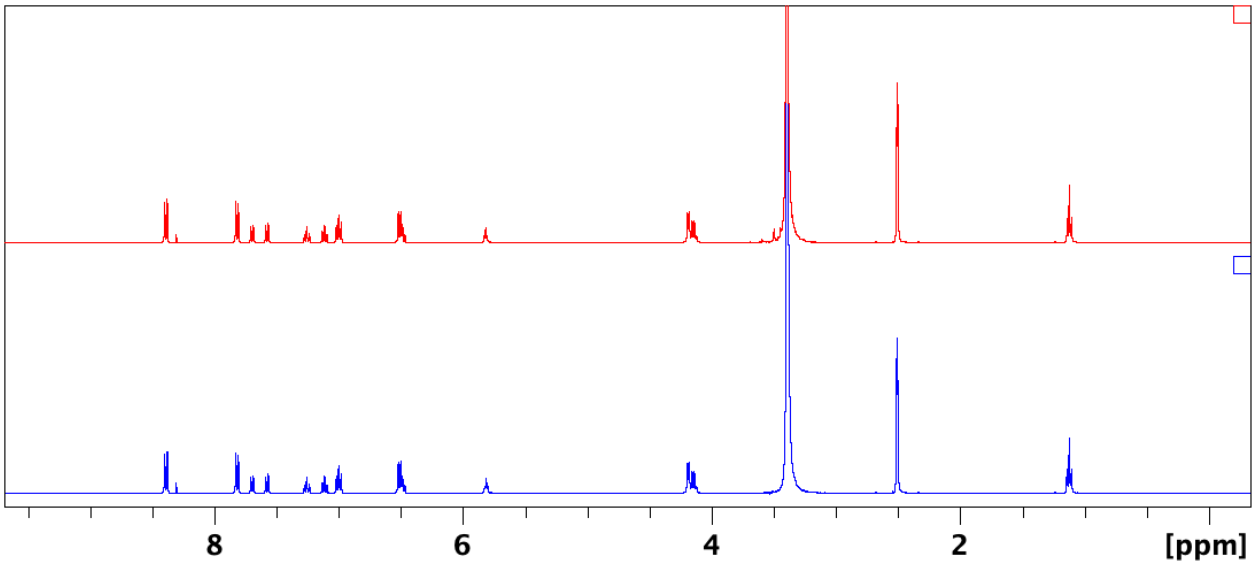

Figure S25. Thermal stability test of **NPIM-Aniline**, ^{1}H NMR of **NPIM-Aniline**, bot: before heatting; top: after heated 24h.

Uncaging reaction of NPIM derivatives

Procedures: dissolve NPIM derivatives in DMSO-d_6, transfer sample to NMR tube and irradiated with 405 nm LED lamp, reaction process was traced by ^{1}H NMR.

Uncaging of **NPIM-Benzoate**:

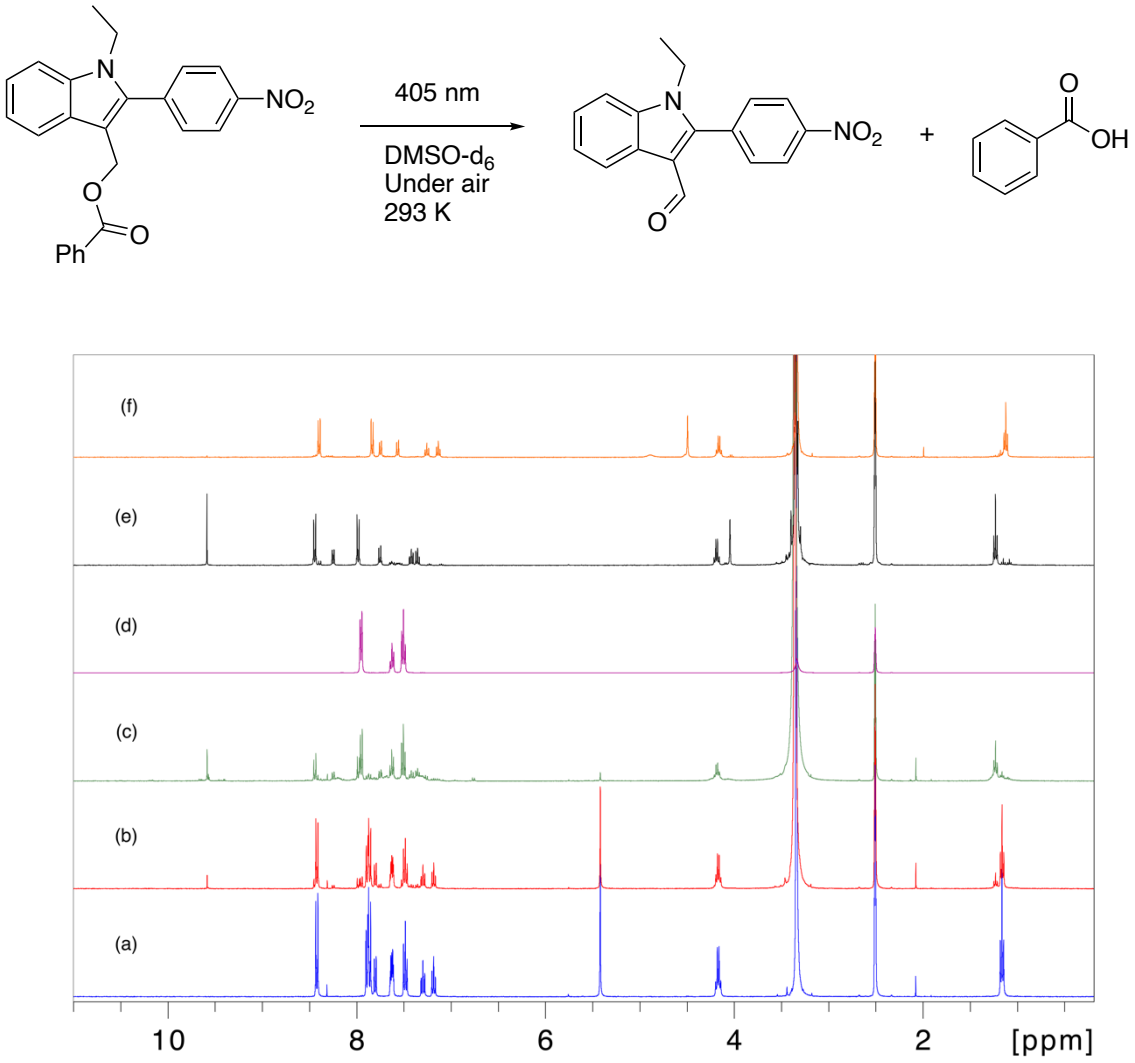

Figure S26. ^{1}H NMR spectroscopy analysis of **NPIM-Benzoate** photolysis (12 mM) at 405 nm in DMSO-d_6; (a) before irradiation; (b) after 1 h irradiation; (c) after 4 h irradiation; (d) ^{1}H NMR spectrum of benzoate; (e) 1-ethyl-2-(4-nitrophenyl)-1*H*-indole-3-carbaldehyde (**NPIM-Ald**) in DMSO-d_6; (f) (1-ethyl-2-(4-nitrophenyl)-1*H*-indol-3-yl)methanol, δ 2–10 ppm.

Uncaging of **NPIM-Acetate**:

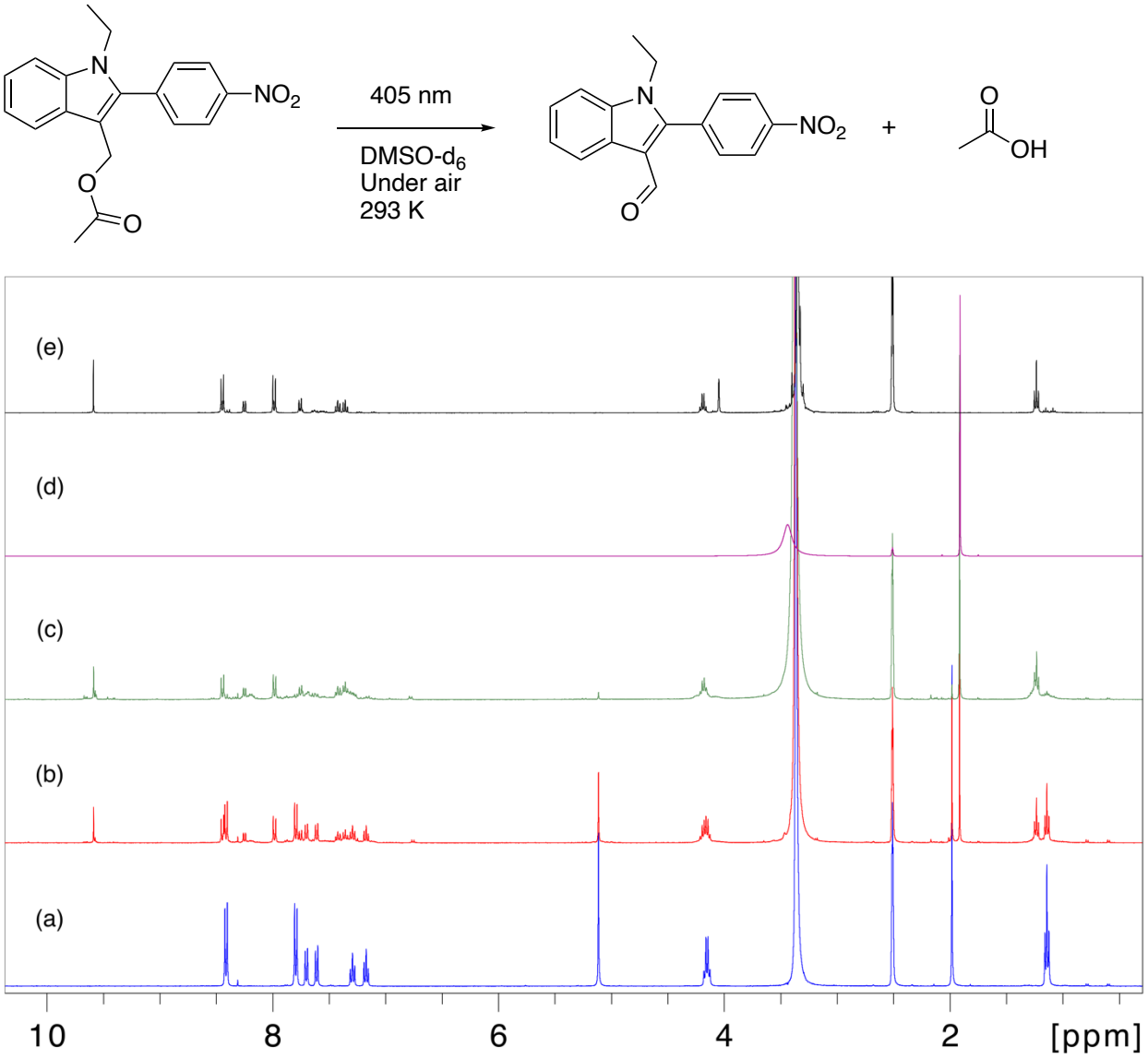

Figure S27. ^{1}H NMR spectroscopy analysis of **NPIM-Acetate** photolysis (10 mM) at 405 nm in DMSO-d_6; (a) before irradiation; (b) after 1 h irradiation; (c) after 2.5 h irradiation; (d) ^{1}H NMR spectrum of acetate; (e) 1-ethyl-2-(4-nitrophenyl)-1*H*-indole-3-carbaldehyde in DMSO-d_6, δ 2–10 ppm.

Uncaging of **NPIM-Phenol**:

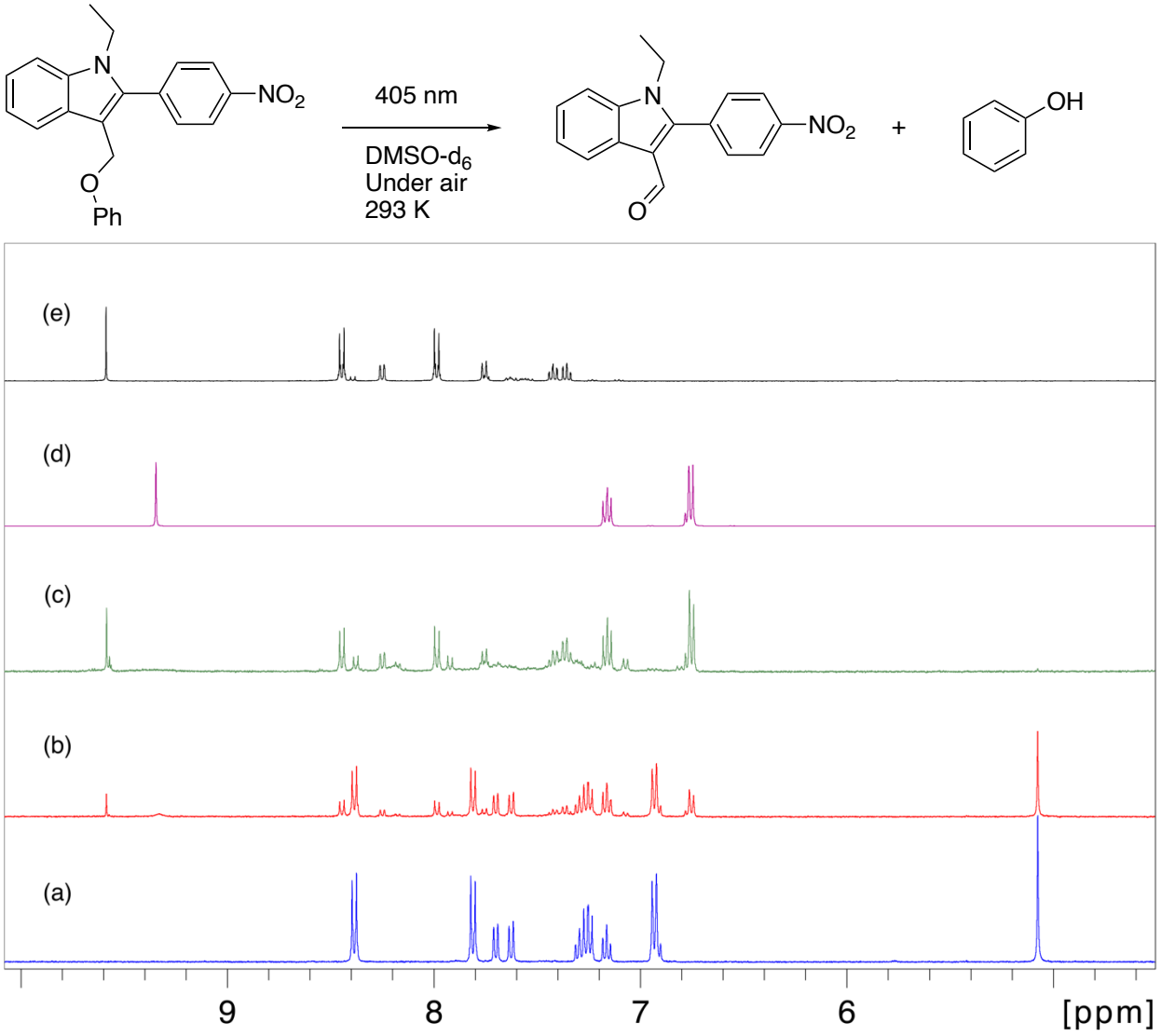

Figure S28. ^{1}H NMR spectroscopy analysis of **NPIM-Phenol** photolysis (5.4 mM) at 405 nm in DMSO-d_6; (a) before irradiation; (b) after 15 min irradiation; (c) after 1 h irradiation; (d) ^{1}H NMR spectrum of phenol; (e) 1-ethyl-2-(4-nitrophenyl)-1*H*-indole-3-carbaldehyde in DMSO-d_6, δ 6–10 ppm.

Uncaging of **NPIM-EtOH**:

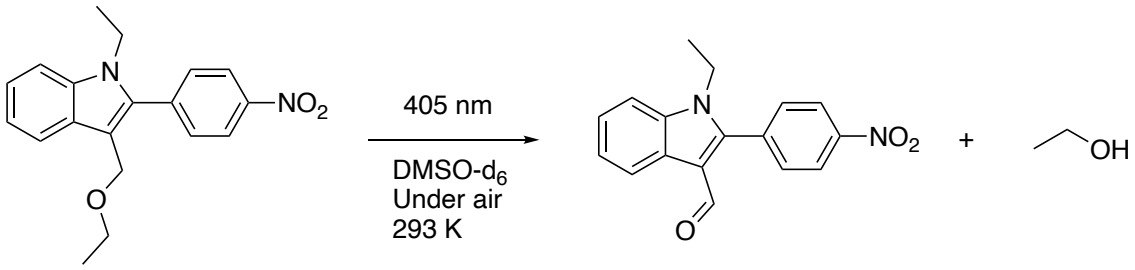

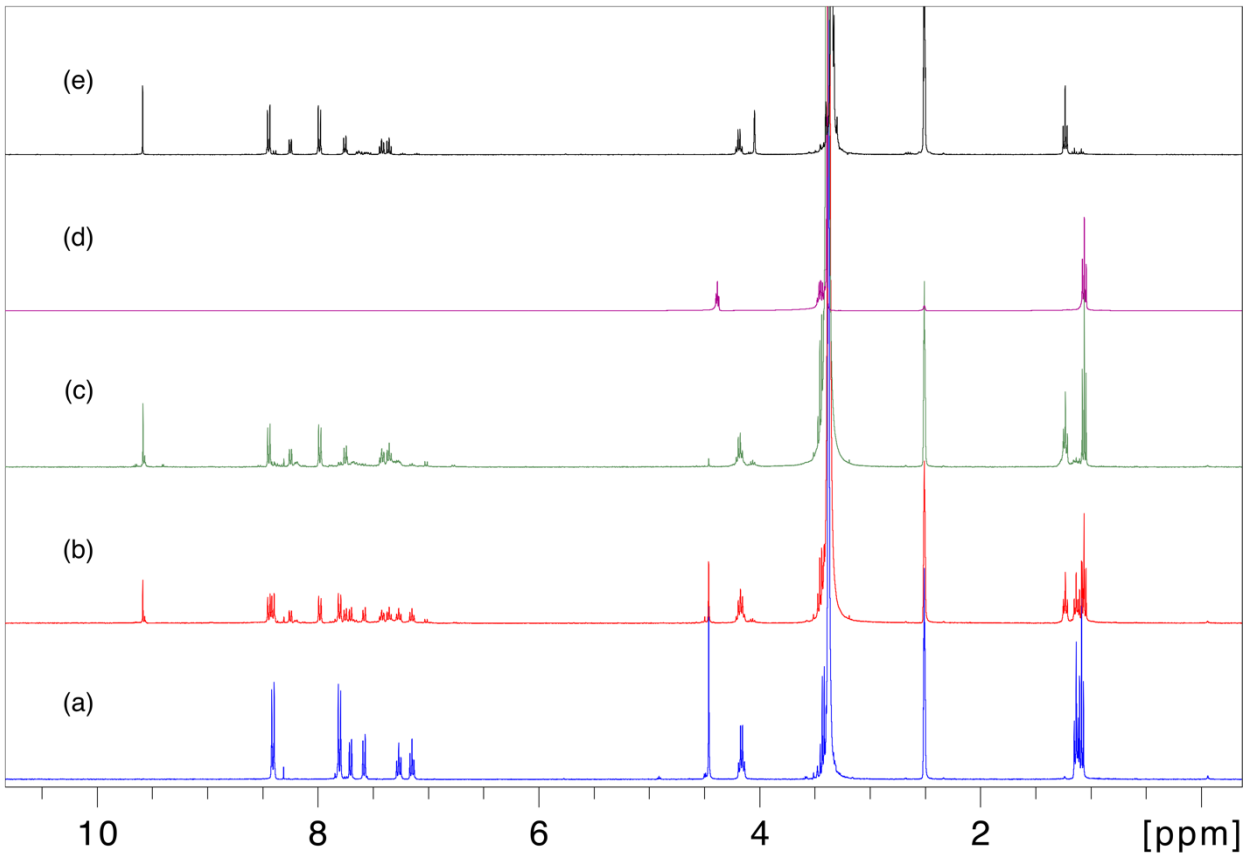

Figure S29. ^{1}H NMR spectroscopy analysis of **NPIM-EtOH** photolysis (13 mM) at 405 nm in DMSO-d_6; (a) before irradiation; (b) after 1 h irradiation; (c) after 3 h irradiation; (d) ^{1}H NMR spectrum of EtOH; (e) 1-ethyl-2-(4-nitrophenyl)-1*H*-indole-3-carbaldehyde in DMSO-d_6, δ 1–10 ppm.

Uncaging of **NPIM-Aniline**:

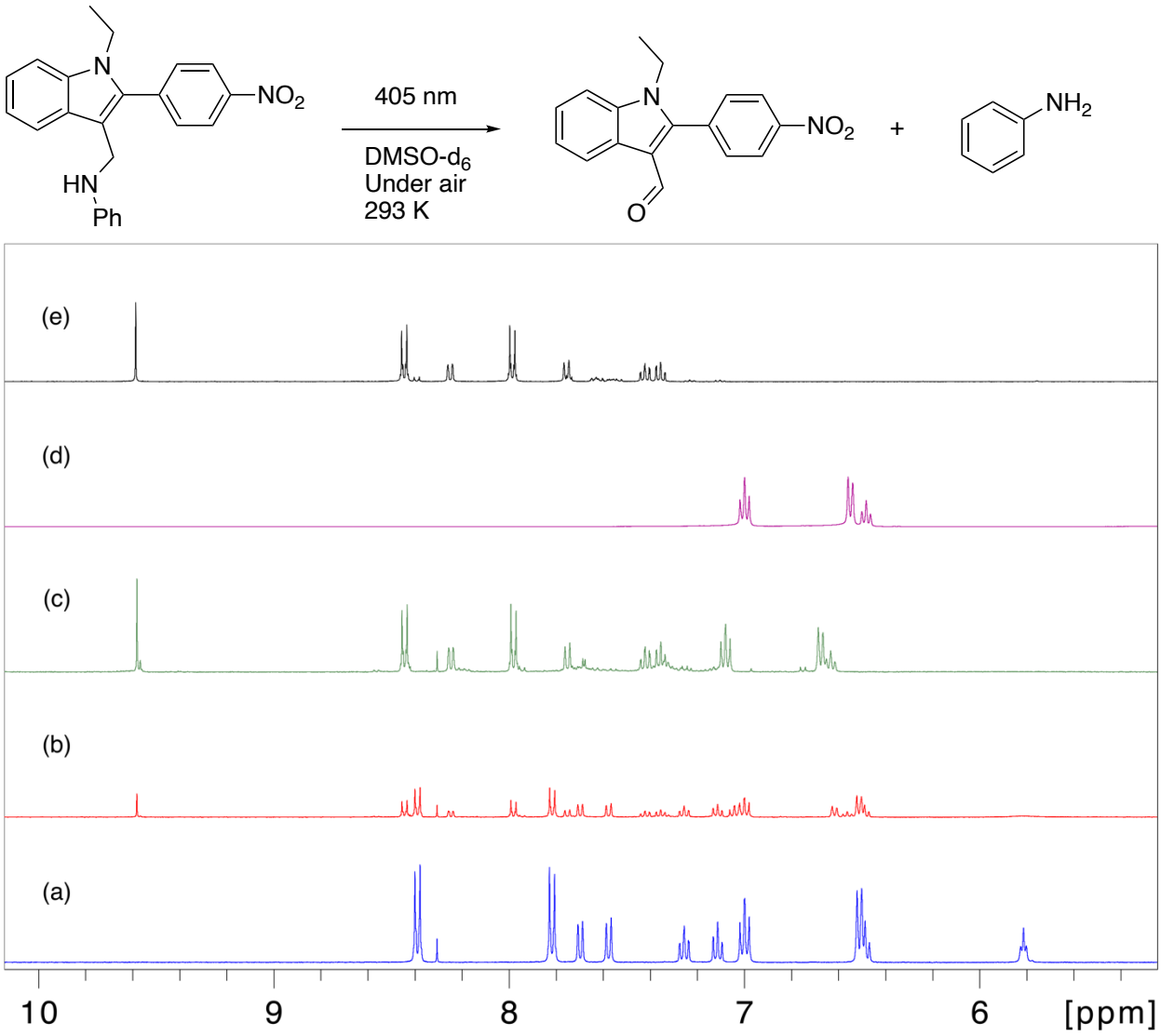

Figure S30. ^{1}H NMR spectroscopy analysis of **NPIM-Aniline** photolysis (8.1 mM) at 405 nm in DMSO-d_6; (a) before irradiation; (b) after 1.5 h irradiation; (c) after 3 h irradiation; (d) ^{1}H NMR spectrum of aniline; (e) 1-ethyl-2-(4-nitrophenyl)-1*H*-indole-3-carbaldehyde in DMSO-d_6, δ 6–10 ppm.

Uncaging of **NPIM-Benzylamine**:

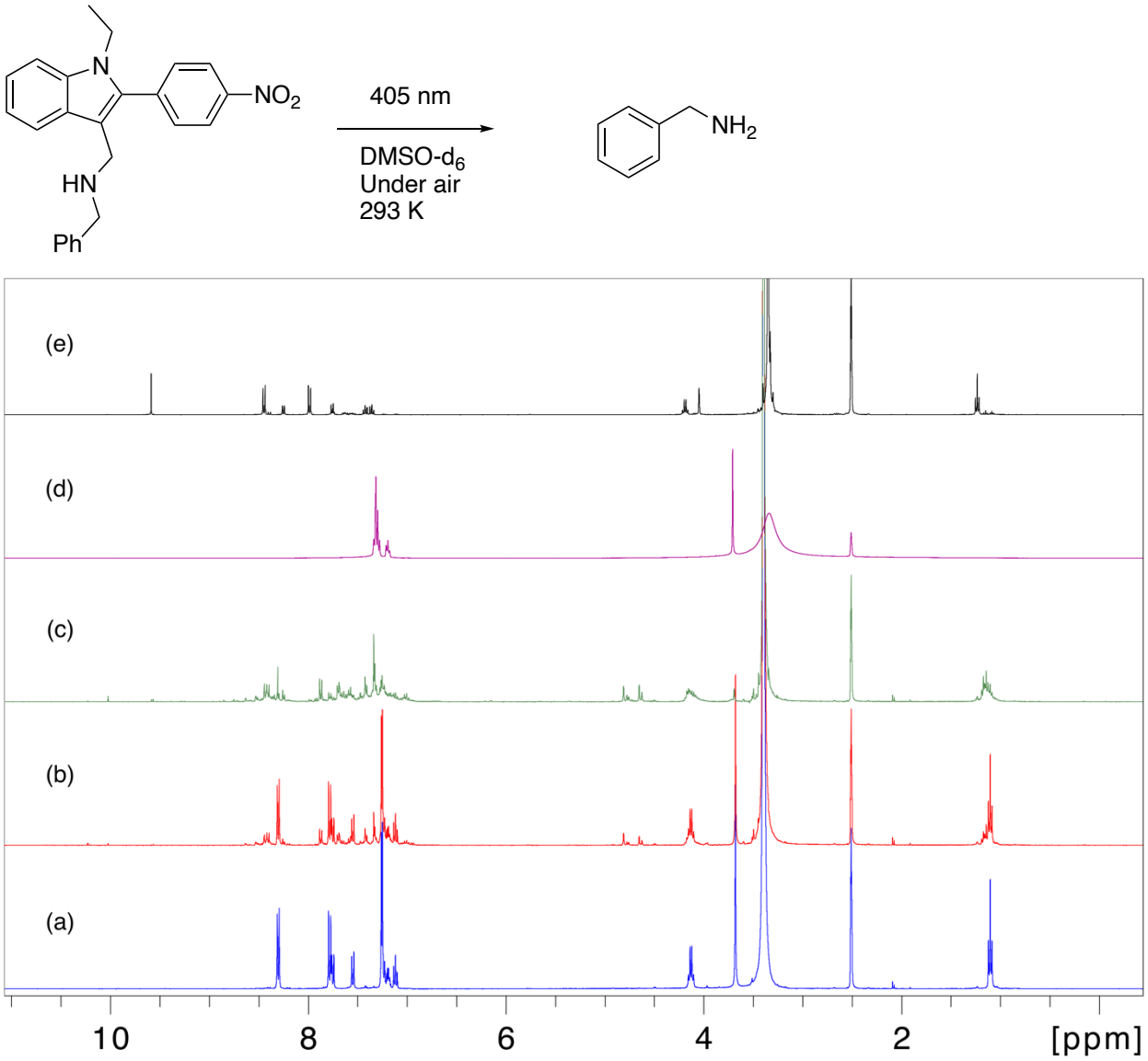

Figure S31. ^{1}H NMR spectroscopy analysis of **NPIM-Benzylamine** photolysis (18 mM) at 405 nm in DMSO-d_6; (a) before irradiation; (b) after 1.5 h irradiation; (c) after 3 h irradiation; (d) ^{1}H NMR spectrum of benzylamine; (e) 1-ethyl-2-(4-nitrophenyl)-1*H*-indole-3-carbaldehyde in DMSO-d_6, δ 1–10 ppm.

Decomposition of NPIM-Ald

Procedures: dissolve **NPIM-Ald** derivatives in DMSO-d_6, transfer sample to NMR tube and irradiated with 405 nm LED lamp, reaction process was traced by ^{1}H NMR.

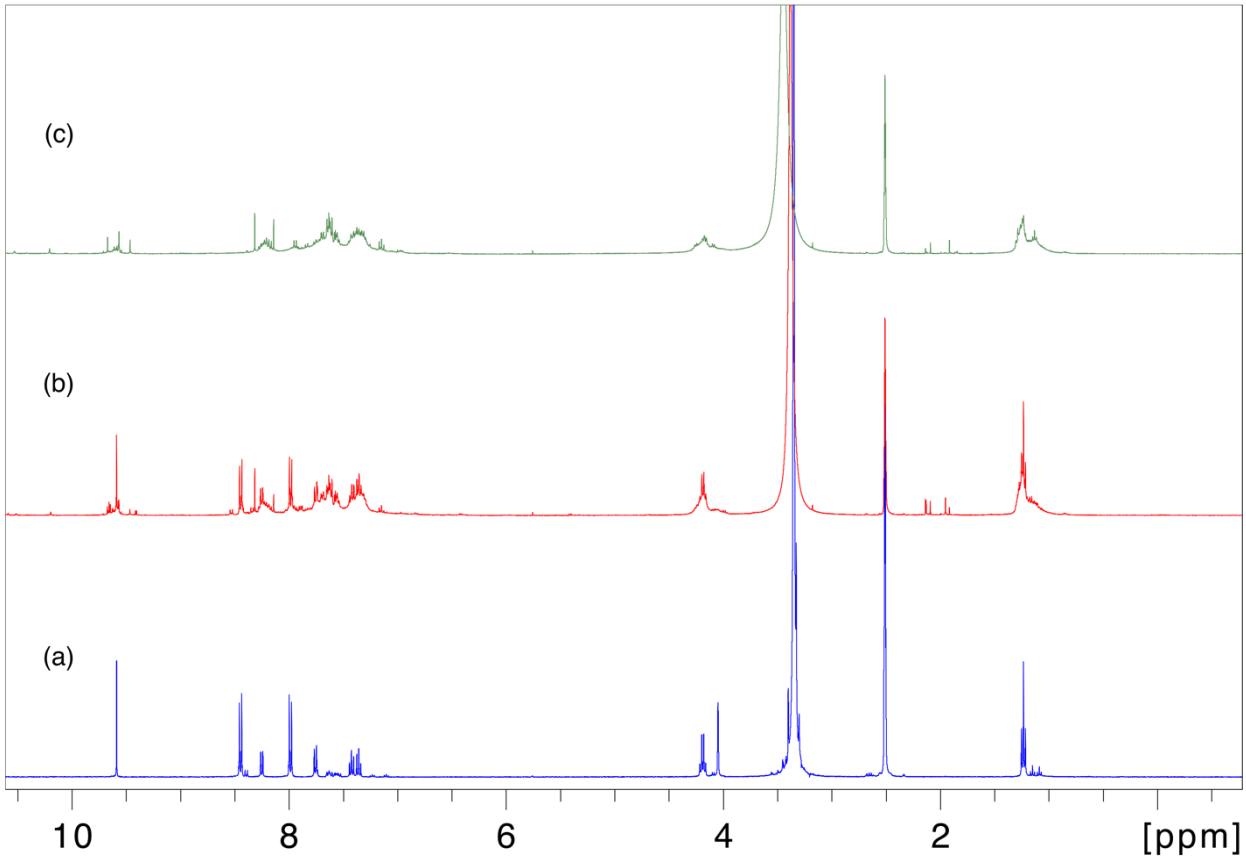

Figure S32. ^{1}H NMR spectroscopy analysis of **NPIM-Ald** photolysis (20 mM) at 405 nm in DMSO-d_6; (a) before irradiation; (b) after 4 h irradiation; (c) after 10 h irradiation, δ 1–10 ppm.

Uncaging of NPI-Benzoate in different conditions

First, uncaging of **NPI-Benzoate** in CD_3CN:

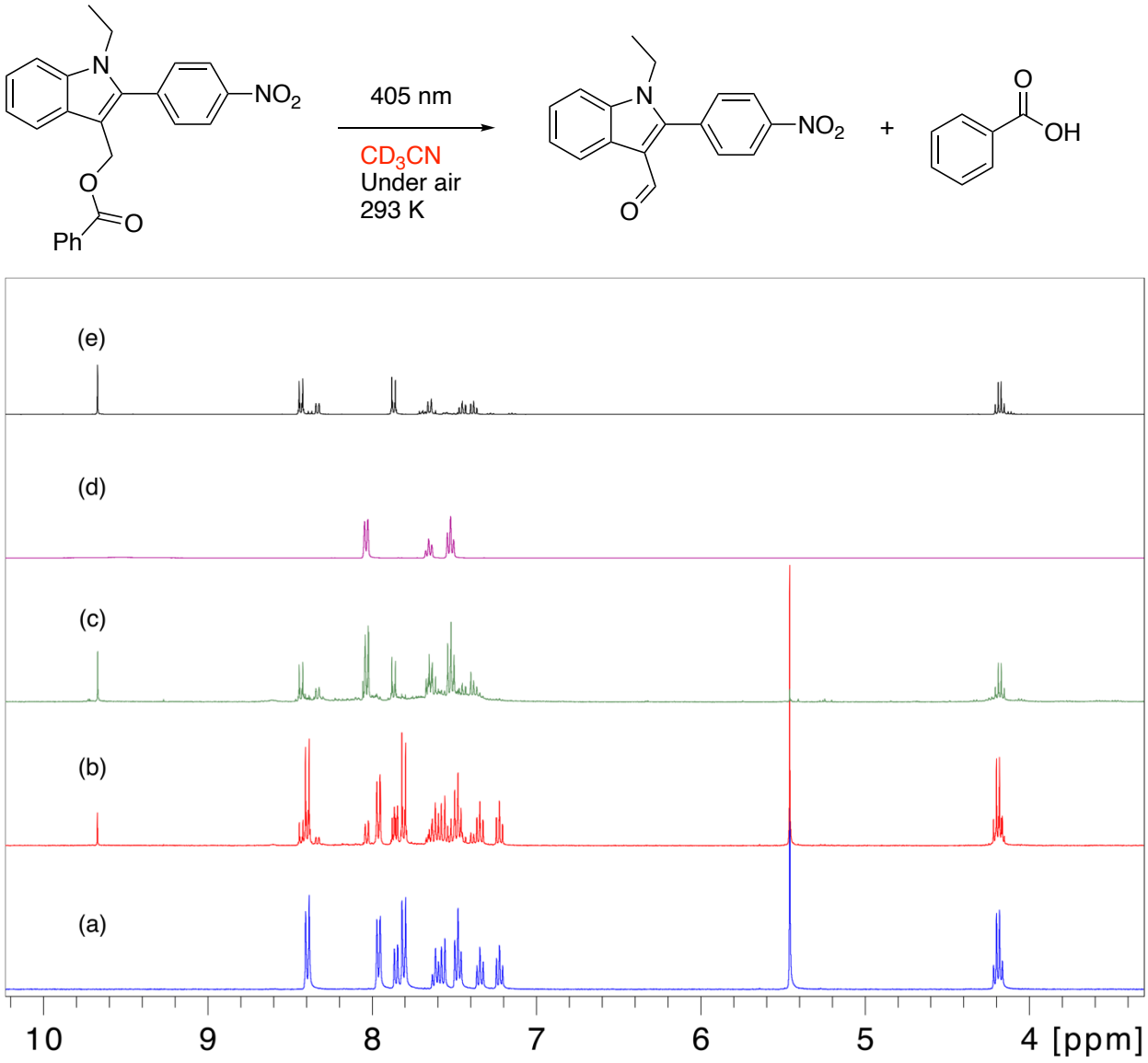

Figure S33. ^{1}H NMR spectroscopy analysis of **NPI-Benzoate** photolysis (12 mM) at 405 nm in CD_3CN; (a) before irradiation; (b) after 10 min irradiation; (c) after 40 min irradiation; (d) ^{1}H NMR spectrum of benzoate; (e) 1-ethyl-2-(4-nitrophenyl)-1*H*-indole-3-carbaldehyde in CD_3CN, δ 4–10 ppm.

Uncaging of **NPI-Benzoate** in CD_3CN after N_2 bubbling for 20min:

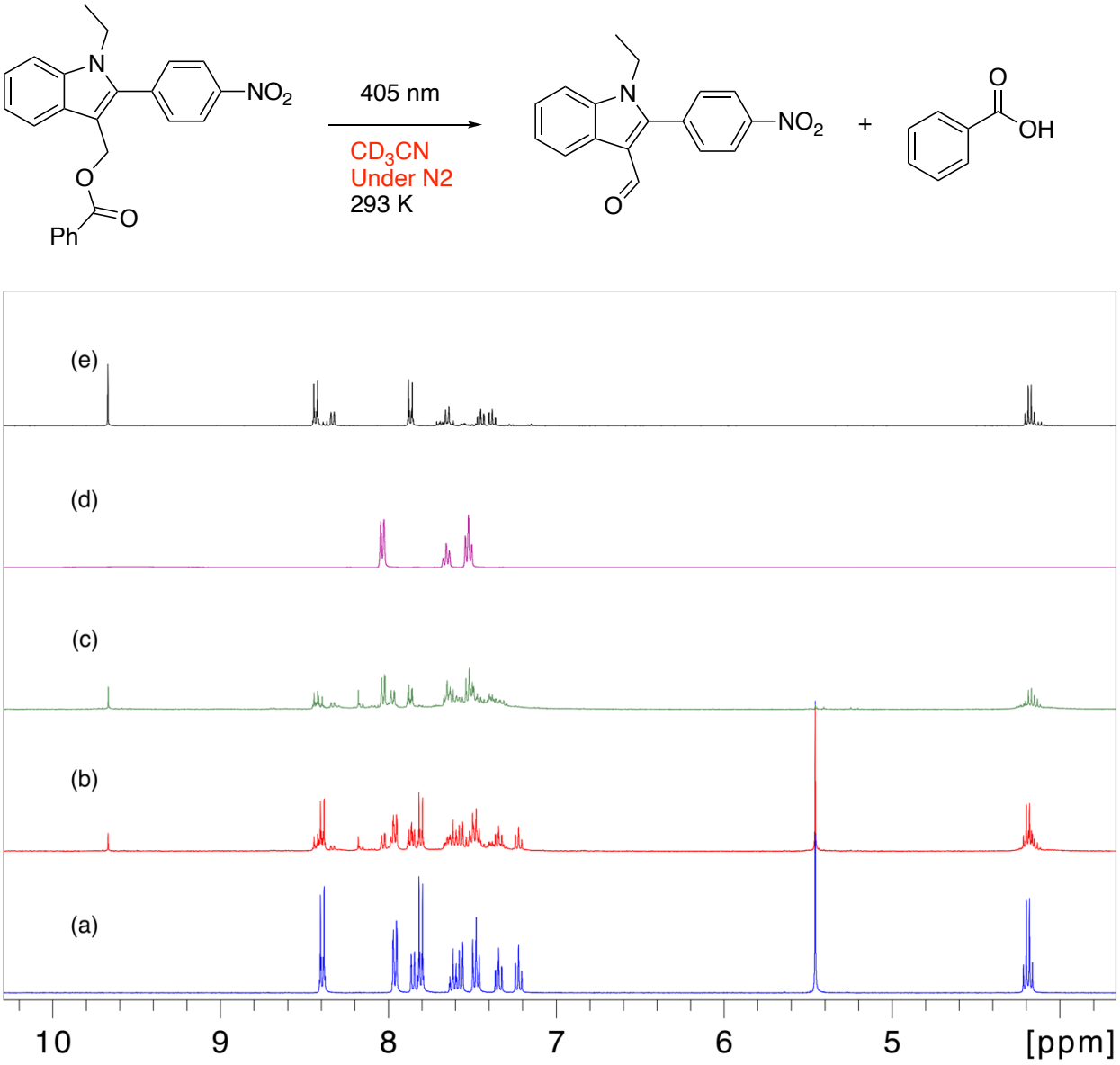

Figure S34. ^1H NMR spectroscopy analysis of **NPI-Benzoate** photolysis (12 mM) at 405 nm in CD_3CN; (a) before irradiation; (b) after 60 min irradiation; (c) after 90 min irradiation; (d) ^1H NMR spectrum of benzoate; (e) 1-ethyl-2-(4-nitrophenyl)-1*H*-indole-3-carbaldehyde in CD_3CN, δ 5–10 ppm.

Uncaging of **NPI-Benzoate** in C_6D_6:

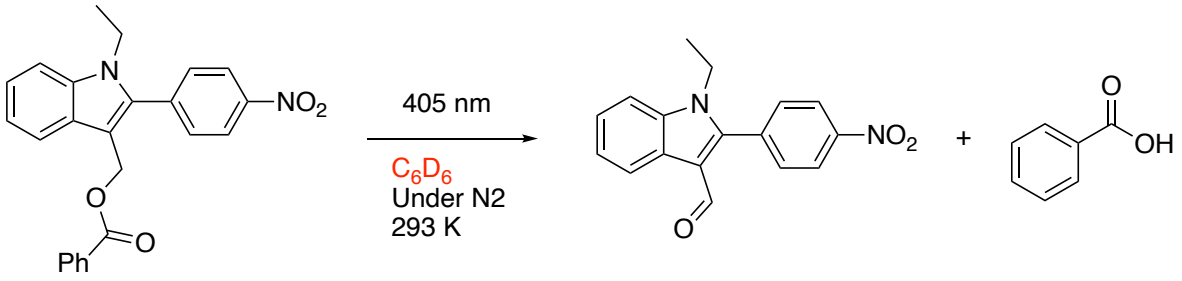

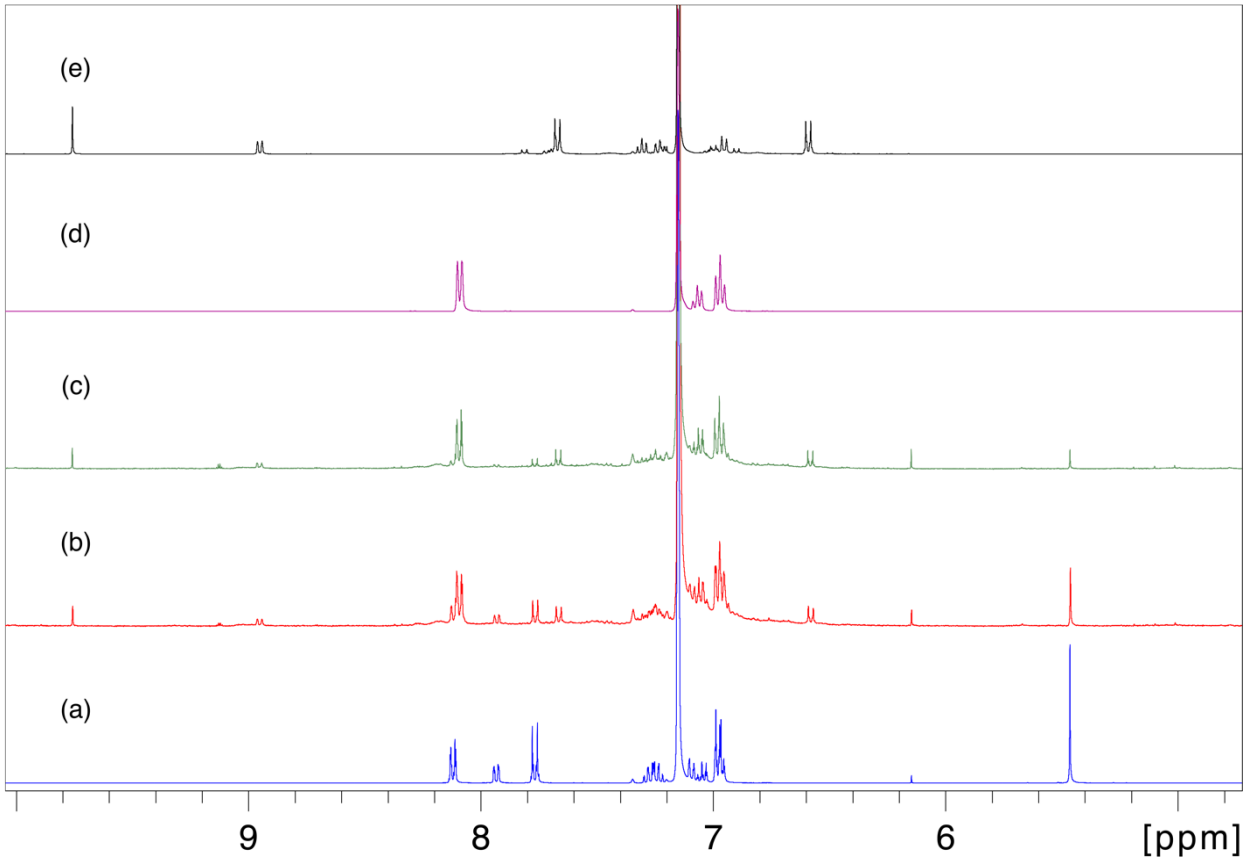

Figure S35. ^{1}H NMR spectroscopy analysis of **NPI-Benzoate** photolysis (12 mM) at 405 nm in C_6D_6; (a) before irradiation; (b) after 5 min irradiation; (c) after 10 min irradiation; (d) ^{1}H NMR spectrum of benzoate; (e) 1-ethyl-2-(4-nitrophenyl)-1*H*-indole-3-carbaldehyde in C_6D_6, δ 6–10 ppm.

Quantum yield of uncaging reaction

Chemical actinometer for quantum yield measurement: The rate of photo uncaging reaction can be quantified by quantum yield (Φ).

$$\Phi = \frac{\text{number of reacted molecules per time unit}}{\text{number of photons absorbed per time unit}}$$

Chemical actinometers are widely used to measure photon fluxes, one of the most popular and reliable one i.e., ferrioxalate, during the photo irradiation the potassium ferrioxalate decomposes according to the following equations.

$$Fe(C_2O_4)_3^{3+} \xrightarrow{h\nu} Fe^{2+} + C_2O_4^{-} + 2C_2O_4^{2-}$$

$$Fe^{2+} + 3phen \longrightarrow Fe(phen)_3^{2+}$$

The number of ferrous ions formed during a photoirradiation is measured by conversion to the colored tris-phenanthroline compound at 510 nm (ε = 11100 M^{-1} cm^{-1}). The original ferric ions are not substantially complexed by phenanthroline and the complex does not absorb at 510 nm.

$$I\ (mol/s) = \frac{\text{moles of } Fe^{2+}}{\Phi_\lambda \times t \times F} = \frac{V_1 \times V_3 \times \Delta A(510\ nm)}{10^3 \times V_2 \times l \times \varepsilon\ (510\ nm) \times \Phi_\lambda \times t}$$

V_1: the irradiated volume (mL)

V_2: the aliquot of the irradiated solution taken for the determination of the ferrous ions (mL)

V_3: the final volume (mL)

ΔA: the optical difference in absorbance between the irradiated solution and that taken in

the dark

l: optical pathlength of the irradiation cell

ε (510 nm): ε of the complex $Fe(phen)_3^{2+}$

Φ_λ: the quantum yield of ferrous ion production at the irradiation wavelength

t: the irradiation time

F: mean function of light absorbed by the ferrioxalate solution

Experiment procedures,

117.7 mg of $K_3[Fe(C_2O_4)_3] \cdot 3H_2O$ was dissolved in 20 mL of 0.05 M H_2SO_4. (0.012 M Ferrioxalate was prepared)-①

10.2 mg of 1,10-phenanthroline monohydrate and 1.78 g of CH_3COONa were dissolved in 10 mL of 0.5 M H_2SO_4-②

3 mL solution of ① irradiated at 370 nm for 0, 10, 20 and 30 seconds, 0.5 mL of solution ② was added each time then measured the absorption spectra at 510 nm to measure the change in absorbance with respect to an irradiation time was used to calculate the light amount.

Calculated number of photons from LED-lamp at 405 nm= 1.10081×10^{-5} mol/min.

Number of reacted molecules per time unit was confirmed by HPLC:

1. **NPIM-Benzoate** dissolved in DMSO (0.45mM);

2. Irradiated with 405 nm LED-lamp for 0, 15, 30, 60 s, injected 5uL of irradiated solution to HPLC for analysis;

3. Measure the change of **NPIM-Benzoate** peak area with respect to an irradiation time to

calculate the conversion rate, then calculate quantum yield:

Quantum yield = numbers of reacted molecules per time unit / numbers of photons absorbed per time unit.

	peak area		
time/s	npi-benzoate	conversion rate	quantum yield
0	501582.14	0	
15	495789.625	0.011548487	0.018883551
30	490460.155	0.022173806	0.018128789
60	487373.2	0.028328242	0.011580257

Two-photon absorption (TPA) cross section measurement

We apply NPBF-BA[43] as reference to estimate TPA cross section for NPI chromophore:

$$\delta_{NPI} = \sigma_{1a} \times \phi_{1a} = \sigma_{NPBF-BA} \times \phi_{NPBF-BA} \times \frac{k_{1a}}{k_{NPBF-BA}}$$

σ NPBF−BA:2PA cross-section of NPBF-BA at 720 nm (18 GM) [43]

ϕ NPBF−BA: quantum yield of NPBF-BA at 720 nm (0.09)

k NPBF-BA: rate constant of NPBF-BA at 720 nm (0.0183)

In this experiment, the mode-locked Ti: Sapphire laser (Mai Tai, Spectra Physic Inc.) was used as the light excitation source which delivers ~80 fs pulses with the repetition rate of 80 MHz. By irradiated with Ti: Sapphire laser and analyze with HPLC to estimate reaction rate of **NPIM-Benzoate**.

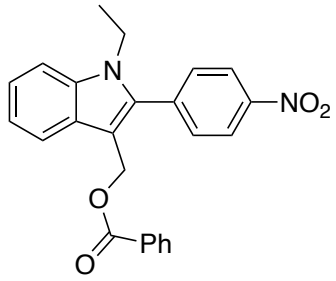

Solvent: DMSO; concentration: 9*10-5 mol/L

HPLC condition: MeCN:H20:TFA=80:20:0.01; flow rate: 1.5 ml/min; pressure: 7.3 MPa; detect: 255 nm; rage: 0.16.

Peak area of starting compound was shown as follow:

wavelength	20 min	40 min	60min
700nm	4799680	4786215	4776035
720nm	4796755	4788470	4777515
750nm	4805530	4787405	4766510
780nm	4766625	4734505	4722010

Then we calculate ln [NPI]/[NPI0]:

ln [NPI]/[NPI0]	20min	40min	60min
700nm	-0.0072595	-0.0100688	-0.012198
720nm	-0.0078691	-0.0095978	-0.0118882
750nm	-0.0060414	-0.0098202	-0.0141944
780nm	-0.0141702	-0.0209316	-0.0235742

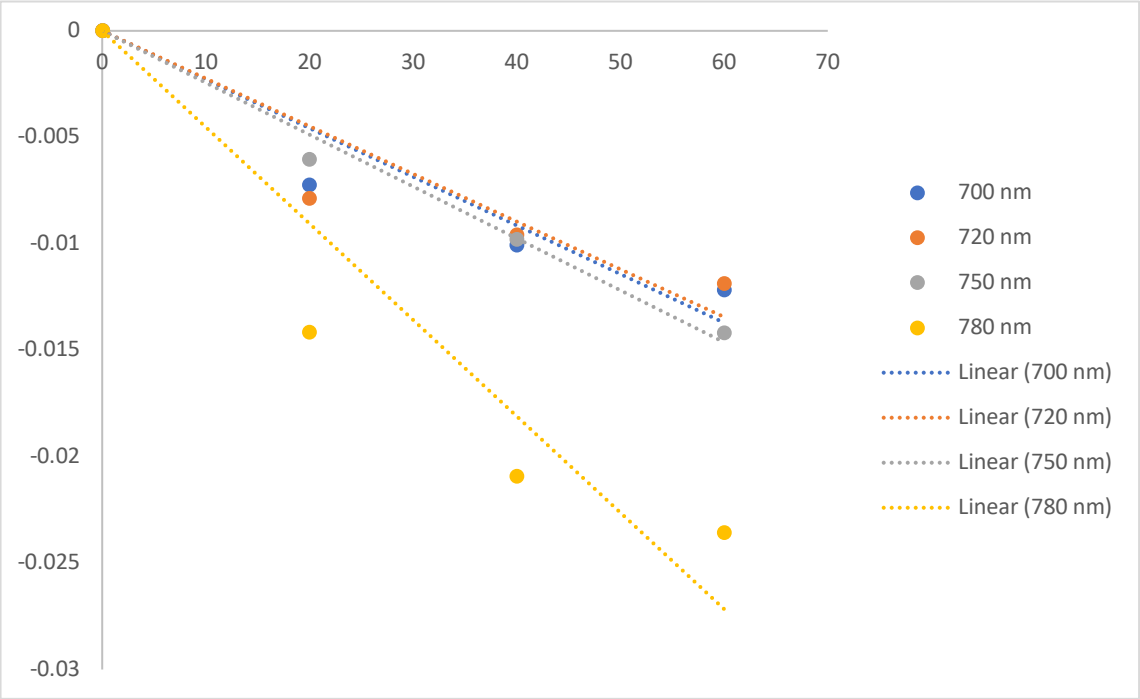

	TPA cross-section	k NPIM-Benzoate
700	100.47541	0.0227
720	98.704918	0.0223
750	107.114754	0.0242
780	198.295082	0.0448

Reference

1 T. Schmierer, S. Laimgruber, K. Haiser, K. Kiewisch, J. Neugebauer and P. Gilch, Femtosecond spectroscopy on the photochemistry of ortho-nitrotoluene, *Phys. Chem. Chem. Phys.*, 2010, **12**, 15653–15664.

2 S. Laimgruber, W. J. Schreier, T. Schrader, F. Koller, W. Zinth and P. Gilch, The photochemistry of o-nitrobenzaldehyde as seen by femtosecond vibrational spectroscopy, *Angew. Chemie - Int. Ed.*, 2005, **44**, 7901–7904.

3 V. Leyva, I. Corral, T. Schmierer, P. Gilch and L. González, A comparative analysis of the UV/Vis absorption spectra of nitrobenzaldehydes, *Phys. Chem. Chem. Phys.*, 2011, **13**, 4269–4278.

4 T. Schmierer, G. Ryseck, T. Villnow, N. Regner and P. Gilch, Kasha or state selective behavior in the photochemistry of ortho-nitrobenzaldehyde, *Photochem. Photobiol. Sci.*, 2012, **11**, 1313–1321.

5 N. Komori, S. Jakkampudi, R. Motoishi, M. Abe, K. Kamada, K. Furukawa, C. Katan, W. Sawada, N. Takahashi, H. Kasai, B. Xue and T. Kobayashi, Design and synthesis of a new chromophore, 2-(4-nitrophenyl)benzofuran, for two-photon uncaging using near-IR light, *Chem. Commun.*, 2016, **52**, 331–334.

6 S. Jakkampudi, M. Abe, N. Komori, R. Takagi, K. Furukawa, C. Katan, W. Sawada, N. Takahashi and H. Kasai, Design and Synthesis of a 4-Nitrobromobenzene Derivative Bearing an Ethylene Glycol Tetraacetic Acid Unit for a New Generation of Caged Calcium Compounds with Two-Photon Absorption Properties in the Near-IR Region and Their Application in Vivo, *ACS Omega*, 2016, **1**, 193–201.

7 Q. Lin and M. Abe, Light-triggered elimination of CO_2 and absorption of O_2 (artificial breathing reaction) in photolysis of 2-(4-nitrophenyl)-1H-indole derivatives, *Photochem. Photobiol. Sci.*, 2021, **20**, 421–434.

8 P. Klán, T. Šolomek, C. G. Bochet, A. Blanc, R. Givens, M. Rubina, V. Popik, A. Kostikov and J. Wirz, Photoremovable Protecting Groups in Chemistry and Biology: Reaction Mechanisms and Efficacy, *Chem. Rev.*, 2013, **113**, 119–191.

9 D. B. G. Williams and M. Lawton, Drying of Organic Solvents: Quantitative Evaluation of the Efficiency of Several Desiccants, *J. Org. Chem.*, 2010, **75**, 8351–8354.

Chapter 4

Summary and outlook

In this study, we aim to design suitable 2P responsive PPGs for caging & uncaging, which can make contributions to understand the effects of bioactive compounds. The 2-(4-nitrophenyl)-1*H*-indole (NPI) chromophore is first designed as a 2P responsive chromophores for caged compounds, due to its efficient 2P sensitivity. As results, NPI chromophore can release leaving group successfully when the leaving group is introduced to the ortho position of nitrobenzene ring. Surprisingly, an unexpected aldehyde was isolated during product analysis, which was transformed from a carboxylic acid moiety without any catalysts. Such unusual reaction pushed us to investigate the mechanism of the transformation and the excited-state dynamics. By employ the TA spectroscopy and TD-DFT computation, it is proposed that the intramolecular electron transfer to the excited state was the initial step of the chemical transformation to generate the zwitterion intermediate. The later CO_2 elimination and absorption of O_2 produced the hydroperoxide together with its photoinduced decomposition products, the alcohol and aldehyde. The photoinduced breathing-type reaction may open a new gate of transition metal free oxidation of amino acids.

Inspired by the photoreaction of NPI derivatives, 2-(4-nitrophenyl)-1*H*-indolyl-3-methyl (NPIM) chromophore was designed for 1P and 2P uncaging. The NPIM chromophore shows excellent performance in uncaging reaction: 1. high chemical yields of leaving groups; 2. clean photoreaction; 3. efficient uncaging reaction with large quantum yield. Generally, direct release of alcohols and amines is tough, because of the low leaving group properties of OR and NHR. However, the NPIM can release alcohols and amines directly. The high 2P absorption cross section and low cytotoxicity of NPIM chromophore were also determined. Such features make NPIM a promising PPG for biological studies.

Publication List

(1) Light-triggered elimination of CO_2 and absorption of O_2 (artificial breathing reaction) in photolysis of 2-(4-nitrophenyl)-1*H*-indole derivatives.
Qianghua. Lin, Manabu. Abe
Photochem. Photobiol. Sci. **2021**, *20*, 421.

(2) 2-(4-Nitrophenyl)-1*H*-indolyl-3-methyl chromophore: A versatile photocage that responds to visible-light one-photon and near-infrared-light two-photon excitations.
Qianghua Lin, Runzhao Guo, Kozue Hamao, Ryukichi Takagi, and Manabu Abe
Chemistry Letters, (Accepted).

Acknowledgment

This research is carried out by the guidance of Professor Manabu Abe at the Department of Chemistry, Graduate School of Science, Hiroshima University.
I would like to express my tons of thanks to Professor Manabu Abe for his kind support, guidance and encouragement during my research.
I would like to express my appreciation to Dr. Ryukichi Takagi and Dr. Sayaka Hatano for their guidance and discussion for my research. I sincerely express my thanks to our lab members.
Finally, I would like to thank my families for their supporting and encouragement.

LIN QIANGHUA December

.....